Synaptojanin1 is involved in endolysosomal trafficking in cone photoreceptors

Ashley Amelia George

A dissertation
submitted in partial fulfillment of the
requirements for the degree of

Doctor of Philosophy

University of Washington
2015

Reading Committee:
Susan E Brockerhoff, Chair
Alexey J. Merz
Sharona E. Gordon

Program Authorized to Offer Degree: Biochemistry

University of Washington

Abstract

Synaptojanin1 is involved in endolysosomal trafficking in cone photoreceptors

Ashley Amelia George

Chair of the Supervisory Committee:
Professor Susan E. Brockerhoff
Biochemistry

Cells require the ability to properly sort and traffic proteins to their correct subcellular destination. The production of new proteins must be balanced by the turnover of old and damaged proteins. A breakdown in this process is detrimental to any cell; however highly polarized, non-proliferating cells, such as neurons, are particularly vulnerable to defects in protein turnover. Photoreceptors are highly polarized, specialized neurons that have high protein trafficking demands. At one end of the photoreceptor is the outer segment; the site of photon detection and phototransduction. The outer segment requires a constant supply of new proteins and membranes to maintain proper function. At the opposite end of the cell is the site of synaptic transmission. The synapse also undergoes large amounts of membrane trafficking and turnover due to the release of neurotransmitter and subsequent synaptic vesicle recycling. Although both ends of the photoreceptor require efficient membrane trafficking, the majority of studies of protein trafficking in photoreceptors have focused on the outer segment. In addition, photoreceptors do not need to degrade old and damaged proteins and membranes from the outer segment; the retinal pigment epithelium phagocytoses outer segment discs.

Therefore the focus on outer segment trafficking has resulted in a deficit in our understanding of the process of protein degradation in photoreceptor cells.

In this study we establish that the zebrafish *nrc*^{a14} mutant has a specific defect in endolysosomal and autophagic trafficking and can therefore be used as a model to understand these processes in cone photoreceptors. The trafficking defects in the *nrc*^{a14} cones begin early in photoreceptor development. The accumulation of autophagosomes in the *nrc*^{a14} mutant is due, at least in part, to impaired autophagosome maturation that is not caused by a decrease in autophagosome mobility. The causative mutation in the *nrc*^{a14}mutant is in the gene encoding a polyphosphoinositide phosphatase Synaptojanin1; highlighting the importance of the phosphoinositide lipids in protein degradation pathways. We analyzed the distribution of the phosphoinositides PI(3)P, PI(4)P, PI(3,5)P_2 and PI(4,5)P_2 in wild type and *nrc*^{a14} photoreceptors. We found that the distribution of these lipids in wild type photoreceptors is the same as in non-neuronal cell types; PI(3)P on endosomes, PI(4)P on the Golgi, PI(3,5)P_2 on late endosomes/lysosomes and PI(4,5)P_2 in the plasma membrane. We found no gross change in the distribution of these phosphoinositides in *nrc*^{a14} mutant photoreceptors. Further, we use the *nrc*^{a14} mutant phenotypes to discover that the Synaptojanin1 dephosphorylates a PIP species with a 5'phosphate to regulate autophagy and endolysosomal trafficking. Collectively, my work has generated a large tool set for studying membrane trafficking in zebrafish cone photoreceptors and has defined a specific role for Synaptojanin1 in regulating autophagy and degradative trafficking pathways in cones.

Table of Contents

List of Figures

Glossary

BFA: Brefeldin A

CC: connecting cilia

CFP: Cyan fluorescent protein

CNG: cyclic-nucleotide gated

crx: cone-rod homeobox

dpf: days post fertilization

EM: embryo media

ER: Endoplasmic Reticulum

ER-GFP: Endoplasmic Reticulum targeted GFP

FAPP1: Four-phosphate-adaptor protein 1

FYVE: Fab1, YotB, Vac1p, and EEA1

GFP: green fluorescent protein

hpf: hours post fertilization

IS: inner segment

LC3: Microtubule-associated protein 1A/1B-light chain 3

Man2a: mannosidase2a

ML1N: N-terminus of Mucolipin 1

nrc^{a14}: no optokinetic response c

OKR: Optokinetic Response

OPL: Outer Plexiform Layer

OS: outer segment

PH: pleckstrin homology

PIP: phosphatidylinositol

PI(3)P: phosphatidylinositol 3-phosphate

PI(3,4)P_2: phosphatidylinositol 3,4-bisphosphate

PI(3,4,5)P_2: phosphatidylinositol 3,4,5-trisphosphate

$PI(3,5)P_2$: phosphatidylinositol 3,5-bisphosphate

PI(4)P: phosphatidylinositol 4-phosphate

$PI(4,5)P_2$: phosphatidylinositol 4,5-bisphosphate

PI(5)P: phosphatidylinositol 5-phosphate

PLCδ: Phospholipase C delta

PTU: 1-phenyl-2-thiourea

RPE: retinal pigment epithelium

SJC: Synaptojanin1 construct

spH: SynaptopHluorin

SynJ1: Synaptojanin1

Syp: Synaptophysin

TαCP: cone transducin alpha promoter

TEM: transmission electron microscopy

Tg: transgenic

UPS: ubiquitin-proteasome system

YFP: yellow fluorescent protein

zf: zebrafish

Acknowledgments

This work would not have been possible if not for the combined efforts of many people. Sue Brockerhoff welcomed me in to her lab and provided the resources I needed to grow as a scientist. Jim Hurley provided valuable advice and input during joint lab meetings.

Luckily for me, the foundations for the *nrc*^{a14} project had been well established before I joined the lab. I owe a great debt to Lars Holzhausen for training me and then handing me the reins to his work on Synaptojanin. Alaron Lewis was a wonderful resource and roll model. George Stearns was there to help with zebrafish. Neil Wilson was there to help with cloning projects and keep me company in the lab. Amy Lassen was there to share my excitement in writing ImageJ macros. Eva Ma was always there to provide words of encouragement.

The Seattle Zebrafish community was incredibly welcoming and helpful. I would also like to thank members of the Hurley lab. The move to the South lake Union campus would have been much harder were it not for the hard work of Jonathon Linton. Jing Huang and Ed Parker in the Vision core were incredibly helpful and provided much needed technical assistance as well as great conversations.

Above all I would like to thank my family for all their support. My parents for always encouraging me in whatever I did. My husband for putting up my long work hours and helping me cope with the inevitable stressful days.

Dedication

To my Dad,

Thank you for everything.

Chapter 1

Introduction

The retina and photoreceptors

The vertebrate retina is made up of ordered layers of specialized neuronal cells (Figure 1.1A). At the back of the retina is a layer of pigmented cells, the retinal pigment epithelium (RPE). The pigment of these cells helps absorb scattered photons to improve image focus and prevent light-induced damage to the retina. In addition, these cells pass nutrients and ions from the bloodstream to the retina (Strauss, 2005). The RPE cells interact tightly with the next layer of cells, the photoreceptors. Photoreceptors are the main light detecting cells of the retina involved in image formation. After detecting changes in light, the photoreceptors signal to downstream neurons, the bipolar cells, which synapse onto ganglion cells. The ganglion cell axons then project into the brain. The signals in the retina are also modulated by inhibitory interneurons, horizontal cells and amacrine cells (Rodieck, 1973).

There are two main types of photoreceptors in the vertebrate retina; rods for dim light vision, and cones for bright light and color vision. Both rods and cones have similar cellular morphology. They consist of an outer segment (OS), inner segment (IS) and synaptic terminal (Figure 1.1B). The OS is the structure that gives rods and cones their names and is the site of photon detection (Sung and Chuang, 2010). Both rod and cone OSs consist of stacks of membranous discs. Rod OSs are rod shaped and the discs are non-continuous with the cellular plasma membrane. In cones, the stacks of discs contact the plasma membrane and have an overall cone-shaped appearance. In both rods and cones, the function of the OS is to detect photons and transform the light energy into an electrical signal in a process known as phototransduction. In the absence of light, cyclic nucleotide gated (CNG) channels in the OS are constitutively open allowing cations to flow into the cell. This cation influx results in a depolarized membrane potential. Upon absorption of a photon, the net result of the

phototransduction cascade is the closing of the CNG channels, resulting in a hyperpolarization of the membrane (Yau and Hardie, 2009; Sung and Chuang, 2010).

At the opposite end of the photoreceptor cell is the synaptic terminal. The synaptic terminal responds to the changes in membrane potential caused by phototransduction by altering the release of the neurotransmitter glutamate, transforming the electrical signal into a chemical signal. In the dark, the depolarized membrane results in the influx of calcium from voltage-gated calcium channels at the synaptic terminal. In turn, the calcium triggers the fusion of synaptic vesicles with the plasma membrane releasing glutamate onto downstream bipolar cells. While photoreceptor synaptic terminals share many of the same proteins and mechanisms as conventional neurons, they contain specialized structures known as ribbon synapses (Figure 1.1.B) that are unique to sensory neurons (Vollrath et al., 1989; Ullrich and Südhof, 1994; Vollrath and Spiwoks-Becker, 1996; Prescott and Zenisek, 2005). Unlike conventional neurons, photoreceptors require the ability to respond to not just the presence and absence of light, but to changing light levels over a magnitude of up to 11 log units. Ribbon synapses allow photoreceptors to transmit small changes in light intensity to the downstream neurons and maintain tonic release of neurotransmitter in the dark (Sterling and Matthews, 2005).

The inner segment of photoreceptors contains the cellular machinery for generating energy and synthesizing proteins. Photoreceptors are energetically demanding cells and contain many mitochondria in their IS at the base of the OS (Figure 1.1B). In addition to energy, proteins are synthesized and modified in the IS. These proteins must be properly sorted and trafficked to their correct subcellular destination (Papermaster et al., 1985; Papermaster et al., 1986; Schmied and Holtzman, 1989). Proper synthesis, sorting and trafficking of proteins destined for the OS, including the phototransduction machinery, is a vital process for proper photoreceptor health and function. Dysfunctional protein folding, sorting and trafficking is linked to multiple photoreceptor degenerative diseases (Ramamurthy and Cayouette, 2009). Because OSs require a constant supply of new proteins and membranes to maintain proper phototransduction, the bulk of protein trafficking studies in photoreceptors have focused

on OS protein trafficking. The proteins trafficked to the OS do not need to return to the IS to be degraded; RPE cells phagocytose OS discs from the tip of the OS in a circadian fashion (O'Day and Young, 1978). In contrast to OS protein trafficking, little is known about the processes involved in the trafficking of synaptic proteins between the inner segment and the synapse. Like the OS, the synaptic terminal is a site of large amounts of membrane trafficking. After synaptic vesicles fuse with the plasma membrane to release glutamate, the membranes and proteins must be retrieved via endocytosis. The cell must properly remove synaptic vesicle proteins from the plasma membrane, and sort them for recycling or degradation. However, unlike OS proteins, synaptic proteins must be turned over and degraded by the photoreceptors themselves.

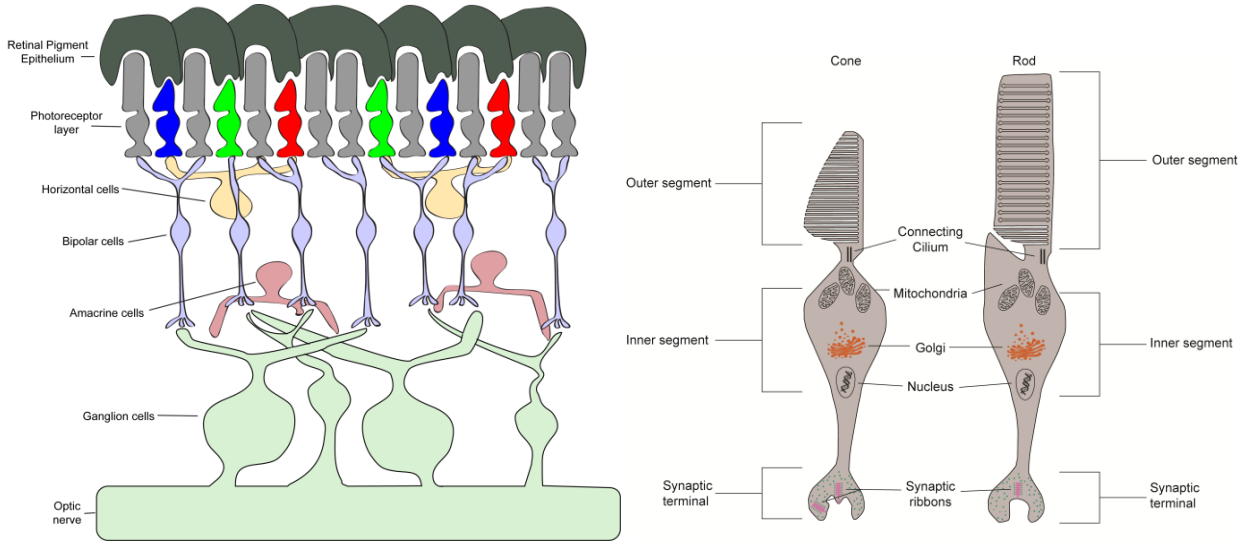

Figure 1.1 Schematics of the vertebrate retina and photoreceptors

The vertebrate retina is composed of layers of specialized cells. At the back of the retina is the retinal pigment epithelium (RPE) followed by the photoreceptor layer. Next are the bipolar cells then the ganglion cells. Signals between neurons are modulated by inhibitory interneurons. Horizontal cells modulate the signals between photoreceptors and bipolar cells, and amacrine cells modulate signals between bipolar and ganglion cells. Both rod and cone photoreceptors are highly polarized cells. They have an outer segment (OS) composed of membranous discs, an inner segment (IS) that contains the mitochondria and other organelles, and a synaptic terminal.

Zebrafish as a model organism to study the retina

Because the retina is a complex tissue, it is difficult to study without an animal model. Early work on the retina employed the mouse as the main model organism. Recently the zebrafish, *Danio rerio*, has emerged as a valuable tool for studying retinal biology (Branchek, 1984; Branchek and Bremiller, 1984; Brockerhoff et al., 1995; Easter and Nicola, 1996; Morris and Fadool, 2005; Muto et al., 2005; Fadool and Dowling, 2008). The zebrafish is a useful laboratory tool; it can easily be lab-reared, develops rapidly *ex vivo*, is transparent during the early developmental stages allowing for microscopic observations and has a fully sequenced genome to allow for genetic studies and manipulations (Westerfield, 1995). In addition to these advantages, the zebrafish retina develops quickly. By 55 hours post fertilization (hpf) photoreceptors have begun forming OSs. At 4 days post fertilization (dpf) the zebrafish larval retina has all of the layers and connections found in the typical vertebrate retina (Schmitt and Dowling, 1999). By this developmental time point it is also possible to observe robust vision-mediated behaviors, allowing for high-throughput screening of mutations that affect vision (Brockerhoff et al., 1995). The rapid development of the zebrafish retina and visual behaviors also makes it possible to study mutations that cause early lethality. In contrast to the nocturnal mouse, the larval zebrafish is diurnal and has a cone dominated retina. This makes the zebrafish a particularly useful tool for studying cone-mediated vision, which is responsible for the daytime and color vision possessed by humans.

Protein homeostasis

The ability to maintain a balance between the synthesis of new proteins and the degradation of old proteins is critical for all cell types. Dysfunction in protein homeostasis can result in proteotoxicity and, if not corrected, cell death (Goldberg, 2003). Neuronal cell types are particularly susceptible to misregulated protein turnover. Because they are post-mitotic, they cannot dilute old and damaged proteins through cell division. In addition, due to their polarized and elongated morphology, neuronal cell types must often traffic proteins long distances to reach the site(s) of protein degradation. These factors contribute to the observation that diseases affecting protein

folding, trafficking or degradation often result in very pronounced neuronal phenotypes, even when the affected protein is ubiquitously expressed (for recent reviews see (Martin et al., 2014; Tanaka and Matsuda, 2014; Vidal et al., 2014)).

Cells have two main pathways for the degradation of proteins; the ubiquitin-proteasome system (UPS) and the lysosomal system. The ubiquitin-proteasome system is involved the degradation of newly synthesized proteins and acts a source of quality control. Unfolded or misfolded proteins are targeted to the proteasome before they can aggregate. The UPS is capable of turning over proteins in a very short timeframe which allows the tight control of the levels of signaling proteins within cells (Goldberg, 2003; Tai and Schuman, 2008).

The second route to protein degradation in the cell is through the endolysosomal system (Stack et al., 1995). Proteins in or on membranes are removed from the membrane by pinching off vesicles. If this vesicle is budding form the plasma membrane, this process is known as endocytosis. The resulting vesicle undergoes fission, fusion and maturation processes to determine the fate of the proteins and membranes it contains. The proteins destined for degradation are first sorted within early endosomes. Subdomains of early endosomes that contain the components destined for degradation mature into multivesicular bodies and then travel to late endosomes. The late endosomes then fuse with the lysosome where a low pH environment and various hydrolytic enzymes degrade the macromolecular contents (Goldberg, 2003).

Proteins, as well as other macromolecules and even organelles, can be delivered to the lysosome using a process known as macroautophagy (Gordon and Seglen, 1988; Seglen et al., 1996; Meijer and Codogno, 2004). Macroautophagy occurs in response to cellular stresses such as starvation with the intent of supplying nutrients to the cell by degrading and recycling the cell's own contents. Even in the absence of stress such as starvation, macroautophagy is an important process and serves as a quality control mechanism (Mizushima, 2005). During the process of macroautophagy a double membrane structure known as a phagophore begins to form in the cytoplasm. There is still some mystery surrounding the origin of the phagophore membrane; however recent

studies have found that many different organelles including the endoplasmic reticulum (ER) (Axe et al., 2008), Golgi (Mari et al., 2010), recycling endosomes (Puri et al., 2013) and the plasma membrane (Ravikumar et al., 2010) supply membrane precursors for phagophore formation. The phagophore continues to elongate and engulfs cytoplasmic components. Finally, the phagophore closes resulting in a double-membrane structure known as an autophagosome. The autophagosome does not possess the proper machinery to break down its contents on its own; it must fuse with the lysosome in order to hydrolyze the materials it contains. In order to reach the lysosome, the autophagosome travels along microtubules. Once it has reached the lysosome, the autophagosome fuses with the lysosome, becoming an autolysosome. In mammalian cell types, the autophagosome can also fuse with other endosomal compartments, becoming an amphisome, before fusing with the lysosome (Shen and Mizushima, 2014). After the contents of the autolysosome have been degraded, the molecules are released back into the cytoplasm, supplying the cell with new substrates for energy and macromolecule synthesis (Klionsky, 2007). The autolysosome undergoes a process known as autophagic lysosome reformation to recreate the lysosome(s) and maintain lysosome homeostasis in the cell (Shen and Mizushima, 2014).

While much has been uncovered about the molecules and mechanisms involved in macroautophagy, many of these studies used yeast or cell culture as a model. More recent studies have begun to analyze the roles and mechanisms of macroautophagy in neuronal cell types. These studies have shown that basal levels of macroautophagy are important in neuronal development and maintenance, and may play a protective role in neurodegenerative diseases (Damme et al., 2014). Even less is known about the regulation and roles of macroautophagy in the retina and how it contributes to normal retinal function and pathology.

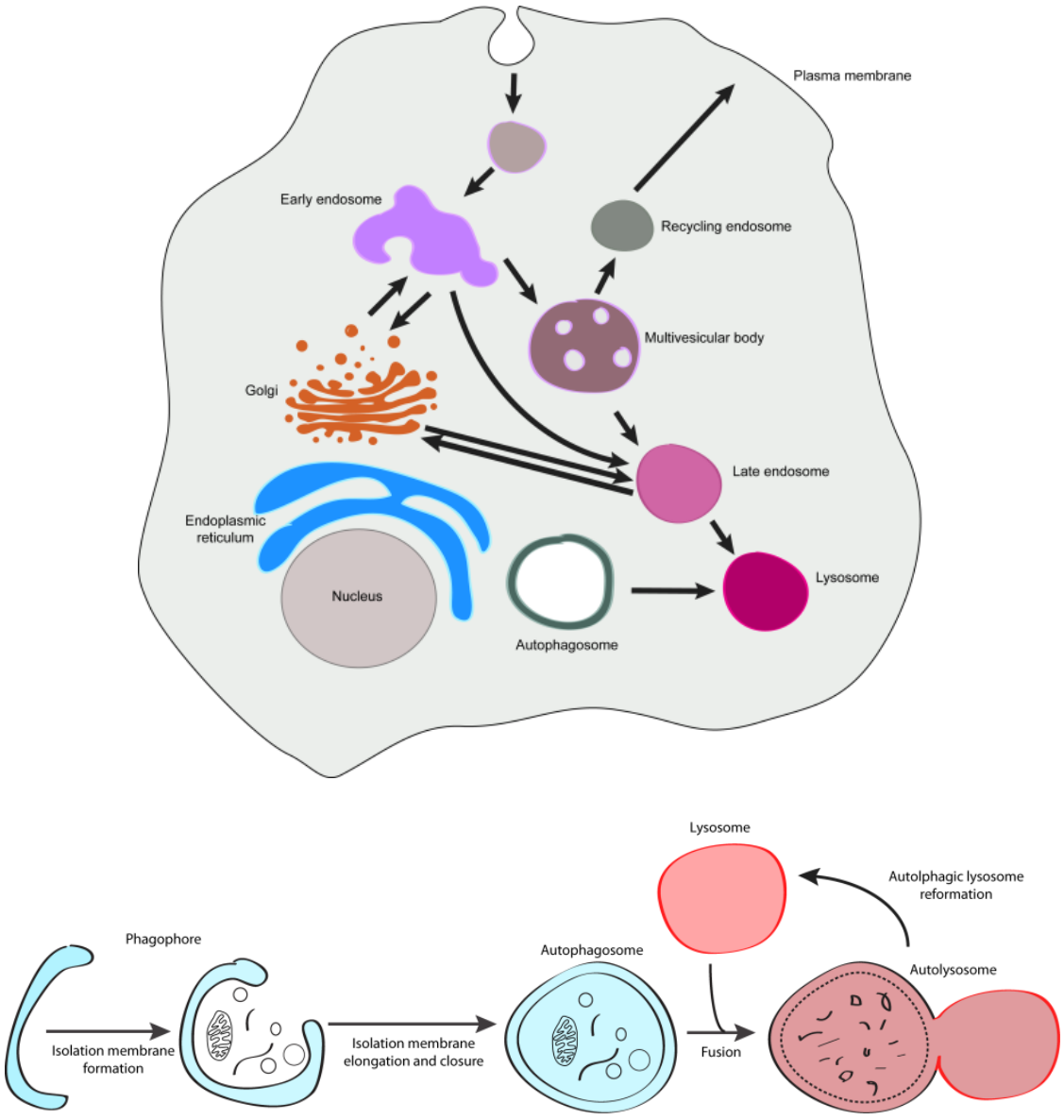

Figure 1.2: The endolysosomal system and autophagic pathway

Schematic drawing of the organelles in the endolysosomal pathway. Proteins can reach the lysosome for degradation via endocytosis or autophagy. After endocytosis, membranes and proteins are sorted in early endosomes and either recycled back to the plasma membrane via recycling endosomes, or sent to the lysosome via multivesicular bodies and late endosomes. Upon induction of macroautophagy, a phagophore begins to form in the cytoplasm. Cytosolic proteins, aggregates and organelles can be engulfed by the forming phagophore to form an autophagosome. The autophagosome fuses with endosomal compartments to begin degradation of its contents. The autophagosome (or amphisome if it has fused with an endosomal compartment) ultimately fuses with the lysosome to complete the degradative process. Finally, the degraded macromolecules will be released from the autolysosome, and the lysosome will be regenerated.

The *nrc^{a14}* zebrafish has a mutation in a polyphosphoinositide phosphatase

The zebrafish visual mutant *nrc^{a14} (no optokinetic response c)* was identified in a large scale mutagenesis screen for zebrafish larvae with visual defects. Upon characterization, the *nrc^{a14}*zebrafish was found to have an abnormal electroretinogram that indicated that while phototransduction did occur in the photoreceptors, the downstream neurons did not properly respond. Histological examination of the *nrc^{a14}* retina showed that the overall morphology of the retina was normal, with all the correct cellular layers. However; closer inspection of the photoreceptor layer showed that the synaptic layer, also known as the outer plexiform layer, was disordered. Ultrastructural studies showed that the cone synapses had an altered morphology, abnormal floating ribbon synapses, a decrease in synaptic vesicle number and a clustering of synaptic vesicles (Allwardt et al., 2001; Van Epps et al., 2001).

Chromosome mapping was performed to identify the causative mutation in the *nrc*^{a14} zebrafish, and the mutation was found to reside within the *synj1* gene (Van Epps et al., 2004). The *synj1* gene encodes the polyphosphoinositide phosphatase Synaptojanin1 (SynJ1). SynJ1 is composed of two lipid phosphatase domains, an N-terminal Sac1 domain, followed by a 5'phosphatase domain. The C-terminus of SynJ1 is involved in protein-protein interactions (McPherson et al., 1994a; de Heuvel et al., 1997; Ringstad et al., 1997; Cestra et al., 1999). The causative mutation in the *nrc^{a14}* zebrafish is a c→t point mutation that results in a premature stop codon after the Sac1 domain. Although a premature stop codon could result in a truncated protein, no truncated SynJ1 protein is detected in *nrc*^{a14} mutants (Van Epps et al., 2004; Holzhausen et al., 2009). The two enzymatic domains of SynJ1 act on phosphoinositides.

Phosphoinositides (PIPs) are glycerophospholipids with an inositol head group. The inositol ring can be reversibly mono-, di-, or tri-phosphorylated at the 3, 4 or 5' position of the ring, generating seven different PIP species. PIPs are found on the cytosolic face of membranes and account for only a small fraction of the total cellular phospholipid content. Despite their low abundance, PIPs are key mediators in a variety of cellular processes including cytoskeletal remodeling, cell signaling and many membrane

trafficking pathways. The different PIP species can be interconverted by many different kinases and phosphatases, giving cells high spatial and temporal control of PIP levels (De Camilli et al., 1996; Cremona et al., 1999; Odorizzi et al., 2000).

One of the roles of PIPs in cells is to impart membrane identity to different subcellular compartments. Different PIP species are asymmetrically distributed in different membranes. The most abundant PIP, PI(4,5)P_2, is found primarily on the plasma membrane. Membranes of the Golgi apparatus contain PI(4)P (Godi et al., 2004; D'Angelo et al., 2008). PI(3)P is localized to endosomes and autophagosomes (Gillooly et al., 2000). As endosomes mature into late endosomes they begin to acquire PI(3,5)P_2, which is also found on lysosomes (Dove et al., 2009). PI(3,4,5)P_3 is synthesized transiently at the plasma membrane in response to extracellular signals such as growth factors and cytokines, and results in downstream signaling cascades (Jackson et al., 1995; Heo et al., 2006). PI(3,4)P_2 is present in small amounts in the plasma membrane and has been shown to play a role in clathrin-mediated endocytosis (Posor et al., 2013). Finally, PI(5)P has been found in many different membranes including the nucleus (Gozani, 2003), plasma membrane, Golgi, ER (Sarkes and Rameh, 2010) and autophagosomes (Vicinanza et al., 2015). Because of their differential distributions, PIPs are able to recruit specific effector proteins to specific membrane compartments. For example, PI(4,5)P_2 in the plasma membrane interacts with the clathrin adapter AP-2. The recruitment of AP-2 ultimately leads to clathrin-mediated endocytosis from the plasma membrane. After endocytosis, PI(4,5)P_2 is removed from the newly formed endosome and converted to PI(3)P through the sequential action of phosphatases and kinases. With its newly acquired PI(3)P, the endocytosed membrane is able to interact with specific effector proteins required for endosome function (Gaidarov and Keen, 1999; Shin, 2005; Di Paolo and De Camilli, 2006).

SynJ1 contains two PIP phosphatase domains. The Sac1 domain can hydrolyze phosphates at various positions on the inositol head group and has been found to dephosphorylate PI(3)P, PI(4)P and PI(3,5)P_2 to phosphatidylinositol (PI) *in vitro*. The 5'phospatase domain is more specific and only removes phosphate from the 5'position

of the inositol head group (Guo et al., 1999). With both these domains, SynJ1 could potentially be involved in regulating the levels of many different PIPs.

SynJ1 protein is highly conserved and is involved in synaptic vesicle recycling

The SynJ1 protein is highly conserved in eukaryotes. The yeast *Saccharomyces cerevisiae* expresses three Synaptojanin-like proteins (SJLs) that have both overlapping and distinct roles in this organism. These roles include cytoskeletal remodeling, cell wall integrity and endosome-to-Golgi membrane trafficking (Stolz et al., 1998; Stefan et al., 2002; Ha et al., 2003). SynJ1 has also been investigated in invertebrates; mutations in the *Caenorhabditis elegans synj1* gene (*unc-26*) result in defects in synaptic transmission. The synaptic terminals from *unc-26* worms appear pale in electron microscopy images due to a decreased number of synaptic vesicles. The synaptic vesicles that are present at synaptic terminals have clathrin coats and many appear as "beads on a string" rather than a uniform distribution (Harris et al., 2000). In another invertebrate, the fruit fly *Drosophila melanogaster*, *synj1* mutants show reduced synaptic function (Verstreken et al., 2003).

Synaptojanin1 was first described in 1994 as p145, a phosphorylated protein in rat neurons (McPherson et al., 1994b; McPherson et al., 1994a). In later studies, p145 was found to localize to synaptic terminals and exhibited 5'phosphatase enzymatic activity (McPherson et al., 1996). Later, using a *synj1* mouse knockout, it was demonstrated that the role of SynJ1 at synaptic terminals was to dephosphorylate $PI(4,5)P_2$ during clathrin-mediated endocytosis in synaptic vesicle recycling. By removing the phosphates of $PI(4,5)P_2$, SynJ1 allows the clathrin coated vesicles to lose their coat and be recycled. In the absence on SynJ1, the clathrin coat is unable to disassociate, resulting in an accumulation of clathrin coated vesicles and a decrease in the pool of synaptic vesicles. Studies in cell culture found that SynJ1 also played a similar role in clathrin-mediated endocytosis in non-neuronal cells (Ramjaun and McPherson, 1996).

SynJ1 and human disease

An absence of SynJ1 protein is lethal in all the previously discussed organisms indicating the importance of SynJ1 protein for organism viability. It is therefore

unsurprising that, until very recently, there have been few human diseases linked to the *synj1* gene. Until recently, the best characterized role of SynJ1 in a human disease has been in Down's syndrome. In humans, the *synj1* gene is found on chromosome 21, the most common trisomy in Down's syndrome (Patterson, 2009). Some of the neuronal phenotypes observed in Down's syndrome mouse models can be reproduced by overexpressing SynJ1 in otherwise wild-type mice. Conversely, the neuronal defects in mouse models of Down's syndrome can be rescued by reducing SynJ1 expression (Voronov et al., 2008). Both human patients and mouse models with Down's syndrome exhibit early neuropathological symptoms of Alzheimer's disease (Patterson, 2009). Studies from multiple groups have now shown a link between SynJ1 and Alzheimer's disease (Cossec et al., 2012; McIntire et al., 2012; Zhu et al., 2013). Recently, multiple patients have been identified with loss-of-function SynJ1 mutations. Four families with the same homozygous missense mutation in the Sac1 domain of SynJ1 have been described. The affected members have been found to suffer from seizures and early onset Parkinsonism symptoms (Krebs et al., 2013; Quadri et al., 2013). In addition, a young patient was identified with a homozygous nonsense mutation in *synj1* resulting in an almost complete absence of the protein. This patient suffered from seizures starting shortly after birth, followed by a progressive neurodegeneration until death at 6 years of age. Post-mortem histological examination of this patient's brain showed an accumulation of tau protein in the substantia nigra region of the brain (Dyment et al., 2014). These recent findings suggest that findings in the zebrafish *nrc*^{a14} mutant will be applicable to understanding human disease. Interestingly, all of the neurodegenerative phenotypes associated with altered levels or function of SynJ1 have connections to defects in protein homeostasis. This observation suggests that SynJ1 may play a yet uncharacterized role in protein degradation in addition to its role in clathrin-mediated endocytosis in neurons.

Chapter 2

Synaptojanin1 is required for endolysosomal trafficking of synaptic proteins in cone photoreceptor inner segments

Introduction

Photoreceptors are highly specialized, polarized, light-sensitive cells in the retina. The apical end of the cell, the outer segment (OS), consists of stacked discs of membranes, which are the site of phototransduction. At the opposite end of the cell is the synaptic terminal, which is the site of neurotransmitter release. The inner segment (IS) of the cell is located between the OS and cell nucleus, and contains the cellular machinery required for production of energy and cellular components (Kolb, 2003; Kennedy and Malicki, 2009). Due to their highly polarized structure, photoreceptors must be able to properly sort and transport proteins made in the IS to opposite ends of the cell. The cell must also have mechanisms of removing damaged proteins that have reached their correct subcellular locations. In the case of OS proteins, damaged proteins are removed apically when discs are shed (Young, 1967). Because altered OS trafficking often results in photoreceptor degeneration, studies of protein trafficking in photoreceptors have focused mainly on trafficking of proteins from the Golgi in the IS to the OS (Ramamurthy and Cayouette, 2009; Sung and Chuang, 2010). In contrast, little is known about the mechanisms used to sort and traffic proteins to the photoreceptor synapse, as well as the recycling and degradation of these proteins.

The zebrafish visual mutant *no optokinetic response c (nrc^{a14})* was identified in a mutagenesis screen (Allwardt et al., 2001). The synaptic terminals of *nrc^{a14}* cone photoreceptors have a flattened morphology, decreased number of synaptic vesicles, and unanchored synaptic ribbons (Allwardt et al., 2001; Van Epps et al., 2001; Van Epps et al., 2004; Holzhausen et al., 2009). The causative mutation was determined to be in the gene *synJ1*, resulting in the loss of Synaptojanin1 (SynJ1) protein (Van Epps et al., 2004). SynJ1 is a polyphosphoinositide phosphatase with an established role in synaptic vesicle recycling. In conventional neurons, SynJ1 is concentrated at presynaptic terminals, where it is involved in the hydrolysis of phosphatidylinositol 4,5-

bisphosphate ($PI(4,5)P_2$) and the uncoating of clathrin-coated vesicles (Cremona et al., 1999). Interestingly, there is not an accumulation of clathrin coated vesicles in *nrc*^{a14} cone photoreceptor terminals, suggesting a unique role for SynJ1 at ribbon synapses (Allwardt et al., 2001; Van Epps et al., 2004). SynJ1 is also present in the cell body and dendrites of neurons (McPherson et al., 1994a; McPherson et al., 1996). While SynJ1 has been found to play a role in regulating endocytosis of AMPA receptors postsynaptically in dendrites(Gong and De Camilli, 2008), its function in the cell body of neurons has been less well studied. A recent study found that abnormal endosomal structures accumulate in the cell bodies of neurons from mice overexpressing SynJ1, suggesting that the functional role of SynJ1 is not exclusive to synaptic terminals (Cossec et al., 2012).

We have previously shown that SynJ1 protein is present in the IS of cone photoreceptors in both adult and larval wild type (WT) zebrafish. This previous study also demonstrated that the synaptic protein VAMP2 localizes to the IS of *nrc*^{a14}, but not WT, cone photoreceptors (Holzhausen et al., 2009). Together, these initial results suggested that SynJ1 also has important functions in the IS of zebrafish cone photoreceptors. In this study, we characterized the IS and trafficking defects associated with the loss of SynJ1. We report that the OSs and connecting cilia of *nrc*^{a14} cone photoreceptors are morphologically normal. In contrast, select synaptic proteins and large vesicular structures accumulate in ISs. To dissect the cause of this accumulation, we analyzed markers for biosynthetic and degradative trafficking pathways. Whereas trafficking pathways for newly-synthesized proteins were not severely affected, there was an aberrant distribution and accumulation of acidic vesicles, late endosomes, and autophagosomes. Our findings show a segregation of apical and basal trafficking pathways in cones, and uncover the important role of SynJ1 in trafficking of synaptic proteins that depend on endolysosomal trafficking pathways. Together these results support the hypothesis that SynJ1 is required for proper membrane and protein trafficking at both the synapse and IS.

Results

Loss of SynJ1 does not affect cone photoreceptor connecting cilia or outer segments

Defects in trafficking of proteins to the OS results in morphologically abnormal OSs and often leads to photoreceptor degeneration (Insinna and Besharse, 2008; Wright et al., 2010). To identify possible apical trafficking defects in *nrc*^{a14} mutants, we performed transmission electron microscopy (TEM) on *nrc*^{a14} mutant larvae and their WT siblings at 5 days post fertilization (5dpf), and examined the morphology of the apical ends of their cone photoreceptors. At this age, WT larvae have robust visual responses that can be measured by optokinetic response (OKR) assays and electroretinogram recordings (Branchek, 1984; Brockerhoff et al., 1995; Easter and Nicola, 1996), and *nrc*^{a14} behavioral and synaptic phenotypes are apparent (Allwardt et al., 2001; Van Epps et al., 2001; Van Epps et al., 2004; Holzhausen et al., 2009). TEM images demonstrated that the OSs of *nrc*^{a14} cone photoreceptors appeared indistinguishable from their WT siblings. The OSs of both WT and *nrc*^{a14} cone photoreceptors consist of characteristic, neatly-stacked membranes (Figure 2.1 A, B). The OSs of *nrc*^{a14} cone photoreceptors also showed no differences in length compared to WT cone OSs (Figure 2.1 G; n=100 cells from 4 larvae for both WT and *nrc*^{a14}). These data suggest that protein transport to the OS proceeds normally in the absence of SynJ1.

As further verification of normal apical transport, we examined the structure of the connecting cilia (CC), a microtubule-based structure that connects the inner and outer segments. OS proteins are synthesized in the IS and transported through the CC (Ramamurthy and Cayouette, 2009). We examined the CC using immunohistochemical staining against two components, acetylated tubulin (Tsujikawa and Malicki, 2004) and IFT88 (Krock and Perkins, 2008). Acetylated tubulin is a structural component of the CC, while IFT88 is a component of the intraflagellar transport complex and is required for the formation and maintenance of OSs. Confocal images of either marker showed the presence of CC within both WT and *nrc*^{a14} photoreceptors (Figure 2.1 C-F). No difference was detected in the number of CC structures in WT and *nrc*^{a14} cone photoreceptors with either acetylated tubulin or IFT88 (Figure 2.1 I, J; n=264-502 cells

from 4-5 larvae). Because acetylated tubulin is found along the entire length of the CC, staining with this marker also allowed us to determine the length of CC in WT and *nrc*^{a14} cone photoreceptors. We observed no difference in length of CC structures in WT and *nrc*^{a14} cone photoreceptors (Figure 2.1 E, F, H; n=176-214 CC from 4-5 larvae). These results demonstrate that SynJ1 is not required for proper trafficking of proteins to the CC or the OSs of cone photoreceptors.

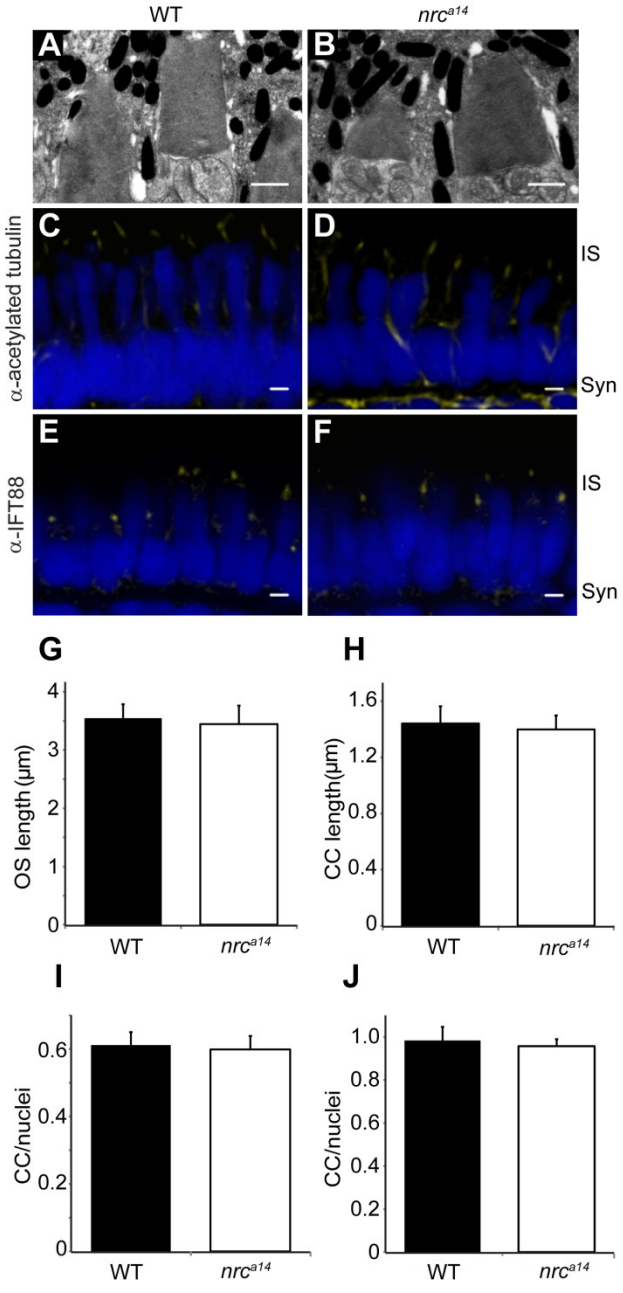

Figure 2.1: *nrc^{a14}* cone photoreceptors have normal outer segments and connecting cilia. (A-B) TEM images of 5dpf WT (A) and *nrc^{a14}* (B) cone photoreceptor OSs. There was no difference in OS appearance or length (G) between *nrc^{a14}* and WT cone photoreceptors at 5dpf (p=0.7). (C-F) Confocal images of 5dpf zebrafish larval retinas immunostained using antibodies against the CC proteins acetylated tubulin (C, D) or IFT88 (E, F). The number (I) and length (H) of acetylated tubulin stained CC was not significantly different between WT and *nrc^{a14}* photoreceptors (p=0.9 and 0.4 respectively). There was no significant difference (p =0.7) in the number of IFT88 stained cilia between WT and *nrc^{a14}* (J). Antibody staining is shown in yellow; nuclei were stained with Sytox Green (D, E) or Hoechst (G, H) and are shown in blue. Syn=photoreceptor synapses, IS= inner segment. Scale bar=1μm in A and B and 2μm in C-F. Graphs show mean values, error bars are STDEV for multiple larvae.

Loss of SynJ1 results in mislocalized synaptic proteins in cone photoreceptors

Our previous studies focused on characterizing synaptic terminals of *nrc^{a14}* cone photoreceptors (Allwardt et al., 2001; Van Epps et al., 2001; Van Epps et al., 2004; Holzhausen et al., 2009). We previously generated the transgenic fish strain *Tg(TαCP:spH)*, which expresses synaptopHluorin (spH) specifically in cone photoreceptors using the transducin alpha cone (TαCP) promoter (Kennedy et al., 2007). SpH is a fusion of a pH-sensitive GFP and the synaptic vesicle SNARE protein VAMP2/synaptobrevin (Miesenbock et al., 1998). In WT larvae, spH localized to synaptic vesicles in cone synaptic terminals, whereas in *nrc^{a14}* mutants, spH accumulated in the ISs and synaptic terminals (Holzhausen et al., 2009); Figure 2.2 B, E). To determine whether other synaptic proteins are mislocalized in *nrc^{a14}* photoreceptors, we examined the distribution of two other proteins, RibeyeB and Synaptophysin. RibeyeB is an active zone protein and a component of the synaptic ribbon in zebrafish cone photoreceptors (Wan et al., 2005). The distribution of endogenous RibeyeB was investigated by immunolabeling of retinal slices of 5dpf *Tg(TαCP:spH)* larvae (Figure 2.2 A, C, D, F). In WT retinas, RibeyeB was localized to photoreceptor synapses, consistent with previous reports (Wan et al., 2005); Figure 2.2 A). In contrast, RibeyeB staining was visible at both the synapses as well as the ISs of *nrc^{a14}* cone photoreceptors (Figure 2.2 D, F). Further, the mislocalized RibeyeB detected in *nrc^{a14}* ISs was coincident with the mislocalized spH (Figure 2.2 F). This mislocalization of endogenous RibeyeB was not due to overexpression of spH, as identical RibeyeB staining patterns were observed in both non-transgenic WT and *nrc^{a14}* cone photoreceptors (Figure 2.3).

Synaptophysin is a synaptic vesicle glycoprotein commonly used as a presynaptic marker (McPherson et al., 1994a; Meyer and Smith, 2006). To examine the distribution of Synaptophysin, we generated the transgenic fish line *Tg(TαCP:Syp-CFP)*, which expresses CFP- tagged zebrafish Synaptophysin in cone photoreceptors. At 5dpf, Synaptophysin-CFP was observed primarily at the synapse, but also in small amounts in the ISs of both WT and *nrc*^{a14} cone photoreceptors. There was no apparent difference in its distribution between *nrc*^{a14} and WT cone photoreceptors (Figure 2.2 G, H). The detection of Synaptophysin at both the synapse and the IS of WT photoreceptors is consistent with previous findings (Mazelova et al., 2009). This result indicates that not all synaptic proteins are mislocalized in *nrc*^{a14} cone photoreceptors, and suggests that there may be multiple pathways for trafficking synaptic proteins in cone photoreceptors, only some of which require SynJ1.

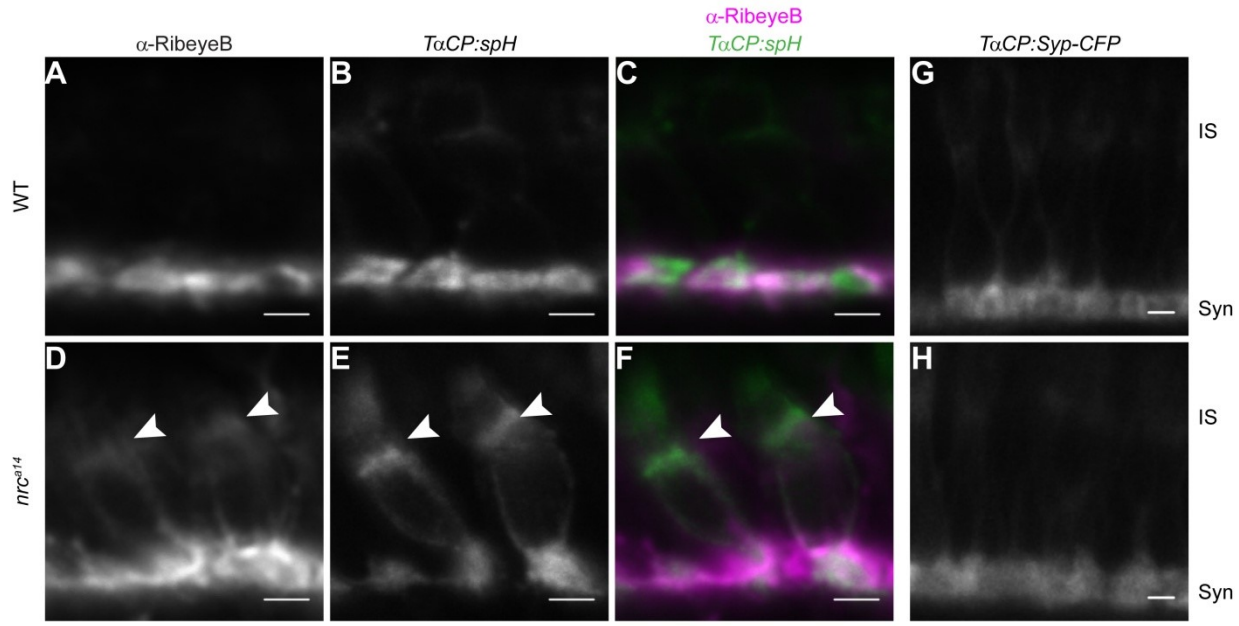

Figure 2.2: Some synaptic proteins are mislocalized in *nrc*^{a14} cone photoreceptors. *Tg(TαCP:spH)* WT and *nrc*^{a14} 5dpf retinal slices were stained with an antibody against the ribbon synapse protein RibeyeB (A-F). In WT photoreceptors, RibeyeB was found only at synaptic terminals (A). In *nrc*^{a14} cone photoreceptors, RibeyeB (D, arrowhead) and VAMP2 (E, arrowhead) were detected in both synaptic terminals and ISs. Mislocalized signals for RibeyeB (magenta) and VAMP2 (green) were coincident in the ISs of *nrc*^{a14} cone photoreceptors (F, arrowhead). In contrast, the synaptic vesicle protein Synaptophysin (Syp-CFP) had a primarily synaptic distribution in both WT (G) and *nrc*^{a14} (H) cone photoreceptors. Live confocal images were taken of 5dpf *Tg(TαCP:Syp-CFP)* WT and *nrc*^{a14} larvae. Syn=photoreceptor synapses, IS= inner segment. Scale bar=2μm.

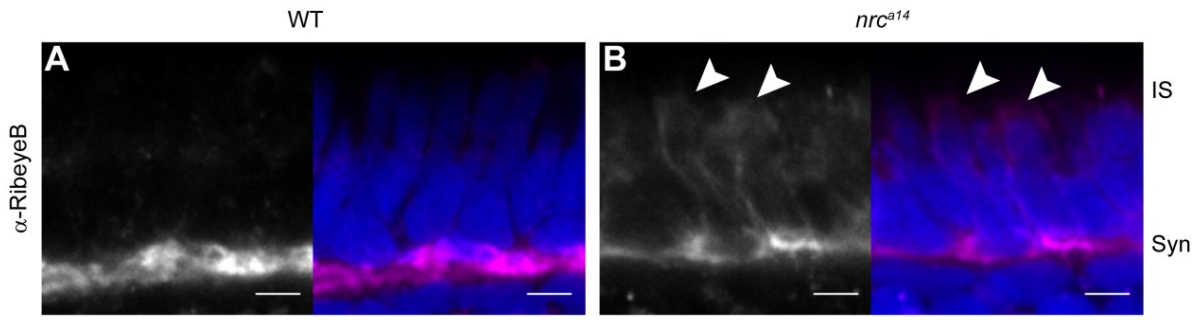

Figure 2.3: RibeyeB is mislocalized in *nrc^{a14}* inner segments even in the absence of *TαCP:spH*. Anti-RibeyeB staining of non-transgenic WT and *nrc^{a14}* 5dpf retinas showed the same staining pattern as *Tg(TαCP:spH)* 5dpf retinas in Figure 2.2. In WT photoreceptors, RibeyeB was found only at synaptic terminals (A, B). In *nrc^{a14}* cone photoreceptors, the RibeyeB staining was visible in both the synaptic terminals and ISs (C, D). Anti-RibeyeB staining is shown in magenta and Hoechst stained nuclei are in blue. Syn=photoreceptor synapses, IS= inner segment. Scale bar= 2μm in all images.

Large vesicular structures accumulate in *nrc^{a14}* inner segments

The presence of SynJ1 protein in the IS of WT cones and the presence of ectopic synaptic proteins in the IS of *nrc^{a14}* cones suggest that SynJ1 plays a functional role at the IS of cone photoreceptors. Therefore, we analyzed the morphology of the *nrc^{a14}* cone IS in 5dpf larvae in more detail using TEM. We made the surprising finding that the IS of *nrc^{a14}* cone photoreceptors contained large vesicular structures that were not often observed in WT cone photoreceptors (Figure 2.4). These structures were present in approximately 80% of *nrc^{a14}* cone photoreceptors and were variable in size, ranging from ~125 to 900 nm in diameter (n=547 cells from 4 *nrc^{a14}* larvae). While many of these structures were devoid of electron density, a few contained electron-dense material (Figure 2.4 E, arrowheads).

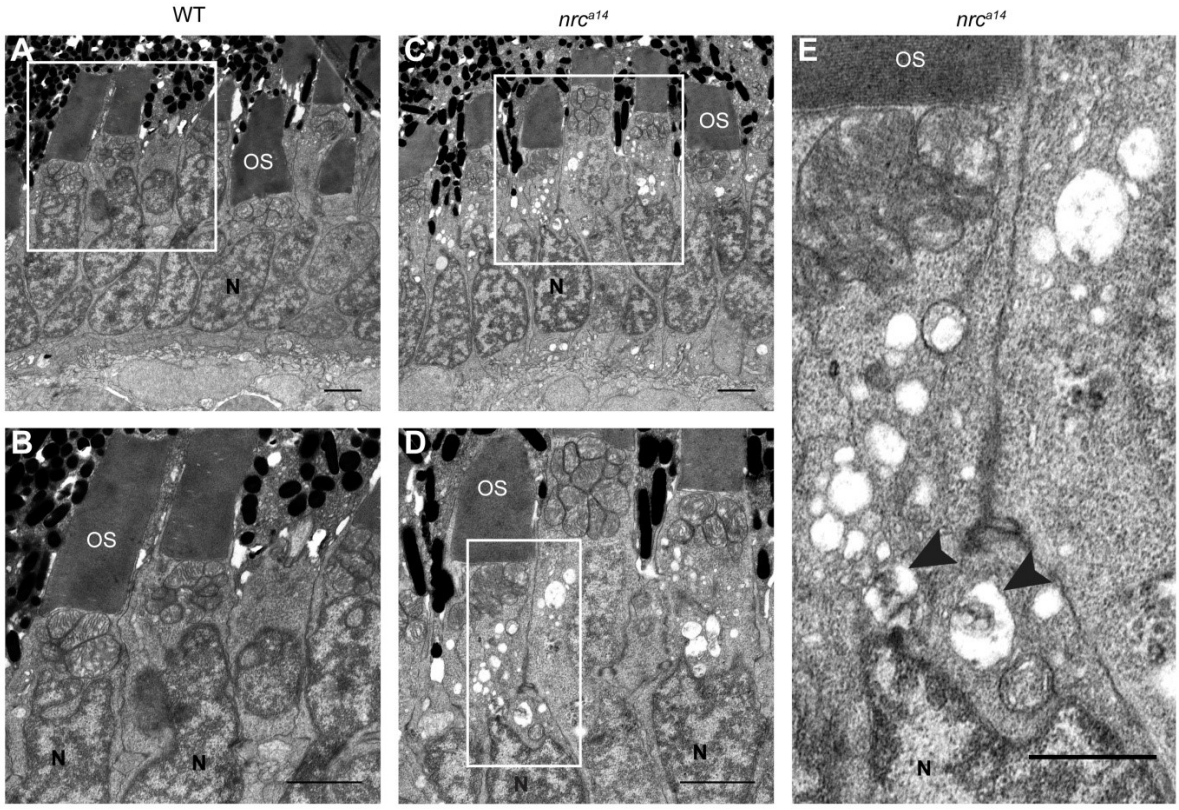

Figure 2.4: Large vesicular structures accumulate in *nrc^{a14}* photoreceptor inner segments. TEM images of cone photoreceptors in WT (A, B) and *nrc^{a14}* (C-E) 5dpf retinas. Large vesicular structures were visible in approximately 80% of *nrc^{a14}* cone photoreceptor ISs. Some vesicular structures contained electron dense material (arrow heads, E). Boxes in A and C show areas enlarged in B and D respectively. Box in D shows area enlarged in E. OS=outer segment, N=nuclei. Scale bar=2μm in A-D, 1μm in E.

Photoreceptors are depolarized in the dark and release glutamate from their synaptic terminals. Both vesicle trafficking to the synapse and recycling of synaptic vesicles would be expected to increase in the dark. Although *nrc^{a14}* photoreceptors show altered synaptic activity, they respond to light (Van Epps et al., 2001). Therefore, we hypothesized that *nrc^{a14}* photoreceptors should similarly modulate trafficking of synaptic proteins between the IS and the synaptic terminal in response to changing light conditions. Furthermore, previous work on zebrafish hair cells lacking SynJ1 has shown that the abnormal, blebbed synaptic morphology of these sensory neurons is dependent upon synaptic activity (Trapani et al., 2009). To investigate whether the IS phenotype of cone photoreceptors lacking SynJ1 was similarly dependent on synaptic activity, we incubated 4dpf WT and *nrc^{a14}* larvae in the dark for 24 hours prior to fixation

for TEM. As a control, light-adapted WT and *nrc*^{a14} sibling larvae were kept on a 14/10hr light/dark cycle for the same 24hr period.

In light-adapted (LA) WT retinas, the majority (80+/-2%) of cone photoreceptors contain "normal" ISs lacking large vesicular structures (Figure 2.5 A and E; n= 504 cells from 5 larvae in 3 independent trials). In contrast, the majority (77+/-3%) of LA *nrc*^{a14} photoreceptors were "vesiculated" and contained at least 3 large (>125nm) vesicular structures (Figure 2.5 B, arrowhead; n=406 cells from 5 larvae in 3 independent trials). We found that 24 hours of darkness caused a slight, but not significant, increase in the number of WT cells with at least 3 vesicular structures in the IS (Figure 2.5 E, ~20% to ~24%; n=508 cells from 5 larvae in 3 independent trials; p=0.2). In contrast, the effect of dark incubation on *nrc*^{a14} ISs produced a dramatic phenotype change (Figure 2.5 D, white arrow). While the total percentage of *nrc*^{a14} cones containing vesicular structures was not affected by dark adaptation, 6+/-3% of cells with aberrant vesicular structures in the IS showed large increases in vesicle number with a concomitant decrease in vesicle size (Figure 2.5 E; n=411 cells from 5 larvae in 3 independent trials). These "severely vesiculated" cells had over 20 vesicles in the IS per cell and was never observed in WT LA or dark-adapted (DA) larval retinas and was rarely seen in LA *nrc*^{a14} ISs (p =0.077 for LA vs. DA *nrc*^{a14}). These results suggest that SynJ1 is involved in trafficking pathways that are modulated during dark adaptation in cone photoreceptors.

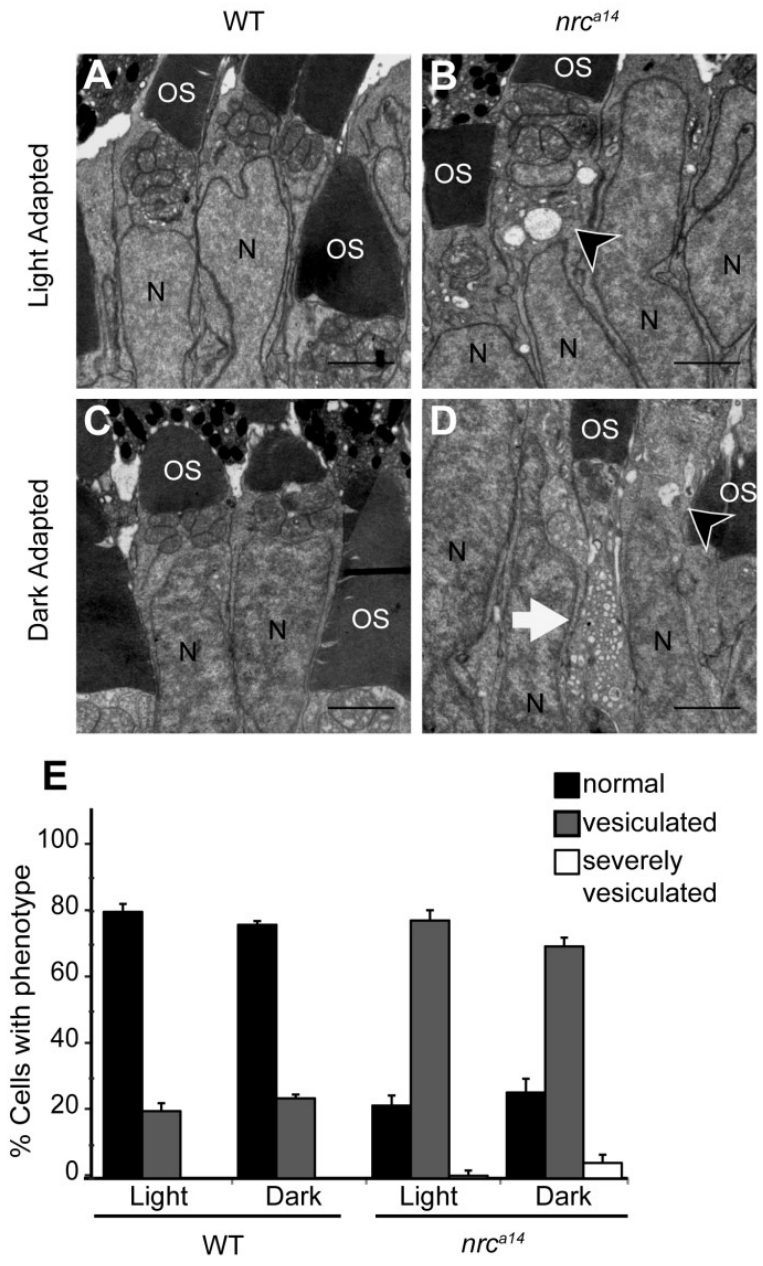

Figure 2.5: Dark adaptation increases the number of vesicular structures in *nrc*^{a14} photoreceptor inner segments. TEM images of cone photoreceptors in light (A, B) or dark-adapted (C, D) WT and *nrc*^{a14} retinas. At 4dpf, larvae were phenotyped by OKR and placed at 28°C either on a normal light/dark cycle, or in complete darkness. 24 hours later, at 5dpf, larvae were fixed for TEM. Dark adaptation exaggerated the vesicular structure phenotype in *nrc*^{a14} cone photoreceptor inner segments (B vs. D). Cells were scored as "normal", "vesiculated" or "severely vesiculated" and the quantification is shown in E. Cells with at least 3 vesicular structures >125nm were scored as "vesiculated" and examples are shown by arrow heads in B and D, cells that contained at least 20 vesicular structures were scored as "severely vesiculated" and an example is shown by an arrow in D. OS=outer segment, N=nuclei. Scale bar=2μm in A-D. Graph shows mean, error bars are STDEV for three independent light/dark experiments. In total at least 400-500 cells from 5 larvae were counted per light condition and genotype.

Nrc^{a14} cone photoreceptor inner segments have normal Endoplasmic Reticulum but acquire a disordered Golgi apparatus

Our experiments demonstrated that the trafficking pathway(s) affected in *nrc^{a14}* mutant cone photoreceptors involve the trafficking of synaptic proteins and can be modulated by changes in photoreceptor activity in the dark. The accumulation of synaptic proteins and vesicles in the IS could be due to either defects in trafficking of newly-synthesized proteins to the synapse, or in the recycling and/or degradation of these proteins. To dissect the trafficking pathways affected in the *nrc^{a14}* cone photoreceptors, we created constructs to express fluorescent markers targeted to various subcellular organelles. We first investigated the Endoplasmic Reticulum (ER) and the Golgi apparatus, which are both involved in the trafficking of newly-synthesized proteins. In addition, we examined the morphology of the Golgi apparatus at various developmental time points. We reasoned that a primary defect in trafficking newly synthesized proteins would result in Golgi disruption during photoreceptor cell differentiation, but prior to onset the of photoreceptor activity. However, if the primary defect is in pathways involved in protein recycling or degradation, we would see no disruption of the Golgi, or that Golgi disruption would occur as a secondary defect after the onset of photoreceptor synaptic activity.

To visualize the ER in cone photoreceptors, we used the ER-targeting sequence from the protein calreticulin (Roderick et al., 1997) to generate a transgenic fish line expressing ER-targeted GFP specifically in cone photoreceptors (*Tg(TαCP:ER-GFP)*). To visualize the morphology of the Golgi apparatus in cone photoreceptors, we generated the transgenic fish line *Tg(crx:Man2a-GFP)* which expresses GFP targeted to the medial Golgi. The *crx* promoter drives expression of the Golgi marker GFP in cones, rods, and bipolar cells at earlier time points in photoreceptor development than the *TαCP* promoter (Suzuki et al., 2013) . We confirmed that the marker Man2a-GFP resides in the Golgi by treating 3 dpf *Tg(crx:Man2a-GFP)* zebrafish larvae with Brefeldin A (BFA). BFA disrupts ER-to-Golgi trafficking and Golgi morphology, resulting in the redistribution of Golgi resident proteins to the ER (Deretic and Papermaster, 1991).

After BFA incubation, the Man2a-GFP signal dispersed to both the ER and fragmented structures distributed throughout the cell (Figure 2.6). This observation indicates that the Man2a-GFP fusion protein mimics the behavior of endogenous medial Golgi proteins.

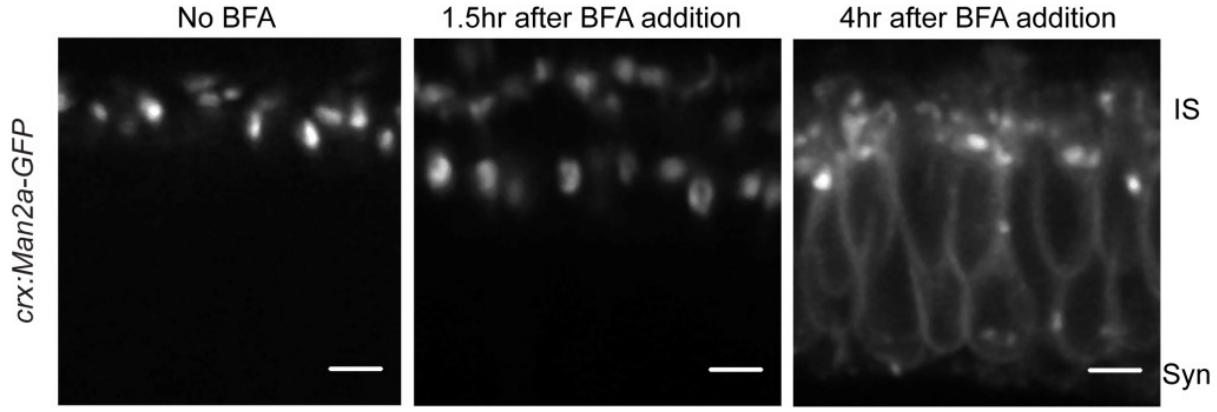

Figure 2.6: Man2a-GFP marks medial Golgi structures. We confirmed that our Golgi marker behaved in the same manner as endogenous Golgi proteins by treating 3dpf *Tg(crx:Man2a-GFP)* zebrafish larvae with 2μM Brefeldin A followed by live imaging. After a 4 hour incubation in BFA, the GFP signal was present in the ER and fragmented Golgi structures.

Confocal microscopy of retinal slices from 5dpf larvae demonstrated no gross differences in ER morphology between WT and *nrc*^{a14} cone photoreceptors (Figure 2.7 A, B), suggesting that the membranes observed in the TEM images (Figures 2.4 and 2.5) were not dilated or disordered ER. Next, we examined WT and *nrc*^{a14} retinas from *Tg(crx:Man2a-GFP)* larvae using confocal microscopy to evaluate Golgi morphology between 3dpf and 5dpf (Figure 2.7 C-H). WT photoreceptors contained rounded or elongated Golgi structures which were located in an ordered manner in the IS on top of the cell nuclei at every time point investigated (Figure 2.7 C, E, G). At 3dpf, Golgi structures in *nrc*^{a14} photoreceptors also appeared as rounded structures located at the apical side of the nucleus (Figure 2.7 D). At 4dpf a few disordered Golgi became visible in *nrc*^{a14} photoreceptors (Figure 2.7 F, arrowhead). By 5dpf the Golgi appear disordered and fragmented in *nrc*^{a14} cone photoreceptors (Figure 2.7 H, arrowheads). We also examined the fish line *Tg(TαCP:Man2a-GFP)* (data not shown) which expresses the Golgi marker in only cone photoreceptors and observed similar disordered Golgi structures. Therefore we can conclude that the disordered structures

we see are present within cone photoreceptors. These data suggest that SynJ1 is not required for the development of the Golgi apparatus in *nrc*^{a14} cone photoreceptors, but is required for the maintenance of Golgi structures after 3dpf.

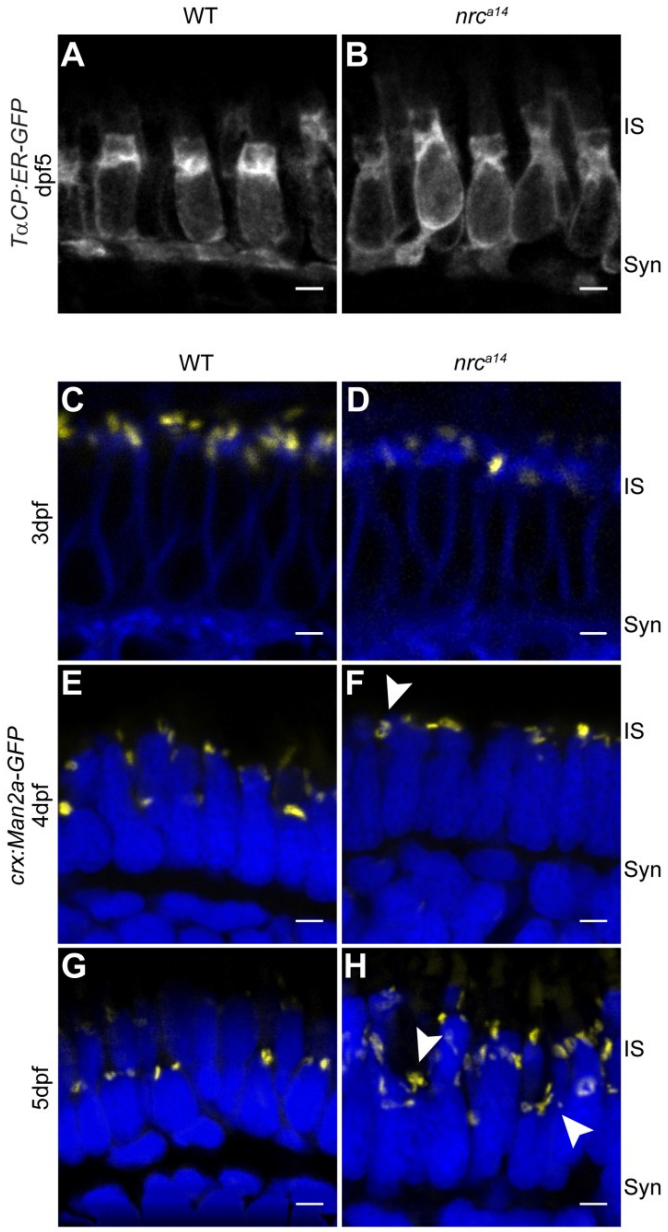

Figure 2.7: SynJ1 is required for Golgi maintenance but not development. The transgenic fish line *Tg(TαCP:ER-GFP)* was used to mark the ER. Retinal slices from 5dpf WT (A) and *nrc*^{a14} (B) larvae showed that the overall ER morphology was unaltered in the absence of SynJ1. Confocal images of *Tg(crx:Man2a-GFP)* WT (C, E, G) or *nrc*^{a14} (D, F, H) larvae retina at 3-5dpf showed that the Golgi is normal during photoreceptor development, but develops abnormalities disordered after cones become functional. No apparent abnormalities were seen

in Golgi morphology of *nrc*^{a14} compared to WT photoreceptors at 3dpf (compare C and D). At 4dpf, some mild morphology changes appeared in *nrc*^{a14} Golgi (F, arrowhead). At 5dpf, fragmented Golgi were visible in *nrc*^{a14} photoreceptors (H, arrowheads). Man2a-GFP signal is shown in yellow, membranes of 3dpf larvae were stained with BODIPY-TR and are shown in blue, and nuclei were stained with Hoechst and are shown in blue for 4dpf and 5dpf images. Syn=photoreceptor synapses, IS= inner segment. Scale bar=2μm in all images.

We had initially hypothesized that the vesicular structures observed in TEM images of *nrc*^{a14} photoreceptors could be disordered Golgi membranes. However, our confocal data (Figure 2.7) suggested that the vesicular structures observed in the TEM images were not derived solely from medial Golgi membranes. The vesicular structures in the TEM images occupied a significant portion of the cone photoreceptor IS. In contrast, the Man2a-GFP-positive structures observed with confocal microscopy did not appear to occupy the same volume of the IS as the vesicular structures (compare Figures 2.4 & 2.5 with Figure 2.7), suggesting that these membranes may be derived from other disrupted trafficking pathways.

Nrc^{a14} cone photoreceptors have abnormal late endosomes and an increase in autophagosomes

Photoreceptors depend on high membrane and protein turnover for their survival and thus defects in the late endosomal degradative pathway would likely cause severe membrane trafficking abnormalities. Furthermore, this pathway is tightly regulated by phosphoinositides (Vicinanza et al., 2008b). To analyze the endolysosomal system, we used LysoTracker Red and followed two major molecules in the degradative pathway, Rab7 and LC3. LysoTracker Red accumulates in acidic organelles and has been used to label lysosomes in live zebrafish larvae (He et al., 2009). Rab7 is a GTPase involved in late endosomal trafficking (Vitelli et al., 1997), lysosome biogenesis (Bucci et al., 2000), maturation of late autophagic vacuoles (Jager et al., 2004) and is commonly used as a marker of the late endolysosomal pathway (Bottger et al., 1996). LC3 is a protein involved in the formation of autophagosome membranes. Changes in the presence of LC3-positive puncta are indicative of alterations in autophagy (Klionsky et al., 2012). To investigate whether late endosomal trafficking pathways are disrupted in *nrc*^{a14}cone photoreceptors we generated transgenic fish lines that target GFP to late endosomes (*Tg(TαCP:GFP-Rab7)*) or autophagosomes (*Tg(TαCP:GFP-LC3*)).

Lysotracker Red staining in WT photoreceptors was observed primarily in synaptic vesicles at the synapse, but also in small punctate structures in the IS (Figure 2.8 A). In contrast, the majority of the Lysotracker Red accumulated in larger, globular structures in the IS of *nrc*^{a14} photoreceptors (Figure 2.8 B, arrowhead) with very little staining at the synapse. The lack of staining at *nrc*^{a14} photoreceptor synapses is consistent with our previous findings of synaptic vesicle defects in *nrc*^{a14} cone photoreceptors (Allwardt et al., 2001).

In WT cone photoreceptors, Rab7 positive structures appeared punctate and localized primarily to the IS (Figure 2.8 C). In contrast, we found that *nrc*^{a14} cone photoreceptors contained abnormal Rab7-positive structures (Figure 2.8 D). While some of the Rab7 structures in *nrc*^{a14} cone photoreceptors appeared punctate and similar in appearance to those in WT cells, the majority of the cells had large perinuclear and/or doughnut shaped structures (Figure 2.8 D, arrowheads and arrow respectively) that were not observed in WT cone photoreceptors. There was also an overall increase in the number of Rab7 structures in *nrc*^{a14} cone photoreceptors compared to WT (Figure 2.8 C, D).

Upon induction of autophagosome formation, the distribution of LC3 changes from diffusely cytosolic to punctate as it becomes concentrated in autophagosome membranes. The GFP-LC3 signal in cone photoreceptors from WT larvae was primarily cytosolic. Few GFP-LC3 puncta were observed in WT cells, with the majority of the GFP-LC3 puncta located in the IS (Figure 2.8 E, G; average of 1.3+/-0.4puncta/cell; median of 1puncta/cell; n=823 cells from 11 larvae). In contrast, *nrc*^{a14} cone photoreceptors contained many more GFP-LC3 puncta. In addition, the GFP-LC3 puncta in *nrc*^{a14} cone photoreceptors were more broadly distributed throughout the IS and at the synapse (Figure 2.8 F, G; average of 5.5+/-2.2puncta/cell; median of 4puncta/cell; n=1055 cells form 12 larvae; p=0.000001). An increase in GFP-LC3 puncta could be indicative of an increase of autophagosome formation, or a decrease in autophagosome clearance.

Together, the abnormalities detected in *nrc*^{a14} cones using all three markers of the endolysosomal/autophagy pathway indicate that the loss of SynJ1 significantly disrupts this important trafficking pathway in cone photoreceptors.

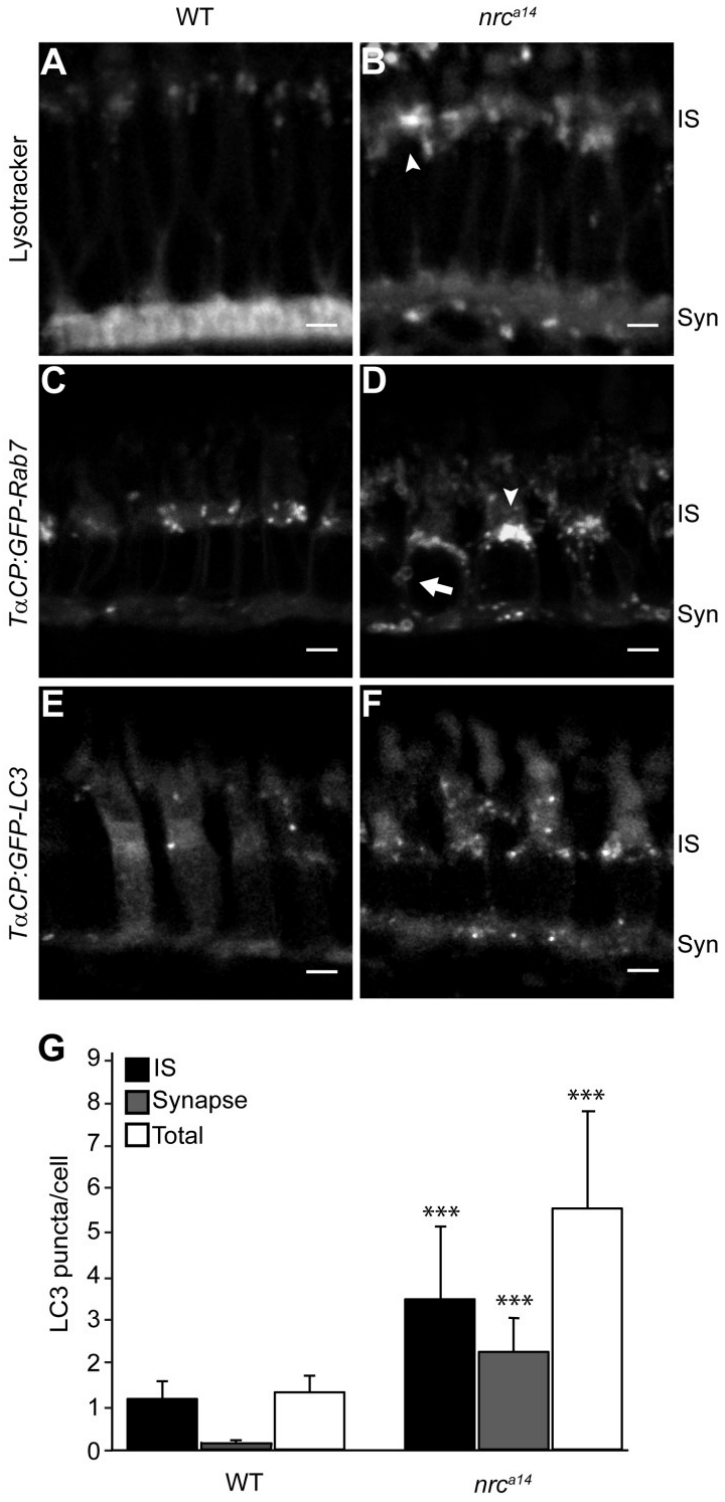

Figure 2.8: Loss of SynJ1 disrupts endolysosomal structures. Confocal images of larvae incubated with Lysotracker Red and the transgenic fish lines *Tg(TαCP:GFP-Rab7)* and *Tg(TαCP:GFP-LC3)* mark the endolysosomal system. 5dpf larvae were incubated in Lysotracker and imaged live. In WT retinas (A), Lysotracker Red accumulated primarily in the synapse and in small punctate structures in the IS of cone photoreceptors. In *nrc*^{a14} cone photoreceptors (B), Lysotracker Red accumulated primarily in larger, abnormal structures in the IS. Retinal slices from WT (C) and *nrc*^{a14} (D) larvae show that abnormal Rab7-positive structures including large perinuclear structures (arrowheads), and doughnut shaped structures (arrows) accumulated in the IS and synapse in the absence of SynJ1. The lack of SynJ1 also caused an increase in the number of LC3-GFP-positive structures, indicating a disruption in autophagy in *nrc*^{a14} cones (F). The number of LC3 puncta is increased in both the IS and synapse of *nrc*^{a14} cones (G). Syn=photoreceptor synapses, IS= inner segment. Scale bar=2μm in all images. Graph shows average LC3 puncta in the IS, synapse or entire cell (Total) per cell, error bars are STDEV for 11 WT larvae and 12 *nrc*^{a14} larvae. The number of LC3 puncta per cell for each subcellular compartment or the entire cell was significantly different between WT and *nrc*^{a14} larvae (p-value<0.001, denoted by ***).

In order to correlate the vesicular structures observed in our TEM images with the autophagic trafficking pathway, we repeated our light/dark experiments using our *Tg(TαCP:GFP-LC3*) fish line. An accumulation of GFP-LC3-positive puncta after dark incubation of *nrc*^{a14} larvae similar to the accumulation of vesicles seen in the "severely vesiculated" photoreceptors in Figure 2.5 would provide strong evidence that the vesicular structures observed in TEM images of *nrc*^{a14} photoreceptors are in the autophagic trafficking pathway. WT and *nrc*^{a14} sibling larvae were incubated in complete darkness, or left on a normal light/dark cycle as described above for 24hours prior to fixation and quantification of GFP-LC3 puncta. We found that dark incubation did not significantly increase the average number of GFP-LC3 puncta in either WT or *nrc*^{a14} cone photoreceptors (Figure 2.9 E, n=2 independent light/dark trials, 3-5 larvae per condition, 60-100 cells per larvae). However, we observed that dark incubation changed the morphology of GFP-LC3 puncta in *nrc*^{a14} cone photoreceptors (Figure 2.9 C, D). While light-adapted *nrc*^{a14} larvae contained numerous small GFP-LC3 puncta, dark adapted *nrc*^{a14} cone photoreceptors contained larger, more intense puncta and less diffuse GFP-LC3 in the cytoplasm (Figure 2.9 D, arrowhead). At the level of confocal resolution, it is unclear whether these larger puncta are due to an increase in size of autophagosomes or large aggregates of puncta that cannot be distinguished from one another. These light/dark experimental results together indicate that increasing synaptic activity with dark adaptation alters both the appearance of vesicular structures in the TEM images (Figure 2.5) as well as the morphology of GFP-LC3 puncta in *nrc*^{a14} cone photoreceptors (Figure 2.9).

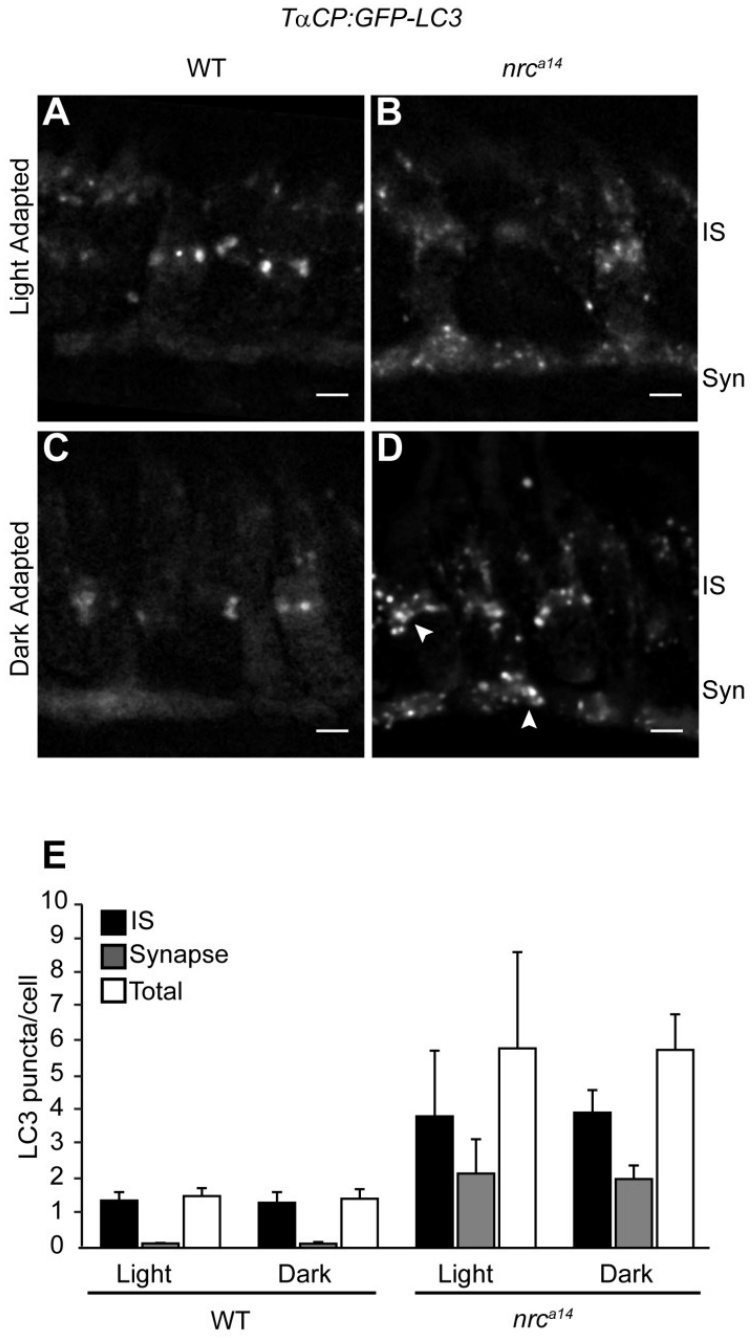

Figure 2.9: Dark adaptation affects autophagosomes in *nrc^{a14}* cone photoreceptors. Confocal images of cone photoreceptors in light (A, B) or dark-adapted (C, D) WT and *nrc^{a14} Tg(TαCP:GFP-LC3)* retinas. At 4dpf, larvae were phenotyped by OKR and placed at 28°C either on a normal light/dark cycle, or in complete darkness. 24 hours later, at 5dpf, larvae were fixed and retinal slices were generated. After dark incubation, the GFP-LC3 positive puncta in *nrc^{a14}* cone photoreceptors appeared enlarged (D, arrowhead). Dark incubation did not significantly affect the number of GFP-LC3 puncta in WT or *nrc^{a14}* cone photoreceptors (E). Syn=photoreceptor synapses, IS= inner segment. Scale bar=2μm in all images. Graph shows average LC3 puncta in the IS, synapse or entire cell (Total) per cell, error bars are STDEV, from two independent light/dark experiments. For each experiment, 3-5 larvae were used per condition, and 60-150 cells were analyzed per larvae.

Discussion

Proteins synthesized in the IS of cone photoreceptors are sorted and transported apically toward the OS or basally toward the synapse. Dysfunctional folding, sorting, or trafficking of OS and ciliary proteins are frequently the cause of photoreceptor degeneration (for example (Hartong et al., 2006)). In addition, OS membranes and proteins are continually shed and must be replaced, resulting in this compartment having a very high demand for protein trafficking. As a consequence, the mechanisms involved in apical transport have been the focus of much more attention than those involved in synaptic protein transport in photoreceptors.

In this study, we identified a novel role for SynJ1 in the IS of cone photoreceptors. We characterized IS trafficking defects in the *nrc*^{a14} zebrafish mutant, which lacks SynJ1. Loss of SynJ1 caused an apparent defect in trafficking of the synaptic proteins VAMP2 and RibeyeB, but no defect in apical trafficking of OS or CC proteins. We extended this analysis and determined that late endolysosomal trafficking pathways are disrupted in *nrc*^{a14} mutant cones. These data suggest that SynJ1 does not play a role in general protein trafficking, but rather a specific role in sorting or transporting synaptic proteins that rely on the endolysosomal and autophagic systems.

SynJ1 is a polyphosphoinositide phosphatase with an established role in synaptic vesicle recycling in conventional neurons. The SynJ1 protein is highly conserved, and consists of two phosphatase domains, a 5'Ptase and a Sac1 domain, and a proline rich C-terminal region involved in protein-protein interactions (McPherson et al., 1996). Mouse *synJ1* knockouts show significantly elevated levels of $PI(4,5)P_2$ (Cremona et al., 1999) ; however, with its dual phosphatase activity, SynJ1 can potentially act on many different phosphatidylinositol (PI) substrates. Synaptojanin-like proteins in yeast have been found to be involved in multiple trafficking processes such as endocytosis and trans-Golgi sorting (Singer-Kruger et al., 1998; Bensen et al., 2000; Stefan et al., 2002). However, in vertebrate neurons the role of SynJ1 in trafficking events other than clathrin-mediated endocytosis is less clear. In a recent study, the overexpression of

SynJ1 in a transgenic mouse line resulted in the accumulation of enlarged early endosomes in neurons (Cossec et al., 2012). In addition, we have previously shown that SynJ1 protein is present in both synaptic terminals and the ISs of cone photoreceptors, suggesting that it may also have additional functions in PIP metabolism at cellular sites other than the synapse (Holzhausen et al., 2009).

In this study, using TEM imaging, we observed the accumulation of large vesicular structures in the IS of *nrc*^{a14} cone photoreceptors at 5dpf. The vesicular structures in the TEM images are abundant, heterogeneous in size and appearance, and often fill the majority of IS between the nucleus and the mitochondria. In order to investigate the trafficking mechanisms that resulted in this vesicle accumulation, we dark adapted WT and *nrc*^{a14} zebrafish larvae. We predicted that increasing synaptic vesicle transport, which is expected to occur in the dark due to increased glutamate release, would enhance appearance of accumulated vesicles. We found that dark adaptation results in an increase in the severity of vesicle accumulation in *nrc*^{a14} ISs (Figure 2.5). As photoreceptors transition between light and dark conditions, they undergo multiple cellular changes including protein translocation (Arshavsky, 2003; Rajala et al., 2009) and redistribution of energy (Linton et al., 2010). The exacerbation of the *nrc*^{a14} phenotype in the dark suggests that SynJ1 could play an important role in facilitating changes in vesicle trafficking required for photoreceptor function in the dark. Dark exposure should result in an increase of trafficking of synaptic proteins basally, as well as an increase in the recycling and/or degradation of synaptic vesicle components. Disruption of either of these two trafficking pathways could result in an accumulation of vesicular structures in ISs. To discriminate between these two possibilities, we targeted GFP to subcellular organelles involved in either the biosynthetic or the degradative pathway.

We found that SynJ1 is required for maintaining, but not establishing, the structure of the Golgi apparatus in cone photoreceptors. In the zebrafish larval retina, cone photoreceptors begin to develop around 2dpf with their OSs and synaptic terminals becoming visible at approximately 2.5dpf. Synaptic contacts between cone and bipolar cell terminals and the first responses become detectable at 3-3.5dpf (Schmitt and

Dowling, 1999; Allwardt et al., 2001). In the *nrc*^{a14} mutant, the Golgi apparatus in the photoreceptors appears to develop normally, but begins to become disordered at approximately 4dpf; at this time point in development, WT photoreceptor synapses are functional. Release of neurotransmitter at the synaptic terminal requires a constant supply of newly synthesized synaptic proteins from the IS, as well as efficient recycling of these proteins. Dysfunction of either of these trafficking pathways would result in a buildup of synaptic proteins in the IS. The disordered Golgi in *nrc*^{a14} photoreceptors would be predicted to cause a defect in trafficking newly synthesized synaptic proteins. Prior to reaching their destinations, many apical and basal proteins both pass through the trans Golgi (Schmied and Holtzman). However, the ability of *nrc*^{a14} cone photoreceptors to maintain proper apical trafficking despite altered Golgi morphology suggests that the disruption of protein transport of newly synthesized proteins is not the primary defect. The developmentally late disruption of the Golgi suggests a secondary defect due to altered endolysosomal trafficking. The Golgi and endolysosomal system exchange proteins and lipids (Pfeffer, 2009) and defects in endolysosomal trafficking caused by genetic diseases (Choudhury et al., 2002; Ganley and Pfeffer, 2006), or genetic and chemical manipulations (Kirkbride et al., 2012) can cause alterations in Golgi morphology and function.

All cell types need to maintain protein quality and homeostasis by degrading damaged proteins. However, due to their high levels of membrane turnover and long life, neuronal cell types, including photoreceptors, are severely affected by impairments in endolysosomal trafficking and protein degradation (Dermaut et al., 2005; Nixon et al., 2008; Chinchore et al., 2009). Disruptions in endolysosomal and autophagic trafficking have been found in many neurodegenerative diseases including Parkinson's disease (Cook et al., 2012; Tofaris, 2012; Dehay et al., 2013; Nixon, 2013). In addition, mutations in SynJ1 have recently been linked to a human familial early-onset Parkinsonism (Krebs et al., 2013; Quadri et al., 2013). In our current study, we found that *nrc*^{a14} cones have multiple abnormalities in the endolysosomal and autophagic systems. These cells contain enlarged acidic vesicles, aberrantly shaped Rab7 positive late endosomes, and an increase in LC3 positive autophagic vesicles (Figure 2.8). These observations indicate that loss of SynJ1 in cones disrupts late endosomal and

autophagic trafficking. In addition, upon dark incubation, LC3-positive puncta appeared larger in *nrc*^{a14} mutant cones compared to puncta observed in the light. Thus, changes in both the number and/or shape of vesicles were observed in darkness by both TEM and when using an autophagy marker, which suggests that the vesicles observed in TEM may also be associated with the autophagic trafficking pathway. These findings are consistent with our observation of morphologically normal apical ends of *nrc*^{a14} cones; OS disc shedding to remove damaged proteins and lipids does not rely on intracellular endolysosomal pathways. Further, while two synaptic proteins, VAMP2 and RibeyeB, mislocalize to the ISs of *nrc*^{a14} photoreceptors, a third synaptic protein, Synaptophysin, does not. Synaptophysin protein can be polyubiquitinated and degraded by the proteasome (Wheeler et al., 2002), and therefore this protein may be able to bypass defects in the endolysosomal system.

Regulation of endosomal and autophagic trafficking is highly regulated by phosphoinositides, and disrupting the activity of phosphoinositide kinases and phosphatases can result in aberrant endosomal trafficking and enlarged endosomal structures (Vicinanza et al., 2008b, a; Ooms et al., 2009). The phosphoinositide $PI(3,5)P_2$ is enriched on late endosome/lysosome membranes. Mice with genetic mutations affecting the phosphatases and kinases involved in regulation of $PI(3,5)P_2$ have neurological defects, cells with large vacuoles, abnormal endolysosomal membranes (Chow et al., 2007; Zhang et al., 2007; Ikonomov et al., 2011; Ferguson et al., 2012), and defective autophagy (Ferguson et al., 2009). Similarly, PI3P is enriched on autophagosome membranes and deletion or mutation of PI3P modulating enzymes result in aberrant autophagy (Vergne and Deretic, 2010). The yeast synaptojanin-like proteins INP52 and INP53 can dephosphorylate both $PI(3,5)P_2$ and PI3P to PI (Guo et al., 1999). The phosphatase domains of SynJ1 are highly conserved from yeast to vertebrates; while the role of SynJ1 in regulating these phosphoinositide species has not been investigated *in vivo*, mouse and human SynJ1 constructs can act on PI(3)P *in vitro* (Guo et al., 1999; Mani et al., 2007; Krebs et al., 2013). Further work will need to be done to characterize the PIP species affected *in vivo* by the *nrc*^{a14} mutation.

Materials and Methods

Ethics statement

This study was carried out in strict accordance with the recommendations in the Guide for the Care and Use of Laboratory Animals of the National Institutes of Health. The protocol, 3113-01, was approved by IACUC of the University of Washington.

Cloning and plasmids

The medial Golgi marker, *TαCP:zfMan2a-GFP*, was obtained from Brian Link (Insinna et al., 2010). The synaptic vesicle marker, *CFP-zfSynaptophysin*, was obtained from Martin Meyer (Meyer and Smith, 2006). The autophagosome marker, *GFP-zfLC3* was obtained from Dan Klionsky (He et al., 2009) and cloned into a pCR8/GW Gateway vector (Invitrogen). The ER marker ER-GFP was created by overhang PCR methods to add a C-terminal KDEL sequence, and N-terminal 17 amino acids (MTALSLLFMAVSVALIT) of zfcalreticulin to GFP (based on (Roderick et al., 1997)) and cloned into a pCR8/GW Gateway vector (Invitrogen). *zfRab7* was cloned from larval zebrafish cDNA using the primers 5'- ATTCGCTAGATCTCCTGCTTT-3' and 5'-AGGCTGAGGGTGAAATGTTG-3', and cloned into a 3'Entry Vector (Invitrogen) using the primers 5'-GGGGACAGCTTTCTTGTACAAAGTGGCTATGACATCAAGGAAGAAAGT-3' and 5'-GGGGACAACTTTGTATAATAAAGTTGCTCAGCAGCTACAGGTCTCTG-3'. Expression constructs were generated using the MultiSite Gateway System (Invitrogen) and the Tol2 kit (Kwan et al., 2007). Expression was driven by either the *cone transducin alpha* promoter (*TαCP*) (Kennedy et al., 2007) or the *cone-rod homeobox* promoter (*crx*). To obtain the *crx* promoter, a 5 kb upstream fragment of *crx* was amplified from zebrafish genomic DNA by PCR using the following primers, 5'-GGGGACAACTTTGTATAGAAAAGTTGTCATGGAAATGGCAAAAACATTC-3' and 5'-GGGGACTGCTTTTTTGTACAAACTTGGCGCTACTCGCTGTCTTCAATAA-3'. The resultant PCR DNA fragment was subcloned into pDONR P4P1r by Gateway BP reaction (Suzuki et al., 2013) .

Fish husbandry and generation of transgenic zebrafish

Zebrafish were reared and maintained in the University of Washington fish facility as previously described (Westerfield, 1995). Embryos were maintained in embryo media (EM) (Westerfield, 1995) at 28°C on a 14/10hour light/dark cycle prior to experimentation or rearing in the fish facility. Homozygous *nrc*^{a14} mutants were identified by the optokinetic response assay (OKR) as previously described (Brockerhoff, 2006) or by genotyping. Genotyping was performed by amplifying the region of the *synJ1* gene containing the *nrc*^{a14} mutation site form genomic DNA using the primers 5'-CACCAGAACCATCCAGAACA-3' and 5'-GTCATACCGCTCAGCCCTAA-3'. The *nrc*^{a14} mutation disrupts a cut site recognition sequence of the restriction enzyme BssSI, allowing *nrc*^{a14} mutants to be identified. Since WT and *nrc*^{a14} heterozygotes appear indistinguishable in every phenotypic assay we have performed, we refer to all OKR-positive larvae as WT. The *Tg(TαCP:*spH) fish line has been previously described (Holzhausen et al., 2009). We created other transgenic fish lines by injecting DNA expression constructs described above and mRNA encoding the tol2 transposase simultaneously into zebrafish embryos at the one-cell stage. Once injected zebrafish reached sexual maturity, pair-wise crosses were performed to identify fish that could transmit the desired transgene (Kikuta and Kawakami, 2009). Newly identified transgenic fish were assayed by OKR at 5dpf to ensure that transgene expression did not affect visual responses. For dark adaptation, larvae were raised in the dark for 24hrs starting at 4dpf. Light-adapted WT and *nrc*^{a14} larvae were kept on a normal 14/10 hour light/dark cycle. The 24hr incubations started in the afternoon. After 24hrs (at 5dpf) dark-adapted larvae were fixed in the dark, light-adapted controls were fixed in the light, and then fixed larvae were processed for TEM or histology.

Immunohistochemistry

Retinal slices were prepared as previously described (Brockerhoff et al., 1997). After blocking in 5% normal goat serum, 1% bovine serum albumin, and 0.3% TritonX-100 in PBS, slices were incubated with the following primary antibodies at 4°C overnight: 1:100 anti-RibeyeB (a gift from Teresa Nicolson, (Obholzer et al., 2008)), 1:5000 anti-IFT88 (a

gift from Brian Perkins, (Krock and Perkins, 2008)), or 1:500 anti-acetylated tubulin (Sigma, T6793). Slices were incubated with secondary anti-rabbit Alexa-633 (Invitrogen, A21071) or anti-mouse Alexa 568 (Invitrogen, A11002) at 1:200 for 1 hour at room temperature. Nuclei were counter stained with 5μM Sytox Green (Invitrogen) or 5μM Hoechst (Invitrogen). Slides were mounted with a coverslip and Fluoromount-G (Southern Biotech). Imaging of retinal sections was performed on an Olympus FV300 or FV1000 confocal microscope with a 60X oil immersion objective.

Live Imaging

Larvae were treated with 0.003% 1-phenyl-2-thiourea (PTU) in EM at ~24 hours post fertilization (hpf) to prevent melanization (Westerfield, 1995). For membrane counterstaining, 3dpf larvae were incubated in 25μM BODIPY-Texas Red (Invitrogen) for 1 hour, followed by three washes in EM with PTU prior to imaging. For Brefeldin A treatments, 3dpf larvae were incubated with 2μM Brefeldin A (Cell Signaling) in EM and PTU for 90 minutes prior to imaging. For Lysotracker Red staining, 5dpf larvae were incubated in 10μM Lysotracker Red DND 99 (Invitrogen) in EM and PTU for 2 hours, followed by three washes in EM and PTU prior to imaging. Larvae were anaesthetized in Tricaine (Sigma) and mounted in warm 0.5-1% low mount agarose. Embedded larvae were covered in EM containing PTU and Tricaine and imaged. For BFA treatments, 2μM BFA was included in the EM during imaging. Imaging was done on an Olympus FV1000 using a 40X or 60X water immersion objective.

Transmission electron microscopy

Transmission electron microscopy was performed at the UW Vision Core as previously described (Schmitt and Dowling, 1999). For quantification, the entire retina was imaged.

Image processing and data analysis

Images were processed using NIH ImageJ and Adobe Photoshop. Representative images in Figures are 2μm projections of confocal stacks, or single optical slices of TEM images. Images were randomized prior to analysis. ImageJ was used to measure CC

and OS lengths and vesicles sizes from randomized images. For qualitative comparisons between WT and *nrc*^{a14} larvae, at least 6 larvae of each genotype were analyzed. For quantitative data, the number of larvae analyzed is included in the text and Figure legends. For light/dark experiments cells were scored as "vesiculated" if they contained at least three large (>125nm in diameter) vesicular structures in their ISs. If the number of vesicular structures exceeded 20, the cell was scored as "severely vesiculated". Microsoft Excel and R were used for statistical analysis. Unless otherwise indicated, bar graphs and values in text represent mean values +/- STDEV and p-values were calculated by the Mann-Whitney test.

Acknowledgements

The work described in this chapter was published in PloS ONE. The other authors that contributed to this study were Lars C. Holzhausen, Sara Hayden, Eva Y. Ma, Sachiro Suzuki and Susan E. Brockerhoff. We thank Jing Huang and Ed Parker at the UW Vision core for help with preparing retinal slices and TEM experiments respectively. We thank Brian Link (Medical College of Wisconsin), Martin Meyer (King's College, London), Dan Klionsky (University of Michigan), and Rachel Wong (University of Washington) for contributing plasmids, and Teresa Nicolson (Oregon Health and Science University) and Brian Perkins (Texas A&M) for providing antibodies. We thank Alaron Lewis (University of Washington) for critical reading of the manuscript, Neil Wilson (University of Washington) for assistance with Gateway cloning, and Gail Stanton for assistance with genotyping.

Chapter 3

Autophagy in cone photoreceptors is regulated by Synaptojanin1 5'phosphatase activity

Introduction

Cells must balance synthesis of new proteins with the degradation of old and damaged proteins to maintain their cellular proteome. Protein degradation is accomplished by two main pathways; the ubiquitin-proteasome system or the endolysosomal system. Membrane proteins are removed from the plasma membrane by endocytosis. The endocytosed proteins are delivered to early endosomes where they are sorted. Proteins destined for degradation will continue through the endolysosomal pathway, first through late endosomes and finally to the lysosome. Cytosolic proteins can be degraded either by the proteasome or by autophagy (Goldberg, 2003). The term autophagy generally refers to macroautophagy, a process in which a double membrane structure forms in the cytoplasm, non-specifically engulfing cytoplasmic contents including proteins and organelles. In order to degrade their contents, autophagosomes must fuse with the lysosome. In yeast, autophagosomes fuse directly with the vacuole. In mammalian systems, autophagosomes can also fuse directly with the lysosome or first fuse with other endosomal compartments, forming an amphisome, before fusing with the lysosome (Klionsky, 2007).

Neurons are post-mitotic, long-lived cells which makes them particularly susceptible to breakdowns in protein homeostasis. Many neurodegenerative diseases including Alzheimer's, Parkinson's, and amyotrophic lateral sclerosis show cellular phenotypes that are consistent with abnormalities in protein turnover (Fecto et al., 2014). Understanding the proteins and cellular processes that underlie protein turnover is vital to understanding the underlying pathology of these diseases as well as developing treatments. Important regulators of the endolysosomal pathway are the phosphoinositide (PIP) lipids. The inositol head group of these phospholipids can be mono-, di- or tri-phosphorylated giving rise to seven different PIP species. Despite accounting for only a small percentage of cellular phospholipids, PIPs are vital in a

variety of cellular processes such as cytoskeletal remodeling, signal transduction, and membrane trafficking (Billcliff and Lowe, 2014). The differential distribution of PIPs in different membranes confers membrane identity and allows the spatial and temporal control of effector proteins to endosomal membranes (Huotari and Helenius, 2011). Two PIP's, phosphatidylinositol 3-phosphate (PI(3)P) and phosphatidylinositol 3,5-bisphosphate ($PI(3,5)P_2$) are found on the cytosolic face of membranes of endolysosomal organelles, and play key roles in regulating their formation, maturation and trafficking. PI(3)P is found on early endosomes whereas $PI(3,5)P_2$ is found on late endosomes and lysosomes. The production of PI(3)P is also vital for the process of autophagy; knocking out the kinase that produces PI(3)P prevents autophagosomes from forming in yeast (Dall'Armi et al., 2013).

We have previously shown that cone photoreceptors in zebrafish larvae lacking the PIP phosphatase Synaptojanin1 (SynJ1) have endolysosomal defects. These defects include enlarged acidic vesicles, abnormal late endosomes, an increase in autophagosomes as well as an accumulation of synaptic proteins (George et al., 2014). Due to the involvement of PIPs in regulating endolysosomal trafficking, it is not surprising that mutations in a polyphosphoinositide phosphatase would result in trafficking defects. However, the characterized role of SynJ1 in vertebrate neurons is in regulating phosphatidylinositol 4,5-bisphosphate ($PI(4,5)P_2$) levels during clathrin-mediated endocytosis (Cremona et al., 1999). Recent studies have demonstrated that $PI(4,5)P_2$ is also involved in autophagy in mammalian cells; both in the initial formation of autophagosome precursors (Moreau et al., 2012) as well as in autophagic lysosome reformation (Rong et al., 2012). It is unclear if changes in $PI(4,5)P_2$ levels could sufficiently explain the drastic endolysosomal and autophagic defects we observed in *nrc*^{a14} photoreceptors. One of the yeast Synaptojanin-like proteins, INP53, has been found to play a role in autophagy by modulating PI(3)P levels (Cebollero et al., 2012). The role of vertebrate SynJ1 in regulating PI(3)P *in vivo* has not been demonstrated, however both human and mouse SynJ1 proteins can hydrolyze this lipid *in vitro* (Mani et al., 2007; Krebs et al., 2013). Links between SynJ1 and the two neurodegenerative diseases Alzheimer's (Berman et al., 2008) and Parkinson's (Krebs et al., 2013; Quadri et al., 2013) have recently been described. Understanding the functional role of SynJ1

in protein turnover in the endolysosomal and autophagic pathways would help us understand the pathologies of these diseases.

The goal of this study was to define the specific trafficking steps altered in the SynJ1-deficient zebrafish mutant *nrc^{a14}* and to identify the functional role of SynJ1 in these pathways. We found that defects in late endosomes and autophagosomes in *nrc^{a14}* cones appear early in photoreceptor development. The accumulation of autophagosomes is due to a defect in autophagosome maturation, but not due to a loss of autophagosome mobility. The loss of SynJ1 does not result in a redistribution of $PI(4,5)P_2$, PI(4)P, PI(3)P, or $PI(3,5)P_2$. We also demonstrate the phosphatase activity of the 5'phosphatase domain, but not Sac1 domain, of SynJ1 is involved in regulating endolysosomal and autophagic trafficking in cones.

Results

We have previously shown that photoreceptors from 5 days post fertilization (dpf) zebrafish larvae lacking SynJ1 have abnormal endolysosomal and autophagic trafficking (George et al., 2014). At the developmental time point of 5dpf, cone photoreceptors have fully differentiated and are functional (Schmitt and Dowling, 1999). To correlate the endolysosomal defects observed in *nrc^{a14}* cones with initial stages of photoreceptor development, we examined late endosomes and autophagosomes in cone photoreceptors starting at 3dpf. Retinal development is rapid in zebrafish; at 3 dpf, cone photoreceptors have begun to form both outer segments and synaptic contacts with bipolar cells. By 4dpf, cone photoreceptors have fully formed outer segments, established synaptic connections, and can reliably respond to visual stimuli (Schmitt and Dowling, 1999). We analyzed fixed retinal sections of wild type (WT) and *nrc^{a14} Tg(TαCP:GFP-LC3)* and *Tg(TαCP:GFP-Rab7)* larvae (Figure 3.1); these fish lines express the autophagosome marker GFP-LC3 or the late endosome marker GFP-Rab7 respectively, in cone photoreceptors.

WT cones contain twice as many LC3 positive structures at 3dpf than at 4dpf (Figure 3.1A & C). Autophagy and protein degradation have been found to play roles in neuron development (Rowland et al., 2006; Shen and Ganetzky, 2009). Our results

suggest that similar processes are involved in cone photoreceptor development. At 3dpf, cones lacking SynJ1 already display differences in late endosomes and autophagosomes relative to WT cones (Figure 3.1A-C). These differences include a statistically significant increase in the number of LC3 positive puncta (Figure 3.1A & C), as well as the presence of enlarged and abnormal Rab7 positive structures (Figure 3.1B). By 4dpf, the severity of both phenotypes had sharply increased (Figure 3.1A, B & C). To determine whether the defects in *nrc*^{a14} cones are specific to the late stages of endolysosomal trafficking, we examined the distribution of early endosomes in WT and *nrc*^{a14}cones. We generated the line *Tg(TαCP:GFP-Rab5a)* that expresses the early endosome marker GFP-Rab5a in cones. We observed no apparent difference in the number or distribution of Rab5a positive early endosomes between WT and *nrc*^{a14} cones at 5dpf (Figure 3.1D). These data show that the trafficking defects in *nrc*^{a14} cones are specific to the late endolysosomal pathway and are present at very early stages of cone development.

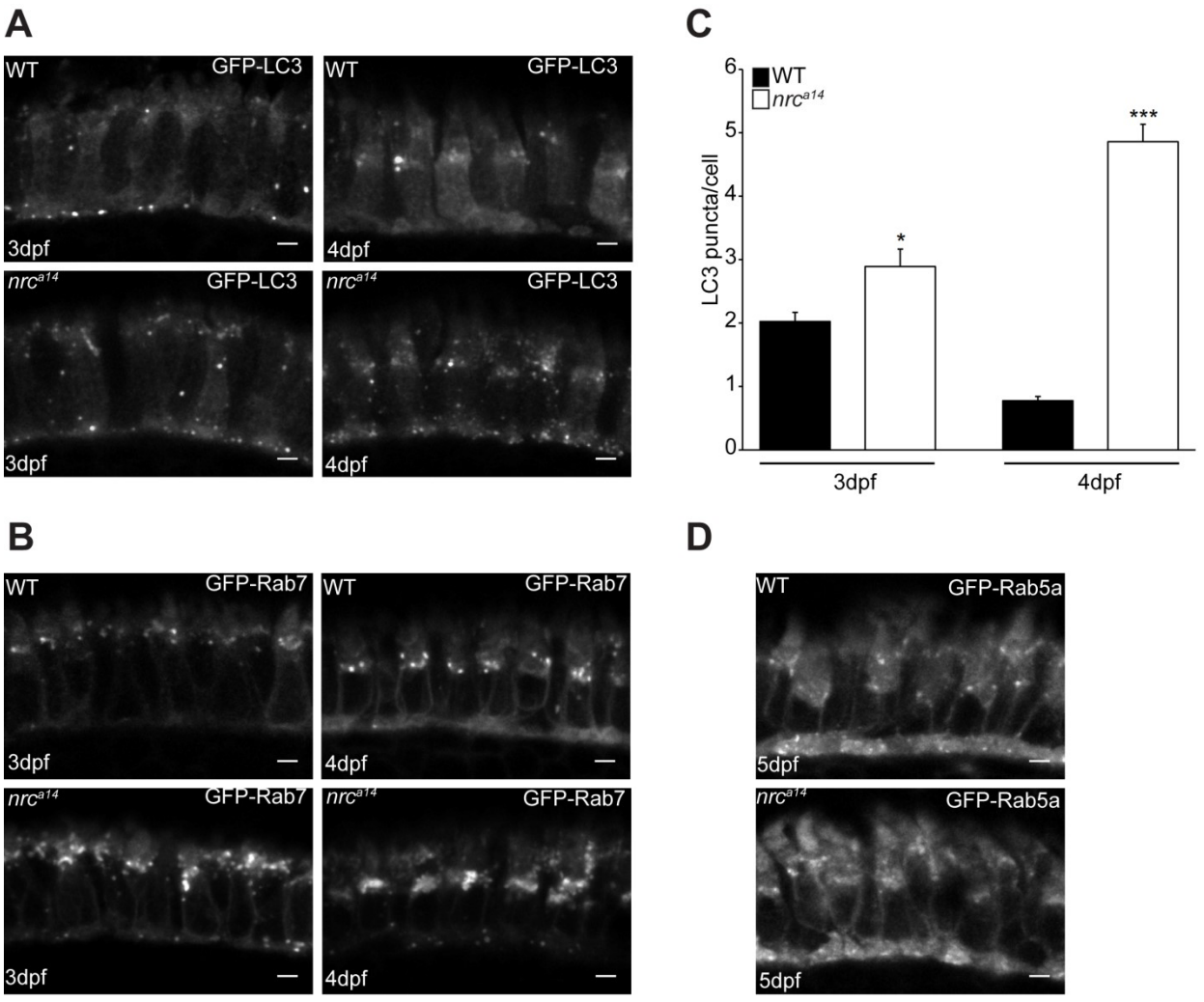

Figure 3.1: Abnormalities in *nrc*^{a14}cones are specific to late endosomes and autophagosomes and appear early in development. Images of fixed WT and *nrc*^{a14} retinas from *Tg(TαCP:GFP-LC3)* (A) and *Tg(TαCP:GFP-Rab7)* (B) larvae at 3 and 4dpf. WT cones contain more LC3 positive puncta at 3dpf than 4dpf (C, and compare top panels in A). At 3dpf *nrc*^{a14} cones contain more LC3 positive puncta than WT cones (C, compare left panels in A), particularly at synapses. By 4dpf *nrc*^{a14} cones contain many more LC3 puncta than WT cones. Abnormally enlarged Rab7 structures are present in *nrc*^{a14} cones by 3dpf (B). At 4dpf most of the Rab7 structures in *nrc*^{a14} cones are abnormal. There is also an increase in the number of Rab7 positive late endosomes at *nrc*^{a14} synapses at both 3 and 4dpf relative to WT cones (compare top and bottom panels in B). There is no difference in the appearance or number of Rab5a positive early endosomes between WT and *nrc*^{a14} cones at 5dpf (D). Scale bar=2μm in all images. Graph (C) shows average LC3 puncta per cell at 3dpf or 4dpf, error bars are SEM. n=8 WT larvae and 7 *nrc*^{a14} larvae on 3dpf and n=8 WT larvae and 9 *nrc*^{a14} larvae on 4dpf. The number of LC3 puncta per cell was significantly different between WT and *nrc*^{a14} at both 3dpf and 4dpf larvae (*=p-value<0.05, ***=p-value<0.001 as assessed by Mann-Whitney test).

SynJ1 is a polyphosphoinositide phosphatase and phosphoinositides (PIPs) are important regulators of membrane trafficking in eukaryotic cells (Di Paolo and De Camilli, 2006). In order to determine if a change in PIP species distribution could account for the trafficking defects in *nrc*^{a14} photoreceptors we analyzed the distribution of different PIPs using live imaging and genetically encoded fluorescent probes specific to different PIP species. Fluorescent probes specific to different phosphoinositides have been used in many studies to examine localized changes in PIP cellular distribution (Balla and Varnai, 2009).

First we analyzed the distribution of the canonical vertebrate SynJ1 substrates, PI(4,5)P_2 and PI(4)P using the genetically encoded probes PLCδ-PH and FAPP1-PH respectively. We transiently expressed these probes under the control of the *crx* promoter. In WT photoreceptors, PI(4,5)P_2 was localized throughout the plasma membrane and concentrated at synaptic terminals (Figure 3.2A & B). Interestingly, although we observed the PLCδ-PH signal extending up until the ends of the calycal processes at the apical end of the IS, we did not detect PI(4,5)P_2 in photoreceptor OSs. Between 3 and 6dpf, the distribution of PI(4,5)P_2 in WT and *nrc*^{a14} photoreceptors appeared the same (Figure 3.2B). We did not observe an accumulation of PI(4,5)P_2 on intracellular structures that could be attributed to abnormal late endosomes or autophagosomes in *nrc*^{a14}photoreceptors.

PI(4)P is found predominantly on the Golgi apparatus (De Matteis et al., 2005). We transiently expressed the PI(4)P probe, RFP-FAPP1, in photoreceptors of WT and *nrc*^{a14} *Tg(crx:Man2a-GFP)* larvae. This line expresses GFP fused to the medial Golgi targeting sequence from Mannosidase2a in photoreceptors and retinal bipolar cells (George et al., 2014). Although we observed variability in the distribution of the RFP-FAPP1 PI(4)P probe in transient expression experiments, we did not observe consistent differences in PI(4)P distribution between WT and *nrc*^{a14} photoreceptors. The probe localized to the Golgi and partially overlapped with the medial Golgi marker in both WT and *nrc*^{a14} photoreceptor cells (Figure 3.2C). Thus, misaccumulation of PI(4)P or PI(4,5)P_2 on endosomal structures within ISs does not appear to explain SynJ1 trafficking defects.

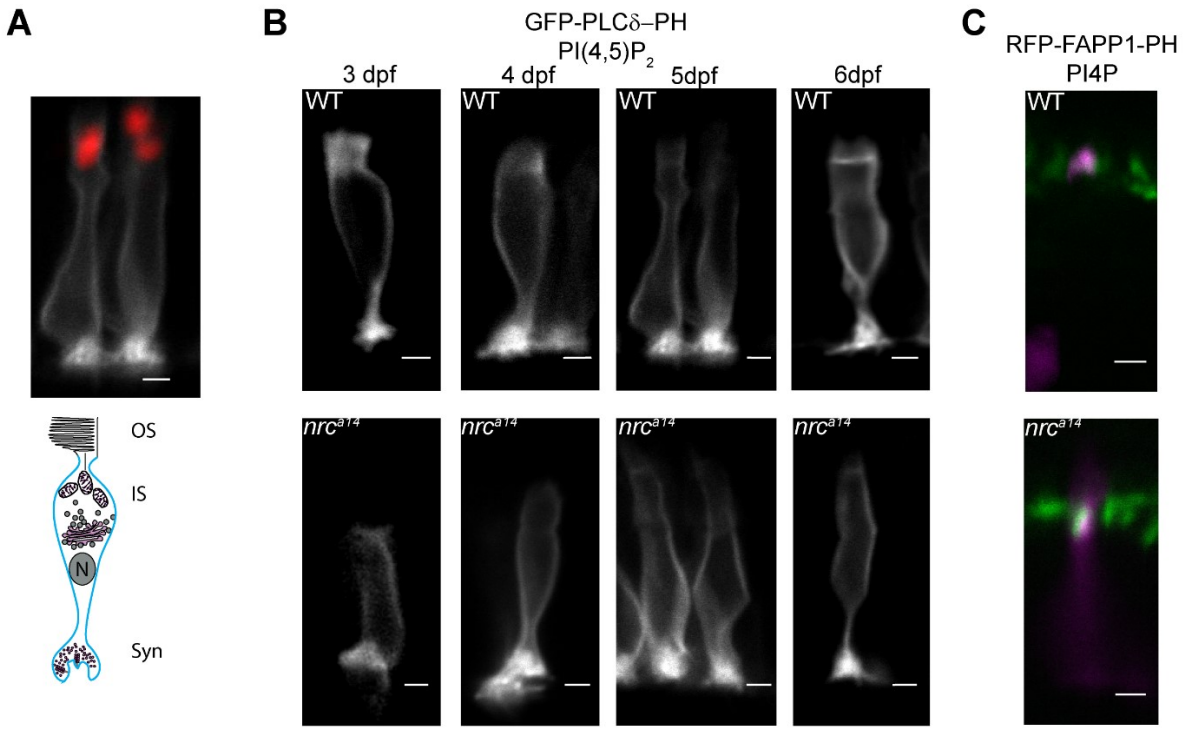

Figure 3.2: PI(4,5)P_2 and PI(4)P distributions are not altered in *nrc^{a14}* cones. The PI(4,5)P_2 probe GFP-PLCδ-PH was expressed in photoreceptors using the *crx* promoter (A, B). In WT cells at 5dpf this probe localized to the plasma membrane and concentrated at synapses, but did not extend above the mitochondria (red) into the OS (A). The PLCδ-PH probe showed the same distribution in *nrc^{a14}* photoreceptors, indicating no gross change in PI(4,5)P_2 distribution in the absence of SynJ1 (B) from 3 to 6dpf. PI(4)P was visualized with the probe RFP-FAPP1-PH (C). In both WT and *nrc^{a14}* photoreceptors at 5dpf, the RFP-FAPP1-PH probe (magenta) overlapped with the medial Golgi marker Man2a-GFP (green). There was no difference in the distribution of PI(4)P between WT and *nrc^{a14}* photoreceptors

Next, we investigated whether the distribution of PI(3)P was altered in *nrc^{a14}*cones. While the role of vertebrate SynJ1 in PI(3)P homeostasis has not been investigated *in vivo*, the yeast SynJ1 homologues INP52 and INP53 are known to play roles in regulating this lipid (Guo et al., 1999; Stefan et al., 2002; Parrish et al., 2004). PI(3)P has established roles in both endosomal and autophagic trafficking(Lindmo and Stenmark, 2006), and alterations of this lipid could account for the types of endolysosomal and autophagy phenotypes observed in *nrc^{a14}* cones. We generated the transgenic fish line *Tg(TαCP:YFP-2XFYVE)* which expresses the PI(3)P probe 2XFYVE (Gillooly et al., 2000) under the cone specific *TαCP* promoter. PI(3)P is found primarily in the membranes of early endosomes and autophagosomes (Gillooly et al., 2000; Lindmo and Stenmark, 2006). Consistent with the location and appearance of Rab5a-

containing structures in WT cones (Figure 3.1), the PI(3)P probe localized to small punctate structures at the synapses and larger punctate structures in the IS (Figure 3.3 A). In *nrc*^{a14} cones, we observed a similar distribution of PI(3)P containing structures although the number of puncta, particularly at synapses, was increased. In contrast, *nrc*^{a14} and WT ISs appeared indistinguishable from each other and we did not detect aberrant large PI(3)P positive structures.

Phosphatidylinositol-3,5-bisphosphate (PI(3,5)P_2) has been found to play multiple roles in endosomal and autophagic trafficking, (for reviews see, (Ho et al., 2012; McCartney et al., 2014) (Takasuga and Sasaki, 2013)) making it an attractive candidate to explain the *nrc*^{a14} phenotypes. It aids in the determination of physical properties and fusogenic potential of endolysosomal membranes by interacting with a membrane channel (Dong et al., 2010); and serves as a precursor for PI(3)P and PI(5)P (Zolov et al., 2012). PI(3,5)P_2-deficient cells have enlarged endolysosomes and trafficking defects in the late endocytic pathway (Gary et al., 1998; Nicot et al., 2006; Zolov et al., 2012). Interestingly, in yeast, inactivation of Synaptojanin-like proteins leads to 2-fold increases in cellular levels of PI(3,5)P_2 (Stefan et al., 2002). To investigate the distribution of PI(3,5)P_2 in WT and *nrc*^{a14} cone photoreceptors, we generated the fish line *Tg(TαCP:mCherry-ML1NX2)* which expresses the PI(3,5)P_2 probe mCherry-ML1NX2 (Li et al., 2013) under the cone specific TαCP promoter. In WT photoreceptors this probe localized to punctate structures in the inner segment and showed diffuse cytoplasmic staining. In *nrc*^{a14} photoreceptors we found a very similar distribution; the probe localized to punctate structures and also showed diffuse signal in the cytoplasm (Figure 3.3 B).

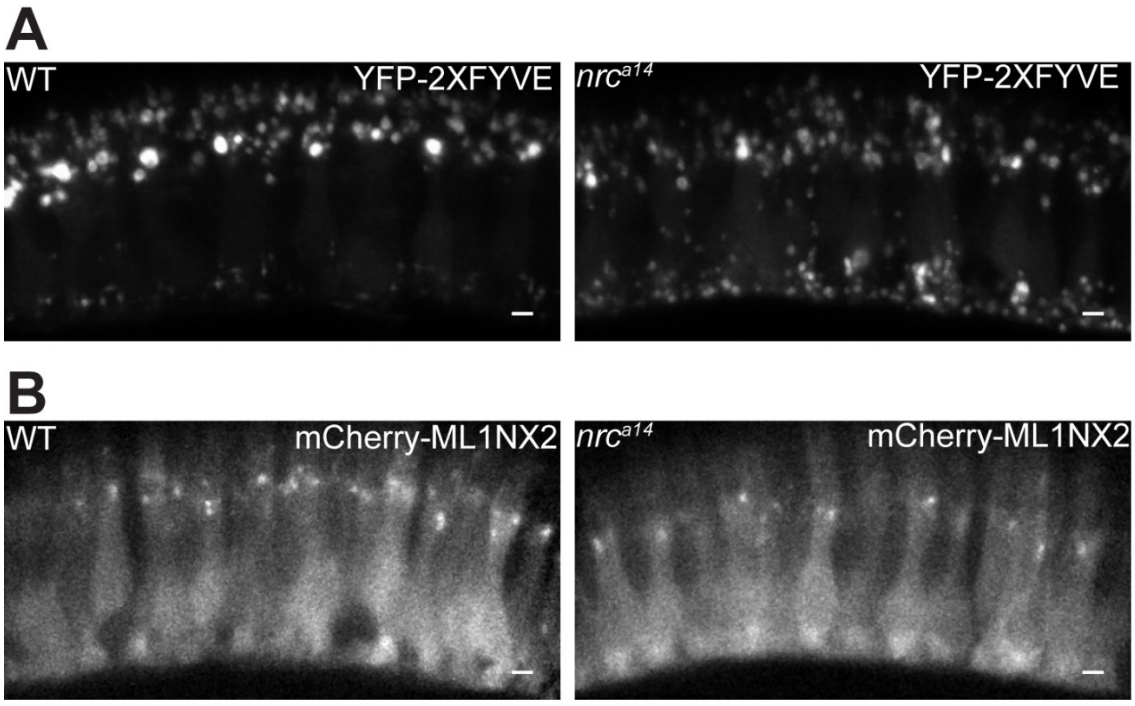

Figure 3.3 *nrc*^{a14} cone photoreceptors have an increased number of PI(3)P positive puncta, but no change in distribution of PI(3)P or PI(3,5)P_2. (A). PI(3)P was detected using YFP-2XFYVE in 5dpf cones. PI(3)P puncta localize to punctate structures consistent with the distribution of early endosomes and autophagosomes in WT cones. In *nrc*^{a14} cones, there is an increase in the number of PI(3)P positive structures at the synapse, which appears similar to the increased presence of autophagosomes. (B) The PI(3,5)P_2 probe ML1NX2 localizes to small, punctate structures in the inner segments of WT and *nrc*^{a14} cone photoreceptors. Scale bar=2μm in all images.

We further characterized the distribution of PI(3)P and PI(3,5)P_2 in WT and *nrc*^{a14} cone photoreceptors by analyzing the colocalization of these two PIPs with our markers for late endosomes and autophagosomes. The PI(3)P marker 2XFYVE has been found to colocalize with the autophagosome marker LC3 in *Drosophila melanogaster* (Juhasz et al., 2008), but not in mammalian cells (Axe et al., 2008). In our zebrafish cones, we found a similar pattern as in mammalian cells; very few LC3 positive puncta were also positive for PI(3)P (Figure 3.4A). The additional LC3 puncta in the *nrc*^{a14} cones did not overlap with the additional PI(3)P puncta in these cells. The hydrolysis of PI(3)P by PIP phosphatases has been found to involved in multiple steps in autophagy (Vergne and Deretic, 2010). Our results suggest that SynJ1 is not responsible for removing PI(3)P from LC3 positive autophagosomes. However; as we only used LC3 as an autophagosome marker, it is possible that the additional PI(3)P puncta in the nrc^{a14}

cones correspond to autophagosome precursor membranes. In the endocytic pathway PI(3)P is found primarily on early endosomes, but is also found on the luminal vesicles of multivesicular bodies (Gillooly et al., 2000), and localizes to Rab7 positive membranes (Stein et al., 2003). In both WT and *nrc*^{a14} cones we observed that some Rab7 positive structures are positive for PI(3)P (Figure 3.4A). There does not appear to be an increase in the proportion of structures that are positive for both Rab7 and PI(3)P between WT and *nrc*^{a14} cells, suggesting that excess PI(3)P does not contribute to the late endosome phenotype. Finally we looked at the colocalization of Rab7 and PI(3,5)P_2. We found that some of the PI(3,5)P_2 positive structures colocalized with Rab7 positive structures in both WT and *nrc*^{a14} cones. Importantly the structures in *nrc*^{a14} that are positive for both Rab7 and PI(3,5)P_2 are punctate; the larger abnormal Rab7 structures were not positive for PI(3,5)P_2. These results show that SynJ1 is not required for negatively regulating PI(3)P or PI(3,5)P_2 on LC3 positive autophagosomes or late endosomes.

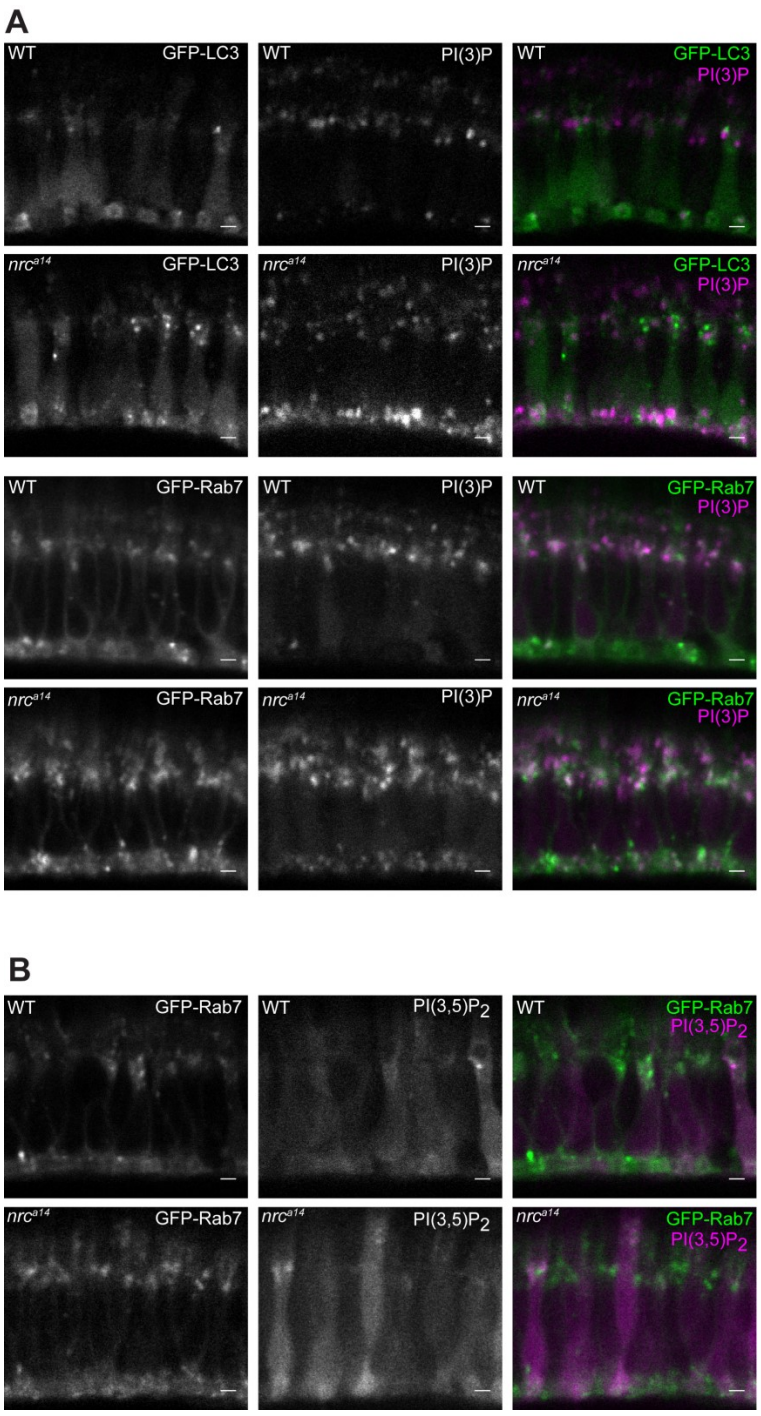

Figure 3.4 Excess PI(3)P or PI(3,5)P_2 is not found on abnormal late endosomes or autophagosomes in *nrc^{a14}* cone photoreceptors. (A). PI(3)P was detected using tagRFPt-2XFYVE in 5dpf cones expressing GFP-LC3 or GFP-Rab7. PI(3)P puncta do not overlap with autophagosomes in WT or *nrc^{a14}* cone photoreceptors. Some PI(3)P signal overlaps with Rab7 signal in both WT and *nrc^{a14}* cones. (B) The PI(3,5)P_2 probe ML1NX2 partially overlaps with Rab7 puncta in both WT and *nrc^{a14}* cone photoreceptors, but is not found on abnormal Rab7 structures in *nrc^{a14}* cones. Single optical slices are shown. Scale bar=2μm in all images.

Autophagy is a dynamic process; the increased GFP-LC3 puncta in *nrc*^{a14} cones could result from increased formation of new autophagosomes, or decreased autophagosome maturation and turnover. To examine autophagic flux, we visualized a tandem mCherry-GFP-LC3 construct in WT and *nrc*^{a14} cone photoreceptors. The LC3 protein concentrates in autophagosome membranes, which have both mCherry and GFP signal. In order to degrade their contents, autophagosomes fuse with the acidic lysosome, becoming an autolysosome. The autolysosomes only have mCherry signal due to quenching and loss of the pH sensitive GFP signal in the tandem construct (Kimura et al., 2007). In WT cones, we observed cytosolic signal from both GFP and mCherry and punctate mCherry-only structures within the IS indicative of autolysosomes (Figure 3.5A left panel). In *nrc*^{a14}cones, we rarely observed mCherry-only puncta; most of the LC3 signal had both signals indicating that autophagosomes had not fused with acidic organelles (Figure 3.5A, right panel). We quantified the GFP/mCherry colocalization using a Pearson's colocalization coefficient and found significantly more colocalization in *nrc*^{a14} photoreceptors (Figure 3.5B). We also determined an "Autolysosome value", which quantified the number of mCherry positive pixels without colocalized GFP positive pixels per cell. The "Autolysosome value", was also significantly reduced, indicating the presence of fewer autolysosomes in *nrc*^{a14} cones (Figure 3.5C).

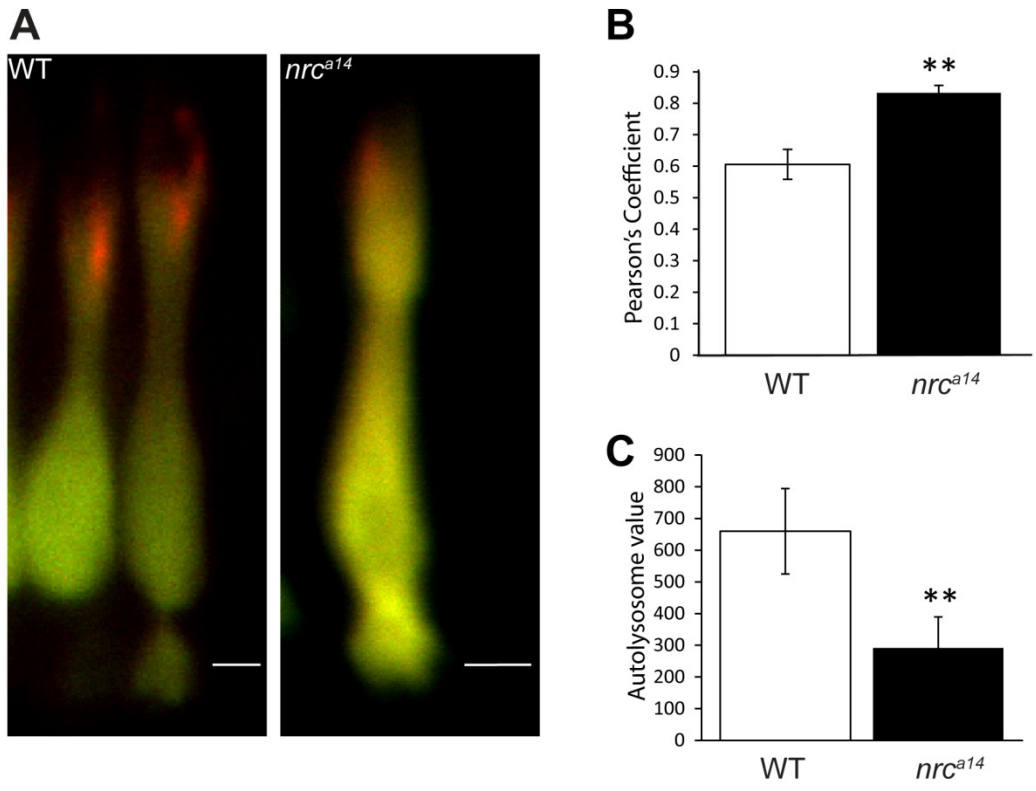

Figure 3.5: Maturation of autophagosomes is blocked in *nrc*^{a14}cones. Expression of the tandem mCherry-GFP-LC3 probe in cones of WT and *nrc*^{a14} 5dpf larvae. In WT photoreceptors autolysosomes (red-only puncta) were visible indicating the presence of autolysosomes (A). Very few red-only puncta were visible in *nrc*^{a14}cones (A), indicating that the LC3 positive autophagosomes had not fused with an acidic compartment. Scale bar=2μm in A. Graph in (B) shows average Pearson's Coefficient, and graph in (C) shows average "Autolysosome value". Error bars are SEM and n=14 cells from 6 WT larvae and 11 cells from 6 *nrc*^{a14} larvae in both C and D. The Pearson's Coefficient and Autolysosome value were both significantly different between WT and *nrc*^{a14} cells (***=p-value<0.001, *=p-value<0.05 respectively as assessed by Student's t-test).

An accumulation of autophagosomes and defect in autophagosome-lysosome fusion could occur due to the inability of autophagosomes to move throughout the cell. Using live time-lapse confocal microscopy we found that LC3-labeled autophagosomes were highly mobile in both WT and *nrc*^{a14} cones (Figure 3.6 and Supplementary Movies). Specifically, we observed that autophagosomes found in the ISs of WT cones displayed limited movements; they traveled short distances in the IS and rarely travelled from the IS to the synapse (Figure 3.6A orange arrow and trace). In contrast, the LC3 puncta found at WT synapses moved rapidly to the IS where they appeared to stop or disappear (Figure 3.6B blue arrow and trace). The movements of autophagosomes in

nrc^{a14} cones were qualitatively similar, although we did note a few differences. As in WT cones, many of the puncta in the IS of *nrc*^{a14} cones traveled short distances; however, some puncta also traveled from the IS to the synapse. In addition, some synaptic puncta did not travel to the IS (Figure 3.6B orange arrow and trace), they remained in the synapse and made short range movements. Similar to WT cells, many synaptic LC3 positive puncta rapidly travelled from the synapse to the IS, but in contrast to what we observed in WT cones, rarely stopped or disappeared after reaching the IS; instead they often travelled back toward the synapse (Figure 3.6B blue arrow and trace). Together these data demonstrate that the loss of SynJ1 causes a significant block in autophagosome maturation, but this block does occur due to a loss of autophagosome mobility.

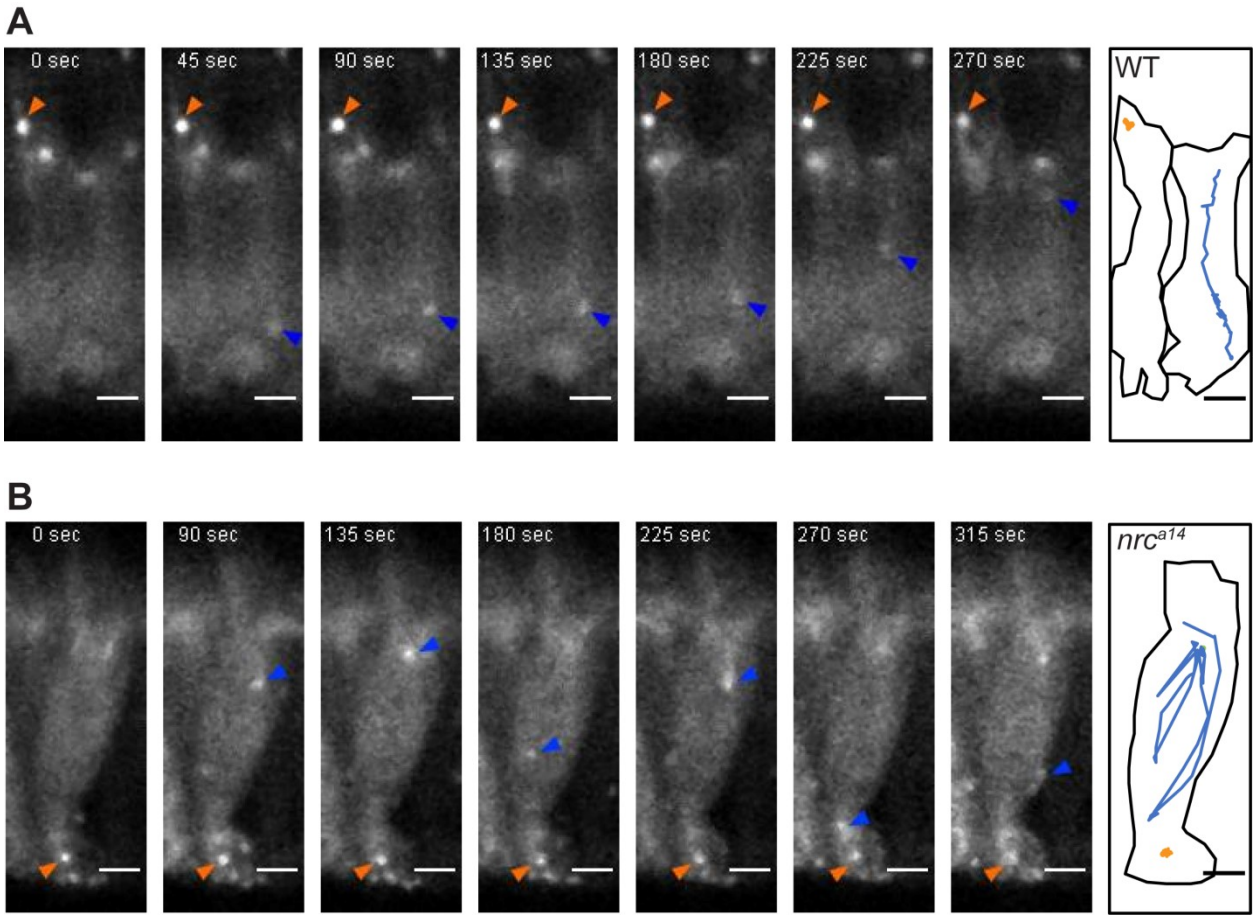

Figure 3.6: Mobility of autophagosomes is not reduced in *nrc*^{a14} cones. Live time-lapse images of *Tg(TαCP:GFP-LC3)* 5dpf zebrafish larvae show that autophagosomes are highly mobile in both WT and *nrc*^{a14} cones. Images were acquired in 5 second frame intervals. Select time points are shown for WT (A) and *nrc*^{a14} (B) cones. A schematic showing the outline of the cell(s) and movement of 2 representative

LC3 positive particles are shown for each video. In WT cells (A), LC3 positive autophagosomes are primarily found in the ISs where they make short movements (A, orange arrow and orange trace). Puncta located at the synapse travel to the IS (A, blue arrow and blue trace). Puncta in *nrc*^{a14} cones are also mobile (B). Puncta exhibit similar movements to those found in WT. Some remain in the IS and some move from the synapse to the IS. However; some puncta remain at the synapse and make short movements (B, orange arrow and trace), and the synaptic puncta that move from the synapse to the IS often remain mobile and return to the synapse (B, blue arrow and blue trace). Scale bar=2μm.

To define the enzymatic activity of SynJ1 involved in regulating the endolysosomal and autophagic systems in photoreceptors, we performed rescue experiments in *nrc*^{a14} cones with WT SynJ1 or SynJ1 containing mutations in the two conserved phosphatase domains. The 5'phosphatase domain has specific activity towards 5'phosphates, and the less-specific Sac1 domain has both 3'- and 4'-phosphatase activities (Guo et al., 1999). We transiently expressed FLAG-tagged zebrafish SynJ1 constructs (SJCs) in cones of *nrc*^{a14} *Tg(TαCP:GFP-LC3)* and *Tg(TαCP:GFP-Rab7)* larvae. Injection of DNA constructs into zebrafish larvae results in mosaic expression (Stuart et al., 1988), allowing us to examine both SJC positive and negative cones within the same retina. Rescue of the autophagosome and late endosome phenotypes by the SJCs in *nrc*^{a14} cones was assessed qualitatively by examining the morphology of Rab7 vesicles and quantitatively by counting the total number of LC3 puncta or synaptic Rab7 puncta per cell. The number of puncta in the SJC expressing cells was normalized to the number of puncta in the non-SJC expressing cells in the same larvae.

Expression of WT SynJ1 in WT cones did not affect the appearance of autophagosomes or late endosomes (Figure 3.7). Expression of WT SynJ1 in *nrc*^{a14} cones significantly (p-value <0.001) rescued the number of LC3 puncta (Figure 3.8A & C), synaptic Rab7 puncta (Figure 3.8B & D) and the abnormally enlarged Rab7 structures in *nrc*^{a14} ISs. Late endosomes appeared punctate in *nrc*^{a14} cones expressing the WT SJC, similar to the Rab7 structures observed in WT cones. Further, we observed significant rescue of both aberrant vesicles in ISs and synaptic morphology by EM analysis of *nrc*^{a14} mutant cones stably expressing a GFP-SynJ1 transgene (Figure 3.9).

Next we determined whether SynJ1 with a point mutation in the Sac1 catalytic domain could rescue the endolysosomal defects in *nrc*^{a14} cones. The Sac1 domain of zebrafish

SynJ1 contains a conserved $CX_5R(T/S)$ catalytic motif (Hughes et al., 2000). Mutating the conserved cysteine to serine results in a catalytically dead Sac1 domain in yeast (Stefan et al., 2002), mouse (Mani et al., 2007) and human (Krebs et al., 2013) Synaptojanin homologues. We generated the homologous C385S mutation in the Sac1 domain of zebrafish SynJ1. This mutation did not affect the localization of SynJ1, or exert dominant negative effects on WT cones (Figure 3.7). We found that the Sac1 mutant SJC was able to significantly rescue the total number of LC3 puncta (Figure 3.8C) and synaptic Rab7 puncta (Figure 3.8D) in *nrc*^{a14} cones, as well as the appearance of abnormal Rab7 structures in cone ISs (Figure 3.8 A & B middle panels). This observation indicates that the Sac1 phosphatase activity of SynJ1 is not required for proper endolysosomal and autophagic trafficking in cones. This suggests that SynJ1 does not play a direct role in regulating PI(4)P or PI(3)P in endolysosomal and autophagic trafficking.

Finally, we generated a catalytically dead D732A mutation in the 5'phosphatase domain of zebrafish SynJ1. The conserved motif XWXGDXN(F/Y)R is found in many 5'phosphatases (Jefferson and Majerus, 1996) and mutating the aspartate to alanine results in the loss of 5'phosphatase activity of yeast (Whisstock et al., 2000) and mouse (Mani et al., 2007) Synaptojanin. As with the C385S mutation, the D732A mutation did not appear to affect the localization of SynJ1 or have an effect on WT cones (Figure 3.7). In contrast to the Sac1 C385S point mutation, the D732A mutation was not able to rescue either the LC3 (Figure 3.8C) or Rab7 (Figure 3.8D) phenotype in *nrc*^{a14} cones. The *nrc*^{a14}cones expressing the D732A SJC still exhibited an accumulation of GFP-LC3 puncta as well as abnormal Rab7 structures (Figure 3.8 A & B bottom panels). This result indicates that SynJ1 is required to regulate a PIP species with a 5'phosphate, and that defects in this process are involved in the observed late endosome and autophagosome abnormalities observed in *nrc*^{a14} cones.

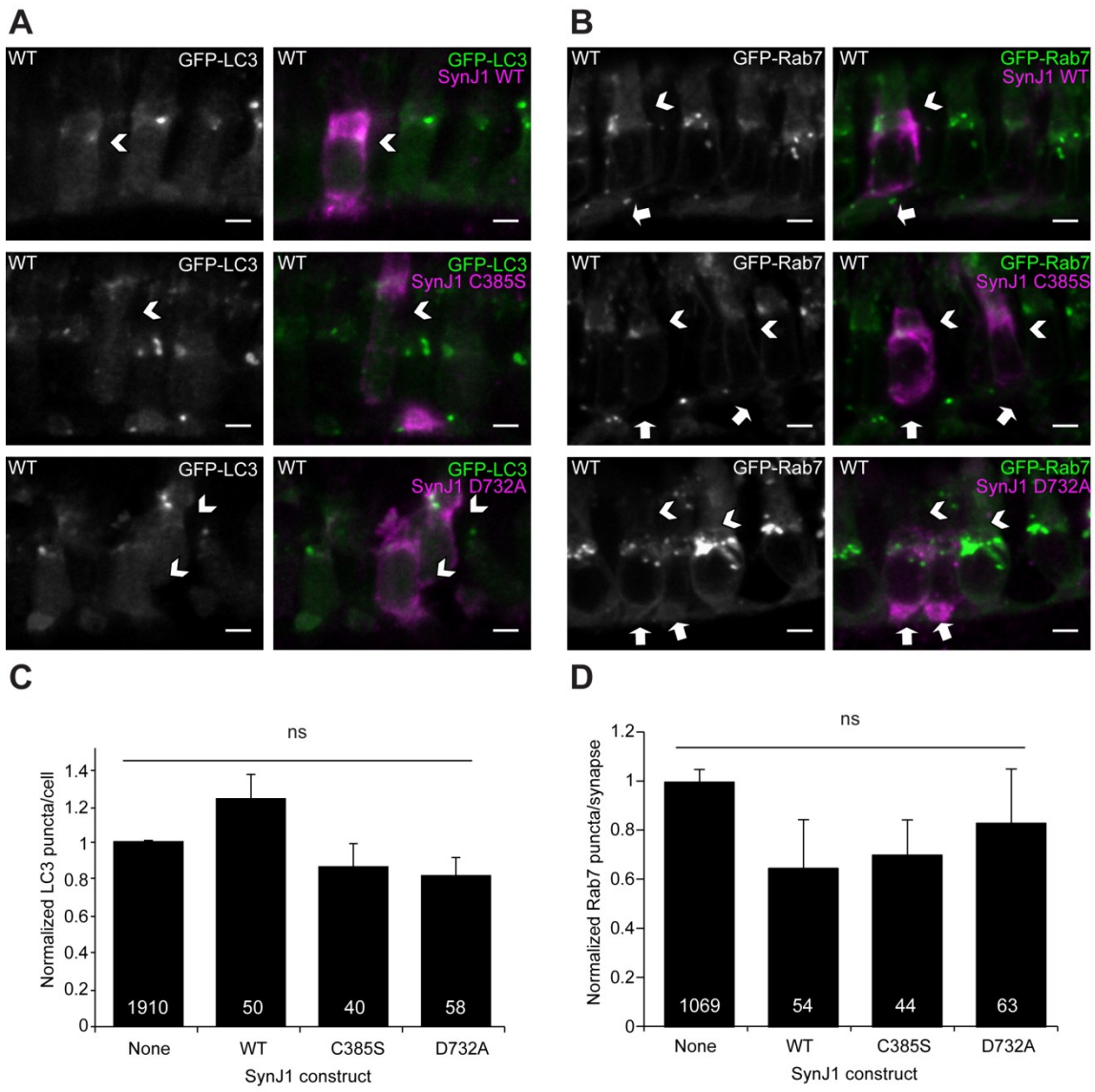

Figure 3.7: Expression of SJCs in WT cones does not affect the appearance of late endosomes or autophagosomes. Fixed sections of 5dpf WT *Tg(TαCP:GFP-LC3)* (A) and *Tg(TαCP:GFP-Rab7)* (B) larvae transiently expressing SJCs in cones. All constructs appeared to have the same cellular distribution and did not affect the number or appearance of LC3 or Rab7 positive vesicles. Arrows point to SJC expressing cells (magenta in merge). Scale bar=2μm in all images. Results were quantified by counting the number of total LC3 puncta (B) or Rab7 synaptic puncta (D) in the SJC expressing cells and normalized to the number of puncta in the non-SJC expressing cells in the same WT larvae. Graph in B shows average normalized LC3 puncta per cell, and Graph in D shows average normalized synaptic Rab7 puncta per cell. Error bars are SEM and n≥40 cells for all conditions (exact n shown on graph). There was no significant change of either the total LC3 puncta or Rab7 synaptic puncta for any SJC (by One-Way ANOVA followed by Dunnett's multiple comparison correction).

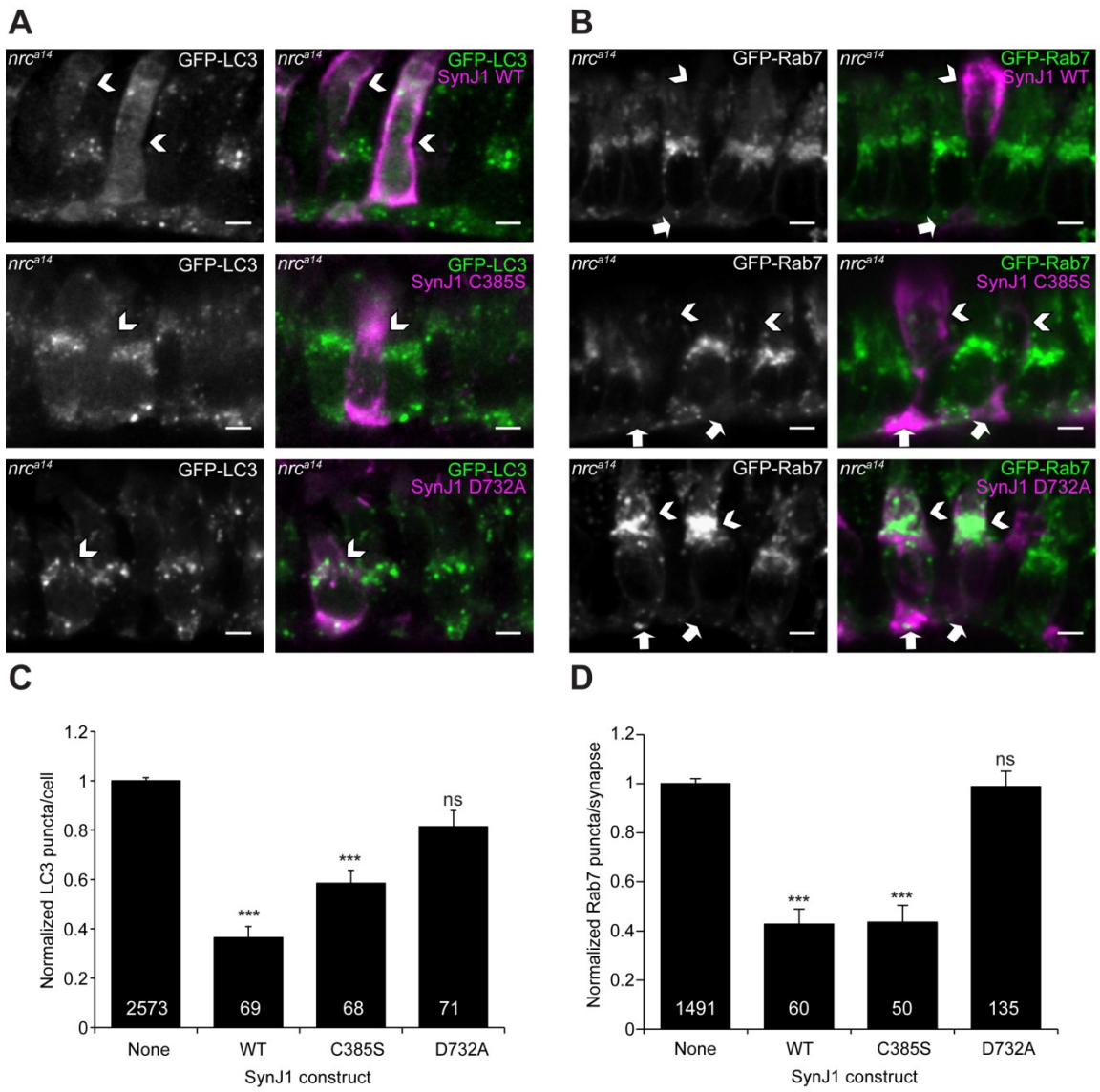

Figure 3.8: 5'phosphatase activity of SynJ1 is required to rescue late endosome and autophagy phenotypes in *nrc^{a14}* cones. Fixed sections of 5dpf *nrc^{a14} Tg(TαCP:GFP-LC3)* (A) and *Tg(TαCP:GFP-Rab7)* (B) larvae transiently expressing SJCs in cones. WT SynJ1 was able to significantly rescue both the late endosome and autophagosome abnormalities in *nrc^{a14}* cones. SynJ1 lacking SacI catalytic activity (C385S) also significantly rescued the late endosome and autophagosome defects. In contrast, the D732A construct was not able to rescue either the late endosome or autophagosome phenotypes. Arrows point to SJC expressing cells (magenta in merge). Scale bar=2μm in all images. Results were quantified by counting the number of total LC3 puncta (B) or Rab7 synaptic puncta (D) in the SJC expressing cells and normalized to the number of puncta in the non-SJC expressing cells in the same *nrc^{a14}* larvae. Graph in B shows average normalized LC3 puncta per cell, and Graph in D shows average normalized synaptic Rab7 puncta per cell. Error bars are SEM and n≥50 cells for all conditions (exact n shown on graph). The rescue of both the total LC3 puncta and Rab7 synaptic puncta was significant for the WT and C385S SJCs, but not for the D732A SJC. (***=p-value<0.001 by One-Way ANOVA followed by Dunnett's multiple comparison correction).

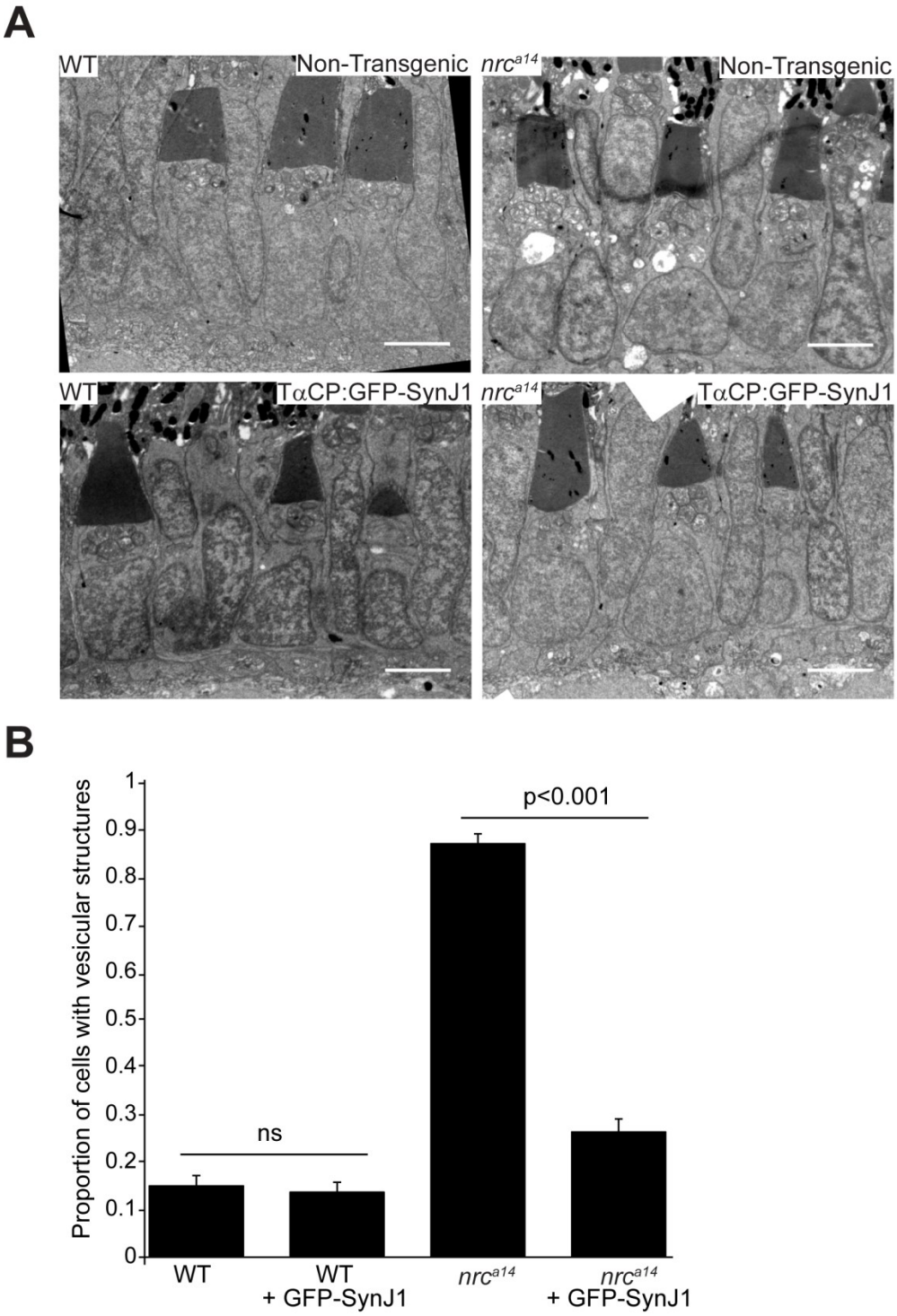

Figure 3.9: Expression of GFP-tagged WT SynJ1 decreases vesicular structures in *nrc^{a14}* cones. Transmission Electron Microscopy (TEM) images of retinas from non-transgenic or *Tg(TαCP:GFP-SynJ1)* WT and *nrc^{a14}* 5dpf larvae. Vesicular structures accumulate in non-transgenic *nrc^{a14}* cone ISs. There is a significant decrease in the number of cells containing vesicular structures in *nrc^{a14}* larvae expressing GFP-SynJ1. Error bars show standard error of a proportion, n≥150 cells for all conditions, p value calculated using Fisher's exact test. TEM was performed at the UW vision core using standard methods.

Together our data show that SynJ1 is acting on a PIP species with a 5'phosphate to cause defects in autophagosome maturation resulting in an increase of PI(3)P positive structures in cones lacking SynJ1. We have established a specific role for SynJ1 in endolysosomal trafficking and defined the functional activity required to regulate this process.

Discussion

SynJ1 is well known for its key role in neurons in clathrin-mediated endocytosis both pre- and post-synaptically (Cremona et al., 1999; Gong and De Camilli, 2008). Recent studies have uncovered links between SynJ1 and Alzheimer's and Parkinson's disease, which highlight the importance of synaptic vesicle recycling and lipid metabolism in maintaining neuronal health (Berman et al., 2008; McIntire et al., 2012; Krebs et al., 2013; Quadri et al., 2013). However, recent studies have also demonstrated roles for this PIP phosphatase in cellular functions other than clathrin-mediated endocytosis. In an Alzheimer mouse model, SynJ1 knockdown resulted in accelerated delivery of amyloid beta (Aβ) to lysosomes (Zhu et al., 2013). Further, our recent work shows that in photoreceptors, SynJ1 plays a role in vesicle trafficking distinct from synaptic vesicle recycling, and is specifically involved in the autophagic and endolysosomal pathways (George et al., 2014). In addition, the involvement of SynJ1 in protein degradation pathways could help explain the pathology observed in a recently identified human *synj1* mutation in a young patient with a taupathy (Dyment et al., 2014). The study we present here represents a detailed mechanistic analysis of SynJ1 function in protein degradation trafficking pathways.

To dissect the defect in the autophagic/endolysosomal pathway we used multiple strategies that exploit the ability to image fluorescent molecules in live zebrafish. The zebrafish model is also a unique tool to characterize vesicle transport and associated diseases in the retina due to the rapid development of the eye. In zebrafish, photoreceptors develop and become functional long before SynJ1-deficient animals die. Using live imaging and genetically encoded indicators for $PI(3,5)P_2$, PI(3)P, PI(4)P or $PI(4,5)P_2$ we did not detect gross changes in distributions of these PIPs. Importantly, we did not detect $PI(4,5)P_2$ containing vesicles within mutant photoreceptor ISs. Thus,

$PI(4,5)P_2$ accumulation on endocytic structures does not underlie defects in endolysosomal/autophagic trafficking.

Our functional analysis of autophagic flux using mCherry-GFP-LC3 indicated that maturation of autophagosomes is impaired in *nrc*^{a14} cones. We found fewer LC3-tagged molecules in acidic compartments in *nrc*^{a14} than in wild type cones. PIPs have been shown to directly modulate kinesin motors (Klopfenstein and Vale, 2004) and autophagosomes are transported along microtubules (Fu et al., 2014). SynJ1 is also known from many studies to modulate the actin cytoskeleton by regulating $PI(4,5)P_2$ levels (Qualmann and Kessels, 2002; Van Epps et al., 2004). Therefore we investigated whether the impaired maturation was due to a change in vesicle mobility. GFP-labeled autophagosomes in *nrc*^{a14} cones showed rapid apical and basal transport and easily traversed from the synapse to the IS, where we observe autolysosomes in WT cones. Like autophagosomes, late endosomes fuse with lysosomes in order to fully degrade their contents (Mullock et al., 1998). An inability of lysosomes to fuse with other compartments, such as autophagosomes and late endosomes, could explain both the accumulation of autophagosomes and abnormal late endosomes observed in *nrc*^{a14} cones.

The requirement for PI(3)P synthesis in the formation of autophagosomes is conserved from yeast to mammalian cells; however, the distribution of PI(3)P on autophagosomal membranes varies from species to species. In yeast, light and electron microscopy studies have also shown that PI(3)P colocalizes with ATG8 (the yeast LC3 homologue) and resides on both the inner and outer membranes of the yeast autophagosome (Obara et al., 2008; Cheng et al., 2014). In the invertebrate model *Drosophila melanogaster*, PI(3)P colocalizes with LC3 positive autophagosomes during starvation-induced autophagy (Juhasz et al., 2008). In mammalian cell lines electron microscopy studies have found PI(3)P on the outer membrane of autophagosomes(Cheng et al., 2014). However; light microscopy studies using the 2XFYVE PI(3)P probe show very little colocalization between PI(3)P and LC3 (Axe et al., 2008). In WT zebrafish cone photoreceptors, we observe very little overlap between LC3 and the PI(3)P marker 2XFYVE. However, it is possible that the increased PI(3)P puncta we observe

correspond to autophagic membranes that have not yet acquired LC3. Indeed, some of the 2XFYVE positive structures appear donut shaped and resemble autophagosome assembly sites known as omegasomes (Axe, 2008; Itakura and Mizushima, 2010). It has been demonstrated that the PI(3)P phosphatase Jumpy is required for autophagosome maturation, suggesting that removal of PI(3)P from the autophagosome membrane is important in this process(Vergne et al., 2009). We observe an increase in both LC3 positive puncta and PI(3)P positive puncta in *nrc*^{a14} photoreceptors. One possibility could be that SynJ1 is required to dephosphorylate PI(3)P in order for autophagosomes to mature. This hypothesis does not appear to be true as there is very little colocalization between LC3 and PI(3)P in *nrc*^{a14} cones.

As an additional strategy, we conducted a mutational analysis of the two SynJ1 phosphatase domains. The 5' phosphatase specifically removes phosphates from the 5' position of the inositol ring. The Sac1-like domain of SynJ1 is less specific and can act on phosphates at both the 3' and 4' positions on the inositol ring (Guo et al., 1999; Mani et al., 2007). Previous studies examining the roles of the different SynJ1 domains have focused on the contribution of these domains in synaptic vesicle recycling. Both the 5' phosphatase and the Sac1-like activity play roles in this process. However, loss of 5' phosphatase activity had more severe consequences than loss of Sac1-like activity and caused impaired endocytosis defects over a broader range of stimuli (Mani et al., 2007). Further, recent studies examining patients with early onset Parkinson's disease have discovered linked mutations in the Sac1 domain of SynJ1 and thus prolonged loss of this activity appears to also have dire effects (Krebs et al., 2013; Quadri et al., 2013). Our work indicates that loss of the 5' phosphatase activity of SynJ1 is more detrimental than the loss of Sac1 activity in endolysosomal trafficking in cone photoreceptors. We found that constructs lacking 5' phosphatase activity could not rescue the accumulation of late endosomes and autophagosomes in *nrc*^{a14} cones; however loss of Sac1 catalytic activity could significantly rescue these phenotypes. Our data revealed a slight (but not significant) impairment in the ability of SynJ1 lacking Sac1 activity to rescue the accumulation of autophagosomes relative to wild type SynJ1. Overall, our data indicates that a PIP with a 5' phosphate is involved in the pathology characterized in this study.

One of the unique features of photoreceptors is their critical dependence on vesicle transport. OSs are partially renewed daily and synapses are specialized for constant vesicle release (Kevany and Palczewski, 2010; Matthews and Fuchs, 2010). These actively studied functions require photoreceptors to maintain optimized and highly regulated vesicle trafficking pathways (Regus-Leidig and Brandstatter, 2012; Pearring et al., 2013; Wang and Deretic, 2014). Surprisingly little is known about other vesicular trafficking pathways such as how proteins are sorted within ISs, recycled and ultimately processed for degradation. Our study has defined a novel role for SynJ1 in a degradative pathway in cone photoreceptors. SynJ1 mutants have impaired autophagosome maturation, and the specific loss of 5' phosphatase, but not Sac1 activity, leads to abnormal accumulation of late endosomes and autophagosomes.

Materials and Methods

Ethics statement. This study was carried out in strict accordance with the recommendations in the Guide for the Care and Use of Laboratory Animals of the National Institutes of Health. The protocol, 3113-01, was approved by IACUC of the University of Washington.

Cloning and plasmids. The PLCδ pleckstrin homology domain was purchased from Addgene (plasmid #21262). The PLCδ PH and FAPP1 PH (Tim Levine, (Levine and Munro, 2002)) were PCR amplified and inserted into Gateway pDONRP2R-P3 vectors using standard Gateway cloning protocols (Invitrogen). The PI(3)P probe 2XFYVE has previously been characterized (Gillooly et al., 2000). The YFP-2XFYVE (Harold Stenmark) clone was created by inserting YFP with a C-terminal linker and EcoRI cut site into a pDONR221 vector. 2XFYVE was then amplified with an N-terminal EcoRI site and inserted into the pME YFP vector. The mCherry-ML1NX2 (Haoxing Xu) clone has been previously characterized (Li et al., 2013), and was inserted into a pDONR221 vector. The full length zebrafish *synJ1* gene cDNA has previously been cloned by our lab (Holzhausen et al., 2009). An N-terminal FLAG tag was added using overhang PCR methods and the full length clone FLAG-tagged clone was inserted into a pCR8/GW Gateway vector (Invitrogen). The C385S and D732A mutations were created using standard site-directed mutagenesis. The tandem mCherry-GFP-LC3 clone was created

by inserting mCherry with a C-terminal linker and EcoRI cut site into a pDONR221 vector. GFP-tagged zebrafish LC3 (He et al., 2009) was then amplified with an N-terminal EcoRI site and inserted into the pME mCherry vector. Expression constructs and other fluorescent protein fusions were generated using the MultiSite Gateway System (Invitrogen) and the Tol2 kit. Expression was driven by the *cone transducin alpha* promoter (*TαCP*) (Kennedy et al., 2007) or the *cone-rod homeobox* promoter (*crx*)(Suzuki et al., 2013).

Fish husbandry and generation of transgenic zebrafish. Zebrafish were reared and maintained in the University of Washington fish facility as previously described (Westerfield, 1995). Embryos were maintained in embryo media (EM) at 28°C on a 14/10hour light/dark cycle prior to experimentation or rearing in the fish facility. Homozygous *nrc*^{a14} mutants were identified by the optokinetic response assay (OKR) or by genotyping as previously described (Brockerhoff, 2006; George et al., 2014). Because WT and *nrc*^{a14} heterozygotes appear indistinguishable in every phenotypic assay we have performed, we refer to all OKR-positive larvae as WT. The *Tg(crx:Man2a-GFP)*, *Tg(TαCP:GFP-Rab7)* and *Tg(TαCP:GFP-LC3)* fish lines have been previously described (George et al., 2014). We created other transgenic fish lines as previously described (Kikuta and Kawakami, 2009; George et al., 2014). Newly identified transgenic fish were assayed by OKR at 5dpf to ensure that transgene expression did not affect visual responses.

Immunohistochemistry. All zebrafish larvae were fixed at the indicated developmental stage between 12pm and 1pm to minimize variation caused by circadian effects. Retinal slices were prepared as previously described (Brockerhoff et al., 1997). To detect FLAG-tagged SJCs, slices were incubated with 1:1000 anti-FLAG M2 (Sigma) primary antibody at 4°C overnight followed by secondary anti-mouse Alexa 568 (Invitrogen, A11002) at 1:200 for 1 hour at room temperature. Nuclei were counter stained with 5μM Hoechst (Invitrogen). Slides were mounted with a coverslip and Fluoromount-G (Southern Biotech). Imaging of retinal sections was performed on an Olympus FV1000 confocal microscope with a 60X 1.35NA oil immersion objective. Fluoview software (Olympus version 2.0c) was used to acquire images.

Live Imaging. Larvae were treated with 0.003% 1-phenyl-2-thiourea (PTU) in EM at ~24 hours post fertilization (hpf) to prevent melanization. Larvae were anaesthetized in Tricaine (Sigma) and mounted in warm 0.5-1% low mount agarose. Embedded larvae were covered in EM containing PTU and Tricaine and imaged. Imaging was performed on an Olympus FV1000 at room temperature using a 40X 0.8NA water immersion objective. Fluoview software (Olympus version 2.0c) was used to acquire images.

Transmission electron microscopy. Transmission electron microscopy was performed at the UW Vision Core as previously described (Schmitt and Dowling, 1999). For quantification, the entire retina was imaged.

Image processing and data analysis. Images were processed using NIH ImageJ (v1.49). Representative images in Figures 3.1-3, 3.6-8 are 2μm MAX projections of confocal stacks; Figures 3.4 and 3.9 show single optical sections; Figure 3.5 shows average projections of a single cell. Contrast was adjusted and a 1 pixel median filter was applied to representative images in ImageJ, any adjustments were applied to in the exact same manner to WT and *nrc*^{a14} images. All analysis was carried out on unprocessed images. Prior to analysis, images were assigned random numbers. For qualitative comparisons between WT and *nrc*^{a14} larvae, at least 6 larvae of each genotype were analyzed. For quantitative data, the number of larvae analyzed is included in the text and Figure legends. Microsoft Excel 2010 and R (v3.0.1) were used for statistical analysis. Error bar values and statistical tests are described in Figure legends.

Colocalization analysis was carried out in Olympus Fluoview (Version 2.0c) software. Each image comprised 7–12 z-slices at 0.5μm depth, for a total of 3.5–6 μm depth depending on the shape of the cell. The integrated density of expression was calculated for the GFP and mCherry channels of cells expressing*TαCP:mCherry-GFP-LC3*. The resulting Pearson's coefficient was recorded and compared between WT and *nrc*^{a14} zebrafish larvae. The "Autolysosome value", a sum of the area of mCherry signal per cell where GFP signal is not present, was calculated for *TαCP:mCherry-GFP-LC3* expressing cells. GFP and mCherry images were cropped to show a single cell and saved separately as text files in ImageJ V1.46r, opened in Microsoft Excel 2010 and

mCherry/GFP ratios were calculated. A threshold of 0.8 was set and values were converted to binary whereby all cells with values above 0.8 were denoted 1 and all below were denoted 0. The autolysosome value is the sum of the 1's.

Acknowledgements. Part of the work described in this Chapter is from a manuscript in preparation. The other authors are Gail R. Stanton, Sara Hayden and Susan E. Brockerhoff. We thank Jing Huang and Ed Parker at the UW Vision core for help with preparing retinal slices and electron microscopy respectively. We thank Harold Stenmark (Oslo University Hospital), Haoxing Xu (University of Michigan) and Tim Levine (University College London) for contributing plasmids. We thank Neil Wilson (University of Washington) for assistance with Gateway cloning and Daryl Phuong (University of Washington) for assistance with genotyping. This work is supported by NIH grant EY015165 (SEB), and NEI grant EY001730, which supports the UW Vision Core. The content is solely the responsibility of the authors and does not necessarily represent the official views of the National Institutes of Health. The funders had no role in study design, data collection and analysis, decision to publish, or preparation of the manuscript.

Supplementary movies 1 and 2: Time-lapse videos of autophagosomes in WT and *nrc^{a14}* cones. Live time-lapse movies of *Tg(TαCP:GFP-LC3)* 5dpf zebrafish larvae show that autophagosomes are highly mobile in both WT (movie 1) and *nrc^{a14}* (movie 2) cones. Live Images were acquired in 5 second frame intervals on an FV1000 Olympus confocal microscope. Arrows are color coded the same as in Figure 3.5, scale bar=2μm.

Chapter 4

Conclusions and Future Directions

Characterization of the trafficking defects in *nrc^{a14}* cones

Previous studies characterizing *nrc^{a14}* cones found that these cells have abnormal synaptic terminals with floating ribbons and a decreased number of synaptic vesicles (Allwardt et al., 2001; Van Epps et al., 2004). An abnormal distribution of the synaptic vesicle protein VAMP2 suggested that these cones might have a defect in protein trafficking (Holzhausen et al., 2009). In order to determine the organelles/trafficking pathways that are disrupted in the *nrc^{a14}* cones we used a combination of genetically encoded probes and dyes to investigate the actin cytoskeleton, endoplasmic reticulum, Golgi apparatus, early endosomes, late endosomes, lysosomes, and synaptic vesicles. We found that *nrc^{a14}* cones had normal endoplasmic reticulum and early endosomes. The Golgi apparatus in *nrc^{a14}* cones develops normally until 4dpf but becomes disordered at 5dpf. There is a decrease in the number of synaptic vesicles at the synapse, and an accumulation of synaptic proteins in the inner segment. Finally we observed abnormal late endosomes and lysosomes, and an accumulation of LC3 positive autophagosomes (Figure 4.1). Unlike the Golgi phenotype, the disrupted late endosomes and autophagosomes were apparent at 3dpf.

Figure 4.1: Summary of trafficking defects in *nrc*^{a14} cone photoreceptors.

To further understand the autophagy defects in *nrc*^{a14} mutants we generated a tandem mCherry-GFP-LC3 construct which allows the differentiation between autophagosomes and amphisomes/autolysosomes (Kimura et al., 2007). Preliminary experiments indicated that there are fewer autolysosomes in *nrc*^{a14} mutants suggesting that the maturation of autophagosomes is blocked. In order to validate these results we have generated a transgenic fish line *Tg(TαCP:mCherry-GFP-LC3)* which expresses the tandem construct in cone photoreceptors. Transient expression of fluorescently-tagged LC3 results in a large amount of cytosolic expression, making the quantification of punctate autophagosomes difficult. Stable lines (both cell lines and whole animal lines) show better distribution of LC3 to punctate structures. In WT cone photoreceptors, the tandem construct has some cytosolic distribution and localizes to punctate structures both with and without mCherry signal (Figure 4.2). Our fish line has been crossed into the *nrc*^{a14} background, however we do not yet have heterozygous breeding adults, and have not been able to analyze *nrc*^{a14} mutants carrying this transgene. This line will be a useful tool for understanding the regulation of autophagy in cone photoreceptors.

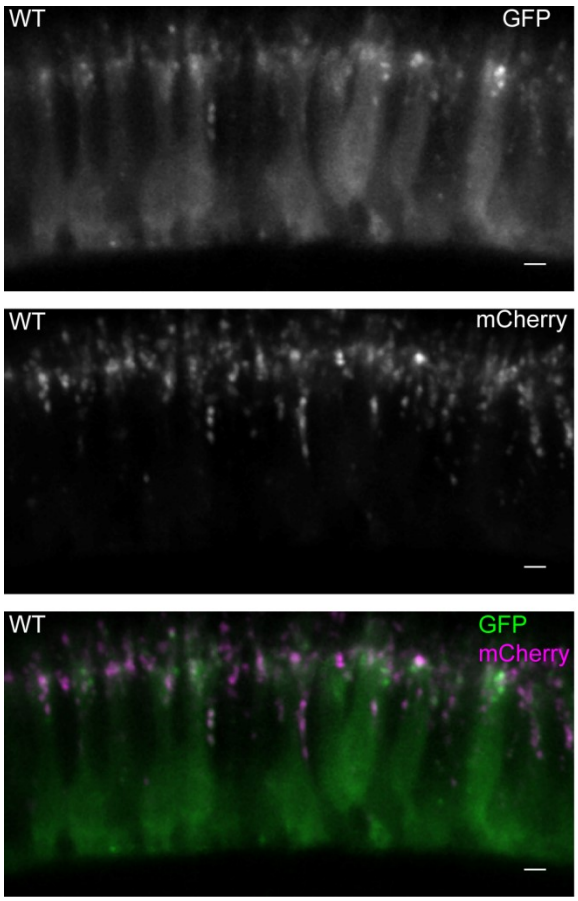

Figure 4.2: Expression of tandem mCherry-GFP-LC3 in *Tg(TαCP:mCherry-GFP-LC3)* WT cone photoreceptors. The tandem construct localizes to autophagosome membranes. Once the autophagosome fuses with an acidic compartment, the GFP signal is quenched. Puncta with both GFP and mCherry signal are autophagosomes, whereas puncta with only mCherry signal are amphisomes and autolysosomes.

A defect in lysosomal protein degradation explains the asymmetric cellular phenotypes in *nrc*^{a14} cones; the OSs appear morphologically normal and are able to undergo phototransduction, whereas the synaptic terminals have severe abnormalities. This correlates with the reliance of these different two subcellular compartments on lysosomal degradation. OS membranes and proteins are degraded by the RPE cells during OS disc shedding (O'Day and Young, 1978). Synaptic proteins rely on protein degradation systems within the photoreceptor cell. Interestingly, there are some proteins which translocate between the OS and the IS depending on light conditions (Arshavsky, 2003). We predict that these proteins would be partially affected by abnormal lysosomal degradation. Many of these proteins are involved in adaptation of

photoreceptors to background light. Interestingly, our lab has previously shown that *nrc*^{a14} retinas have defects in background light adaptation (Van Epps et al., 2001), consistent with distribution of these proteins.

The distribution of phosphoinositides in WT and *nrc*^{a14} cone photoreceptors

In order to understand the role of the polyphosphoinositide phosphatase SynJ1 in regulating endolysosomal and autophagic trafficking in cone photoreceptors we need to determine the relevant SynJ1 PIP substrates involved in these processes. In order to accomplish this, we used two main strategies: analyzing the distribution of PIPs in live cones using genetically encoded PIP probes, and performing rescue experiments in *nrc*^{a14} cones by expressing SynJ1 with point mutations in the catalytic domains. Our analysis of the distribution of PIPs in cone photoreceptors also provided information about the distribution of PIPs in this specialized neuronal cell type. The distribution of PIPs has not been investigated in live vertebrate photoreceptors. We found that in WT cone photoreceptors PI(4,5)P_2 localizes throughout the plasma membrane and is concentrated at synaptic terminals. We found that PI(4)P localized to the Golgi apparatus and partially overlapped with a medial Golgi maker. PI(3)P was found primarily on punctate structures, and colocalized with some Rab7 positive structures. Finally we found that PI(3,5)P_2 localized to punctate structures, some of which were Rab7 positive. Interestingly, we did not detect the presence of any of the PIPs we analyzed in cone outer segments. Previous studies have found the presence of many PIP modulating enzymes including the PI3P kinase Vps34(Chuang et al., 2007), the class IA phosphoinositide 3-kinase(Guo et al., 1997), and the type II phosphatidylinositol 5-phosphate 4-kinase (PIPKIIα) (Huang et al., 2011) in rod outer segments. The presence of these enzymes suggests that PIPs are present and important molecules in OS membranes. These studies have been performed in rod OSs. It is possible that there are differences in the distribution of both PIPs between rods and cones. However, PIPs have also been found to be able to regulate cone-specific CNG channels (Bright et al., 2007; Dai et al., 2013; Dai and Varnum, 2013), suggesting that PIPs are important in both cone and rod OSs. It may be that PIPs are rapidly turned over in Oss and their steady state levels are too low to observe with our

genetically encoded probes. An alternative explanation is that the PIP probes used in our studies might be excluded from the OS in live cones, explaining the absence of a signal. If the genetically encoded probes are excluded from the OS, then the distribution of PIPs in OSs would need to be investigated in fixed retinal sections using anti-PIP antibodies or exogenously applied PIP-binding domains. Examining PIP distribution in dead, fixed cells needs to be performed carefully; both fixation and permeabilization conditions can introduce artifacts, and different PIPs require different conditions for proper detection (Hammond et al., 2006; Hammond et al., 2009). These effects can be even more difficult to control for in a thick tissue than in cell culture. Indeed, a recent study examined the distribution of PIPs using anti-PIP antibodies in fixed retinal slices. They observed $PI(4,5)P_2$ in cell nuclei, and not in the plasma membrane. Additionally, in some of their images PI(3)P also localizes to cell nuclei, whereas in other images it localizes to punctate structures (Rajala et al., 2014).

We found no significant difference between the distribution of PIPs in WT and *nrc*^{a14} cones other than an increase in the number of PI(3)P positive puncta. Because the distribution of early endosomes appears normal in *nrc*^{a14} cones, we suspect these additional PI(3)P puncta correspond to membranes involved early in autophagosome biogenesis such as omegasomes or early isolation membranes. In order to test this theory we would need to examine the distribution of ATG proteins involved in early steps of autophagosome biogenesis such as ATG16L1. .

SynJ1 regulates a PIP with a 5'phosphate

In order to determine which SynJ1 catalytic domain was relevant for endolysosomal and autophagic trafficking we performed rescue experiments in *nrc*^{a14} cones with WT and catalytic domain mutants of SynJ1. We found that SynJ1 with no Sac1 Catalytic activity could rescue the *nrc*^{a14} phenotype, indicating that the Sac1 domain of SynJ1 does not directly regulate PI(3)P in the trafficking pathways we studied. SynJ1 with no 5'phosphatase activity is not able to rescue the autophagy or late endosome phenotypes. The relative importance of the different catalytic domains is consistent with findings in other organisms (Mani et al., 2007). Therefore, the most physiologically relevant PIP substrate of SynJ1 contains a 5'phosphate.

The plasma membrane has been found to be a source of membranes for the formation autophagosome precursors that are positive for ATG16L, but negative for LC3 (Ravikumar et al., 2010). Increasing $PI(4,5)P_2$ on the plasma membrane leads to an increase in both LC3 negative autophagosome precursors as well as LC3 positive autophagosomes (Moreau et al., 2012). The phenotypes we observe in *nrc*^{a14} mutants and the results of our rescue experiments are consistent with an increase in $PI(4,5)P_2$. We hypothesize that an overload within the degradative could also impair fusion of Rab7 vesicles with lysosomes. The pronounced abnormalities in synaptic cellular structure detected in *nrc*^{a14} may also upregulate autophagy. In fact, a significant increase in autophagosome number at the synapse was detected in our analyses, which is consistent with this idea. A marker expressed early during autophagosome formation and our analysis of the transgenic fish line *Tg(TαCP:mCherry-GFP-LC3)* will help us verify these ideas.

Future Directions

There are still many unanswered questions regarding the role of SynJ1 in cone photoreceptors.

What PIP(s) is SynJ1 regulating? Our mutational analysis of SynJ1 has indicated that SynJ1 regulates a PIP with a 5'phosphate. Although this is an important step to identifying the relevant PIP species, further work is still needed. One way to answer this question is to modulate the levels of specific PIPs and observe whether these effects can phenocopy the *nrc*^{a14} mutation in WT cells, or rescue the phenotypes in *nrc*^{a14} cells. Many techniques have been developed for modulating PIP levels; there are pharmacological agents that inhibit specific kinases and phosphatases, and more recent techniques employ inducible dimerization systems to control the levels of specific PIPs with high temporal and spatial control. We have attempted to treat zebrafish with drugs such as LY294002; however we observed no effect on cone photoreceptors, most likely due to an inability of the drug to cross the blood-retina barrier in sufficient quantities. The use of the inducible dimerization systems in our model is also difficult. One system uses a rapamycin analog to induce dimerization. This system suffers from the same pitfalls as other drug treatments; the drug may not sufficiently cross the blood-retinal

barrier. In addition, the added time that a drug would take to diffuse into the retina if it could would result in a loss of the temporal control which is available in cell culture systems. Other inducible dimerization techniques use light as a control mechanism. The fact that we are working with a light-responsive tissue makes these systems also difficult to employ. Because of these issues, we have decided to transiently express proteins involved in the regulation of specific PIPs in cone photoreceptors, similar to our SynJ1 rescue experiments.

One candidate protein that we are using to manipulate PIPs in cone photoreceptors is the small GTPase Arf6. Arf6 is involved in controlling $PI(4,5)P_2$ levels by recruiting the PI5P kinase to the plasma membrane. Additionally, this protein has been implicated in the formation of pre-autophagosomal membranes through its effects on $PI(4,5)P_2$ (Moreau et al., 2012). This small GTPase also has characterized mutations that result in constitutively active (CA) or dominant negative (DN) activity. We have cloned the zebrafish homologue of Arf6 as well as CA and DN constructs and have begun performing experiments to determine the effects of altering $PI(4,5)P_2$ levels on endolysosomal trafficking in cone photoreceptors.

If SynJ1 is regulating endolysosomal and autophagic trafficking through effects on $PI(4,5)P_2$, what is the mechanism? (Figure 4.3) Is it due to an upregulation of autophagy by supplying additional membranes to pre-autophagosomal structures? Another possibility is that SynJ1 affects late endosomes and autophagy through effects on the actin cytoskeleton, a mechanism that has been documented in cell culture (Monastyrska et al., 2009; Kirkbride et al., 2012). The cones in *nrc*^{a14} mutants are known to have alterations in their actin cytoskeleton (Van Epps et al., 2004). We have generated the zebrafish line *Tg(TαCP:Lifeact-GFP*) which labels f-actin (Riedl et al., 2008) in cone photoreceptors to help investigate this possibility.

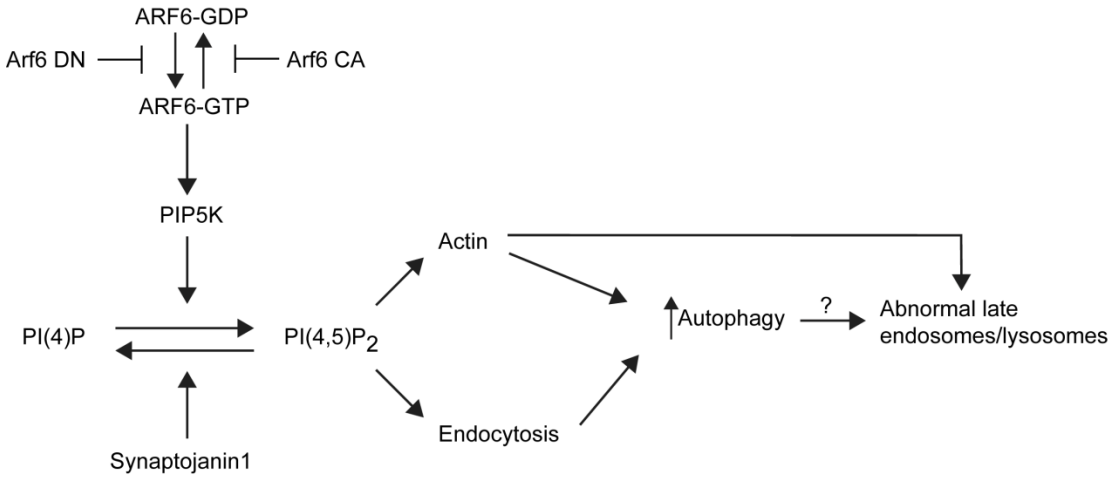

Figure 4.3: Possible mechanisms through which PI(4,5)P_2 could regulate autophagy. SynJ1 negatively regulates PI(4,5)P_2 levels by hydrolyzing PI(4,5)P_2 to PI(4)P (and possibly further to PI). In the absence of SynJ1, increased PI(4,5)P_2 could cause alterations in autophagy by increasing the delivery of membrane from the plasma membrane to preautophagic membranes (Ravikumar et al., 2010; Moreau et al., 2012) . PI(4,5)P_2 could also have effects on autophagy and late endosomes/lysosomes by altering the actin cytoskeleton (Aguilera et al., 2012; Kirkbride et al., 2012)

How is SynJ1 activity regulated in cone photoreceptors? SynJ1 is known to undergo post-translational modifications such as phosphorylation and ubiquitination in multiple organisms (McPherson et al., 1994a; Cousin and Robinson, 2001; Lee et al., 2004; Cao et al., 2014; Guiney et al., 2014). In addition, SynJ1 localization may also change in neurons in response to changing synaptic activity. We have generated transgenic zebrafish lines expressing FLAG- and GFP-tagged SynJ1 specifically in cone photoreceptors. Because the tagged-SynJ1 is only expressed in cones, pull-down experiments using anti FLAG or GFP antibodies would allow the analysis SynJ1 in cones to be separated from the SynJ1 pool from the other neurons in the zebrafish. The effects on SynJ1 of changing cone synaptic activity, through different lighting conditions could then be investigated.

Is the regulation of endolysosomal and autophagic trafficking by SynJ1 unique to zebrafish photoreceptors? Although SynJ1 is expressed in other neurons in the zebrafish, we have not investigated whether the cellular phenotypes of the cone photoreceptors are found in other neuronal cell types in the *nrc*^{a14} mutants. The identification of neurodegenerative disease-causing mutations in the human *syn1* gene

suggests zebrafish *synJ1* mutants could be used as models to understand human neurodegenerative diseases. There are many identified zebrafish *synJ1* alleles, and new technologies in genome editing such as the CRISPR/Cas9 system, allows for the targeted creation of new mutations.

Appendix 1

Transgenic fish lines used in this study

Line name	Description	Generated by
Tg(TαCP:Gal4-VP16,UAS:SpHGFP)	SynaptopHluorin, pH sensitive GFP fused to luminal end of synaptic vesicle protein VAMP2 under cone specific promoter	LCH
Tg(TαCP:EGFP-Rno.VAMP2)	EGFP fused to cytoplasmic end of VAMP2 under cone specific promoter	AAG
Tg (TαCP:sypb-CFP)	CFP fused to synaptic vesicle protein Synaptophysin under cone specific promoter	AAG
Tg (TαCP:man2a1-EGFP)	GFP fused to N-terminal 100 aas of medial Golgi protein Mannosidase2a under cone specific promoter	LCH/AAG
Tg(TαCP:man2a1-tagRFP)	tagRFP fused to N-terminal 100 aas of medial Golgi protein Mannosidase2a under cone specific promoter	AAG
Tg(crx:Man2a1-EGFP)	GFP fused to N-terminal 100 aas of medial Golgi protein Mannosidase2a under crx promoter	SH
Tg(TαCP:ER-EGFP)	GFP with N-terminal 17 aas of ER protein calreticulin with C-terminal KDEL sequence under cone specific promoter	AAG
Tg(TαCP:EGFP-synJ1)	GFP fused to WT full length zebrafish SynJ1 under cone specific promoter	AAG
Tg(TαCP:EGFP-rab7)	GFP fused to late endosome marker Rab7 under cone specific promoter	AAG
Tg(TαCP:EGFP-rab5ab)	GFP fused to early endosome marker Rab5a under cone specific promoter	AAG
Tg (TαCP:EGFP-map1lc3b)	GFP fused to autophagosome marker LC3 under cone specific promoter	EYM
Tg (TαCP:mCherry-EGFP-map1lc3b)	Tandem mCherry-GFP fused to autophagosome marker LC3 under cone specific promoter under cone specific promoter	SH/AAG/ GRS
Tg(TαCP:Lifeact-EGFP)	GFP fused to f-actin marker LIfeact under cone specific promoter	AAG
Tg (TαCP:mCherry-ML1Nx2)	mCherry fused to $PI(3,5)P_2$ probe under cone specific promoter	AAG/GRS
Tg (TαCP:tRFP-t-FYVE)	tRFP-t fused to PI(3)P marker under cone specific promoter	AAG/GRS
Tg(TαCP:YFP-FYVE)	YFP fused to PI(3)P marker under cone specific promoter	AAG

References

Aguilera MO, Beron W, Colombo MI (2012) The actin cytoskeleton participates in the early events of autophagosome formation upon starvation induced autophagy. Autophagy 8:1590-1603.

Allwardt BA, Lall AB, Brockerhoff SE, Dowling JE (2001) Synapse formation is arrested in retinal photoreceptors of the zebrafish nrc mutant. In: J Neurosci, pp 2330-2342. United States.

Arshavsky VY (2003) Protein translocation in photoreceptor light adaptation: a common theme in vertebrate and invertebrate vision. Sci STKE 2003:Pe43.

Axe EL, Walker SA, Manifava M, Chandra P, Roderick HL, Habermann A, Griffiths G, Ktistakis NT (2008) Autophagosome formation from membrane compartments enriched in phosphatidylinositol 3-phosphate and dynamically connected to the endoplasmic reticulum. J Cell Biol 182:685-701.

Balla T, Varnai P (2009) Visualization of cellular phosphoinositide pools with GFP-fused protein-domains. Curr Protoc Cell Biol Chapter 24:Unit 24 24.

Bensen ES, Costaguta G, Payne GS (2000) Synthetic genetic interactions with temperature-sensitive clathrin in Saccharomyces cerevisiae. Roles for synaptojanin-like Inp53p and dynamin-related Vps1p in clathrin-dependent protein sorting at the trans-Golgi network. Genetics 154:83-97.

Berman DE, Dall'Armi C, Voronov SV, McIntire LB, Zhang H, Moore AZ, Staniszewski A, Arancio O, Kim TW, Di Paolo G (2008) Oligomeric amyloid-beta peptide disrupts phosphatidylinositol-4,5-bisphosphate metabolism. Nat Neurosci 11:547-554.

Billcliff PG, Lowe M (2014) Inositol lipid phosphatases in membrane trafficking and human disease. The Biochemical journal 461:159-175.

Bottger G, Nagelkerken B, van der Sluijs P (1996) Rab4 and Rab7 define distinct nonoverlapping endosomal compartments. J Biol Chem 271:29191-29197.

Branchek T (1984) The development of photoreceptors in the zebrafish, brachydanio rerio. II. Function. J Comp Neurol 224:116-122.

Branchek T, Bremiller R (1984) The development of photoreceptors in the zebrafish, Brachydanio rerio. I. Structure. J Comp Neurol 224:107-115.

Bright SR, Rich ED, Varnum MD (2007) Regulation of human cone cyclic nucleotide-gated channels by endogenous phospholipids and exogenously applied phosphatidylinositol 3,4,5-trisphosphate. Mol Pharmacol 71:176-183.

Brockerhoff SE (2006) Measuring the optokinetic response of zebrafish larvae. Nat Protoc 1:2448-2451.

Brockerhoff SE, Hurley JB, Niemi GA, Dowling JE (1997) A new form of inherited red-blindness identified in zebrafish. J Neurosci 20:1-8.

Brockerhoff SE, Hurley JB, Janssen-Bienhold U, Neuhauss SC, Driever W, Dowling JE (1995) A behavioral screen for isolating zebrafish mutants with visual system defects. Proc Natl Acad Sci U S A 92:10545-10549.

Bucci C, Thomsen P, Nicoziani P, McCarthy J, van Deurs B (2000) Rab7: a key to lysosome biogenesis. Mol Biol Cell 11:467-480.

Cao M, Milosevic I, Giovedi S, De Camilli P (2014) Upregulation of Parkin in endophilin mutant mice. J Neurosci 34:16544-16549.

Cebollero E, van der Vaart A, Zhao M, Rieter E, Klionsky DJ, Helms JB, Reggiori F (2012) Phosphatidylinositol-3-phosphate clearance plays a key role in autophagosome completion. Current biology : CB 22:1545-1553.
Cestra G, Castagnoli L, Dente L, Minenkova O, Petrelli A, Migone N, Hoffmuller U, Schneider-Mergener J, Cesareni G (1999) The SH3 domains of endophilin and amphiphysin bind to the proline-rich region of synaptojanin 1 at distinct sites that display an unconventional binding specificity. J Biol Chem 274:32001-32007.
Cheng J, Fujita A, Yamamoto H, Tatematsu T, Kakuta S, Obara K, Ohsumi Y, Fujimoto T (2014) Yeast and mammalian autophagosomes exhibit distinct phosphatidylinositol 3-phosphate asymmetries. Nat Commun 5:3207.
Chinchore Y, Mitra A, Dolph PJ (2009) Accumulation of rhodopsin in late endosomes triggers photoreceptor cell degeneration. PLoS Genet 5:e1000377.
Choudhury A, Dominguez M, Puri V, Sharma DK, Narita K, Wheatley CL, Marks DL, Pagano RE (2002) Rab proteins mediate Golgi transport of caveola-internalized glycosphingolipids and correct lipid trafficking in Niemann-Pick C cells. J Clin Invest 109:1541-1550.
Chow CY, Zhang Y, Dowling JJ, Jin N, Adamska M, Shiga K, Szigeti K, Shy ME, Li J, Zhang X, Lupski JR, Weisman LS, Meisler MH (2007) Mutation of FIG4 causes neurodegeneration in the pale tremor mouse and patients with CMT4J. Nature 448:68-72.
Chuang JZ, Zhao Y, Sung CH (2007) SARA-regulated vesicular targeting underlies formation of the light-sensing organelle in mammalian rods. Cell 130:535-547.
Cook C, Stetler C, Petrucelli L (2012) Disruption of protein quality control in Parkinson's disease. Cold Spring Harb Perspect Med 2:a009423.
Cossec JC, Lavaur J, Berman DE, Rivals I, Hoischen A, Stora S, Ripoll C, Mircher C, Grattau Y, Olivomarin JC, de Chaumont F, Lecourtois M, Antonarakis SE, Veltman JA, Delabar JM, Duyckaerts C, Di Paolo G, Potier MC (2012) Trisomy for synaptojanin1 in Down syndrome is functionally linked to the enlargement of early endosomes. Hum Mol Genet 21:3156-3172.
Cousin MA, Robinson PJ (2001) The dephosphins: dephosphorylation by calcineurin triggers synaptic vesicle endocytosis. Trends in neurosciences 24:659-665.
Cremona O, Di Paolo G, Wenk MR, Luthi A, Kim WT, Takei K, Daniell L, Nemoto Y, Shears SB, Flavell RA, McCormick DA, De Camilli P (1999) Essential role of phosphoinositide metabolism in synaptic vesicle recycling. In: Cell, pp 179-188. United States.
D'Angelo G, Vicinanza M, Di Campli A, De Matteis MA (2008) The multiple roles of PtdIns(4)P -- not just the precursor of PtdIns(4,5)P2. J Cell Sci 121:1955-1963.
Dai G, Varnum MD (2013) CNGA3 achromatopsia-associated mutation potentiates the phosphoinositide sensitivity of cone photoreceptor CNG channels by altering intersubunit interactions. Am J Physiol Cell Physiol 305:C147-159.
Dai G, Peng C, Liu C, Varnum MD (2013) Two structural components in CNGA3 support regulation of cone CNG channels by phosphoinositides. J Gen Physiol 141:413-430.
Dall'Armi C, Devereaux KA, Di Paolo G (2013) The role of lipids in the control of autophagy. Current biology : CB 23:R33-45.

Damme M, Suntio T, Saftig P, Eskelinen EL (2014) Autophagy in neuronal cells: general principles and physiological and pathological functions. Acta Neuropathol.
De Camilli P, Emr SD, McPherson PS, Novick P (1996) Phosphoinositides as regulators in membrane traffic. Science 271:1533-1539.
de Heuvel E, Bell AW, Ramjaun AR, Wong K, Sossin WS, McPherson PS (1997) Identification of the major synaptojanin-binding proteins in brain. The Journal of biological chemistry 272:8710-8716.
De Matteis MA, Di Campli A, Godi A (2005) The role of the phosphoinositides at the Golgi complex. Biochim Biophys Acta 1744:396-405.
Dehay B, Martinez-Vicente M, Caldwell GA, Caldwell KA, Yue Z, Cookson MR, Klein C, Vila M, Bezard E (2013) Lysosomal impairment in Parkinson's disease. Mov Disord 28:725-732.
Deretic D, Papermaster DS (1991) Polarized sorting of rhodopsin on post-Golgi membranes in frog retinal photoreceptor cells. J Cell Biol 113:1281-1293.
Dermaut B, Norga KK, Kania A, Verstreken P, Pan H, Zhou Y, Callaerts P, Bellen HJ (2005) Aberrant lysosomal carbohydrate storage accompanies endocytic defects and neurodegeneration in Drosophila benchwarmer. J Cell Biol 170:127-139.
Di Paolo G, De Camilli P (2006) Phosphoinositides in cell regulation and membrane dynamics. Nature 443:651-657.
Dong XP, Shen D, Wang X, Dawson T, Li X, Zhang Q, Cheng X, Zhang Y, Weisman LS, Delling M, Xu H (2010) PI(3,5)P(2) controls membrane trafficking by direct activation of mucolipin Ca(2+) release channels in the endolysosome. Nature communications 1:38.
Dove SK, Dong K, Kobayashi T, Williams FK, Michell RH (2009) Phosphatidylinositol 3,5-bisphosphate and Fab1p/PIKfyve underPPIn endo-lysosome function. Biochem J 419:1-13.
Dyment DA, Smith AC, Humphreys P, Schwartzentruber J, Beaulieu CL, Bulman DE, Majewski J, Woulfe J, Michaud J, Boycott KM (2014) Homozygous nonsense mutation in SYNJ1 associated with intractable epilepsy and tau pathology. Neurobiol Aging.
Easter SS, Jr., Nicola GN (1996) The development of vision in the zebrafish (Danio rerio). Dev Biol 180:646-663.
Fadool JM, Dowling JE (2008) Zebrafish: a model system for the study of eye genetics. Prog Retin Eye Res 27:89-110.
Fecto F, Esengul YT, Siddique T (2014) Protein recycling pathways in neurodegenerative diseases. Alzheimer's research & therapy 6:13.
Ferguson CJ, Lenk GM, Meisler MH (2009) Defective autophagy in neurons and astrocytes from mice deficient in PI(3,5)P2. Hum Mol Genet 18:4868-4878.
Ferguson CJ, Lenk GM, Jones JM, Grant AE, Winters JJ, Dowling JJ, Giger RJ, Meisler MH (2012) Neuronal expression of Fig4 is necessary and sufficient to prevent spongiform neurodegeneration. Hum Mol Genet.
Fu MM, Nirschl JJ, Holzbaur EL (2014) LC3 binding to the scaffolding protein JIP1 regulates processive dynein-driven transport of autophagosomes. Dev Cell 29:577-590.
Gaidarov I, Keen JH (1999) Phosphoinositide-AP-2 interactions required for targeting to plasma membrane clathrin-coated pits. J Cell Biol 146:755-764.

Ganley IG, Pfeffer SR (2006) Cholesterol accumulation sequesters Rab9 and disrupts late endosome function in NPC1-deficient cells. J Biol Chem 281:17890-17899.
Gary JD, Wurmser AE, Bonangelino CJ, Weisman LS, Emr SD (1998) Fab1p is essential for PtdIns(3)P 5-kinase activity and the maintenance of vacuolar size and membrane homeostasis. J Cell Biol 143:65-79.
George AA, Hayden S, Holzhausen LC, Ma EY, Suzuki SC, Brockerhoff SE (2014) Synaptojanin 1 is required for endolysosomal trafficking of synaptic proteins in cone photoreceptor inner segments. PLoS One 9:e84394.
Gillooly DJ, Morrow IC, Lindsay M, Gould R, Bryant NJ, Gaullier JM, Parton RG, Stenmark H (2000) Localization of phosphatidylinositol 3-phosphate in yeast and mammalian cells. Embo j 19:4577-4588.
Godi A, Di Campli A, Konstantakopoulos A, Di Tullio G, Alessi DR, Kular GS, Daniele T, Marra P, Lucocq JM, De Matteis MA (2004) FAPPs control Golgi-to-cell-surface membrane traffic by binding to ARF and PtdIns(4)P. Nat Cell Biol 6:393-404.
Goldberg AL (2003) Protein degradation and protection against misfolded or damaged proteins. Nature 426:895-899.
Gong LW, De Camilli P (2008) Regulation of postsynaptic AMPA responses by synaptojanin 1. Proc Natl Acad Sci USA 105:17561-17566.
Gordon PB, Seglen PO (1988) Prelysosomal convergence of autophagic and endocytic pathways. Biochem Biophys Res Commun 151:40-47.
Gozani O (2003) The PHD finger of the chromatin-associated protein ING2 functions as a nuclear phosphoinositide receptor. Cell 114:99-111.
Guiney EL, Goldman AR, Elias JE, Cyert MS (2014) Calcineurin regulates the yeast synaptojanin Inp53/Sjl3 during membrane stress. Mol Biol Cell.
Guo S, Stolz LE, Lemrow SM, York JD (1999) SAC1-like domains of yeast SAC1, INP52, and INP53 and of human synaptojanin encode polyphosphoinositide phosphatases. J Biol Chem 274:12990-12995.
Guo X, Ghalayini AJ, Chen H, Anderson RE (1997) Phosphatidylinositol 3-kinase in bovine photoreceptor rod outer segments. Invest Ophthalmol Vis Sci 38:1873-1882.
Ha SA, Torabinejad J, DeWald DB, Wenk MR, Lucast L, De Camilli P, Newitt RA, Aebersold R, Nothwehr SF (2003) The synaptojanin-like protein Inp53/Sjl3 functions with clathrin in a yeast TGN-to-endosome pathway distinct from the GGA protein-dependent pathway. Mol Biol Cell 14:1319-1333.
Hammond GR, Schiavo G, Irvine RF (2009) Immunocytochemical techniques reveal multiple, distinct cellular pools of PtdIns4P and PtdIns(4,5)P(2). Biochem J 422:23-35.
Hammond GR, Dove SK, Nicol A, Pinxteren JA, Zicha D, Schiavo G (2006) Elimination of plasma membrane phosphatidylinositol (4,5)-bisphosphate is required for exocytosis from mast cells. J Cell Sci 119:2084-2094.
Harris TW, Hartwieg E, Horvitz HR, Jorgensen EM (2000) Mutations in synaptojanin disrupt synaptic vesicle recycling. J Cell Biol 150:589-600.
Hartong DT, Berson EL, Dryja TP (2006) Retinitis pigmentosa. In: Lancet, pp 1795-1809. England.

He C, Bartholomew CR, Zhou W, Klionsky DJ (2009) Assaying autophagic activity in transgenic GFP-Lc3 and GFP-Gabarap zebrafish embryos. Autophagy 5:520-526.
Heo WD, Inoue T, Park WS, Kim ML, Park BO, Wandless TJ, Meyer T (2006) PI(3,4,5)P3 and PI(4,5)P2 lipids target proteins with polybasic clusters to the plasma membrane. Science 314:1458-1461.
Ho CY, Alghamdi TA, Botelho RJ (2012) Phosphatidylinositol-3,5-bisphosphate: no longer the poor PIP2. Traffic 13:1-8.
Holzhausen LC, Lewis AA, Cheong KK, Brockerhoff SE (2009) Differential role for synaptojanin 1 in rod and cone photoreceptors. J Comp Neurol 517:633-644.
Huang Z, Anderson RE, Cao W, Wiechmann AF, Rajala RV (2011) Light-induced tyrosine phosphorylation of rod outer segment membrane proteins regulate the translocation, membrane binding and activation of type II alpha phosphatidylinositol-5-phosphate 4-kinase. Neurochem Res 36:627-635.
Hughes WE, Cooke FT, Parker PJ (2000) Sac phosphatase domain proteins. The Biochemical journal 350 Pt 2:337-352.
Huotari J, Helenius A (2011) Endosome maturation. The EMBO journal 30:3481-3500.
Ikonomov OC, Sbrissa D, Delvecchio K, Xie Y, Jin JP, Rappolee D, Shisheva A (2011) The phosphoinositide kinase PIKfyve is vital in early embryonic development: Preimplantation lethality of PIKfyve-/- embryos but normality of PIKfyve+/- mice. J Biol Chem 286:13404-13413.
Insinna C, Besharse JC (2008) Intraflagellar transport and the sensory outer segment of vertebrate photoreceptors. Dev Dyn 237:1982-1992.
Insinna C, Baye LM, Amsterdam A, Besharse JC, Link BA (2010) Analysis of a zebrafish dync1h1 mutant reveals multiple functions for cytoplasmic dynein 1 during retinal photoreceptor development. In: Neural Dev, p 12. England.
Itakura E, Mizushima N (2010) Characterization of autophagosome formation site by a hierarchical analysis of mammalian Atg proteins. Autophagy 6:764-776.
Jackson SP, Schoenwaelder SM, Matzaris M, Brown S, Mitchell CA (1995) Phosphatidylinositol 3,4,5-trisphosphate is a substrate for the 75 kDa inositol polyphosphate 5-phosphatase and a novel 5-phosphatase which forms a complex with the p85/p110 form of phosphoinositide 3-kinase. Embo j 14:4490-4500.
Jager S, Bucci C, Tanida I, Ueno T, Kominami E, Saftig P, Eskelinen EL (2004) Role for Rab7 in maturation of late autophagic vacuoles. J Cell Sci 117:4837-4848.
Jefferson AB, Majerus PW (1996) Mutation of the conserved domains of two inositol polyphosphate 5-phosphatases. Biochemistry 35:7890-7894.
Juhasz G, Hill JH, Yan Y, Sass M, Baehrecke EH, Backer JM, Neufeld TP (2008) The class III PI(3)K Vps34 promotes autophagy and endocytosis but not TOR signaling in Drosophila. J Cell Biol 181:655-666.
Kennedy B, Malicki J (2009) What drives cell morphogenesis: a look inside the vertebrate photoreceptor. Dev Dyn 238:2115-2138.
Kennedy BN, Alvarez Y, Brockerhoff SE, Stearns GW, Sapetto-Rebow B, Taylor MR, Hurley JB (2007) Identification of a zebrafish cone photoreceptor-specific promoter and genetic rescue of achromatopsia in the nof mutant. Invest Ophthalmol Vis Sci 48:522-529.

Kevany BM, Palczewski K (2010) Phagocytosis of retinal rod and cone photoreceptors. Physiology 25:8-15.
Kikuta H, Kawakami K (2009) Transient and stable transgenesis using tol2 transposon vectors. Methods Mol Biol 546:69-84.
Kimura S, Noda T, Yoshimori T (2007) Dissection of the autophagosome maturation process by a novel reporter protein, tandem fluorescent-tagged LC3. Autophagy 3:452-460.
Kirkbride KC, Hong NH, French CL, Clark ES, Jerome WG, Weaver AM (2012) Regulation of late endosomal/lysosomal maturation and trafficking by cortactin affects Golgi morphology. Cytoskeleton (Hoboken) 69:625-643.
Klionsky DJ (2007) Autophagy: from phenomenology to molecular understanding in less than a decade. Nat Rev Mol Cell Biol 8:931-937.
Klionsky DJ et al. (2012) Guidelines for the use and interpretation of assays for monitoring autophagy. Autophagy 8:445-544.
Klopfenstein DR, Vale RD (2004) The lipid binding pleckstrin homology domain in UNC-104 kinesin is necessary for synaptic vesicle transport in Caenorhabditis elegans. Mol Biol Cell 15:3729-3739.
Kolb H (2003) How the retina works - Much of the construction of an image takes place in the retina itself through the use of specialized neural circuits. American Scientist 91:28-35.
Krebs CE, Karkheiran S, Powell JC, Cao M, Makarov V, Darvish H, Di Paolo G, Walker RH, Shahidi GA, Buxbaum JD, De Camilli P, Yue Z, Paisan-Ruiz C (2013) The Sac1 domain of SYNJ1 identified mutated in a family with early-onset progressive Parkinsonism with generalized seizures. Human mutation 34:1200-1207.
Krock BL, Perkins BD (2008) The intraflagellar transport protein IFT57 is required for cilia maintenance and regulates IFT-particle-kinesin-II dissociation in vertebrate photoreceptors. In: J Cell Sci, pp 1907-1915. England.
Kwan KM, Fujimoto E, Grabher C, Mangum BD, Hardy ME, Campbell DS, Parant JM, Yost HJ, Kanki JP, Chien CB (2007) The Tol2kit: a multisite gateway-based construction kit for Tol2 transposon transgenesis constructs. Dev Dyn 236:3088-3099.
Lee SY, Wenk MR, Kim Y, Nairn AC, De Camilli P (2004) Regulation of synaptojanin 1 by cyclin-dependent kinase 5 at synapses. Proc Natl Acad Sci U S A 101:546-551.
Levine TP, Munro S (2002) Targeting of Golgi-specific pleckstrin homology domains involves both PtdIns 4-kinase-dependent and -independent components. Curr Biol 12:695-704.
Li X, Wang X, Zhang X, Zhao M, Tsang WL, Zhang Y, Yau RG, Weisman LS, Xu H (2013) Genetically encoded fluorescent probe to visualize intracellular phosphatidylinositol 3,5-bisphosphate localization and dynamics. Proc Natl Acad Sci U S A 110:21165-21170.
Lindmo K, Stenmark H (2006) Regulation of membrane traffic by phosphoinositide 3-kinases. J Cell Sci 119:605-614.
Linton JD et al. (2010) Flow of energy in the outer retina in darkness and in light. Proc Natl Acad Sci U S A 107:8599-8604.

Mani M, Lee SY, Lucast L, Cremona O, Di Paolo G, De Camilli P, Ryan TA (2007) The dual phosphatase activity of synaptojanin1 is required for both efficient synaptic vesicle endocytosis and reavailability at nerve terminals. Neuron 56:1004-1018.
Mari M, Griffith J, Rieter E, Krishnappa L, Klionsky DJ, Reggiori F (2010) An Atg9-containing compartment that functions in the early steps of autophagosome biogenesis. J Cell Biol 190:1005-1022.
Martin DD, Ladha S, Ehrnhoefer DE, Hayden MR (2014) Autophagy in Huntington disease and huntingtin in autophagy. Trends Neurosci.
Matthews G, Fuchs P (2010) The diverse roles of ribbon synapses in sensory neurotransmission. Nature reviews Neuroscience 11:812-822.
Mazelova J, Ransom N, Astuto-Gribble L, Wilson MC, Deretic D (2009) Syntaxin 3 and SNAP-25 pairing, regulated by omega-3 docosahexaenoic acid, controls the delivery of rhodopsin for the biogenesis of cilia-derived sensory organelles, the rod outer segments. In: J Cell Sci, pp 2003-2013. England.
McCartney AJ, Zhang Y, Weisman LS (2014) Phosphatidylinositol 3,5-bisphosphate: low abundance, high significance. BioEssays : news and reviews in molecular, cellular and developmental biology 36:52-64.
McIntire LB, Berman DE, Myaeng J, Staniszewski A, Arancio O, Di Paolo G, Kim TW (2012) Reduction of synaptojanin 1 ameliorates synaptic and behavioral impairments in a mouse model of Alzheimer's disease. The Journal of neuroscience : the official journal of the Society for Neuroscience 32:15271-15276.
McPherson PS, Takei K, Schmid SL, De Camilli P (1994a) p145, a major Grb2-binding protein in brain, is co-localized with dynamin in nerve terminals where it undergoes activity-dependent dephosphorylation. J Biol Chem 269:30132-30139.
McPherson PS, Czernik AJ, Chilcote TJ, Onofri F, Benfenati F, Greengard P, Schlessinger J, De Camilli P (1994b) Interaction of Grb2 via its Src homology 3 domains with synaptic proteins including synapsin I. Proc Natl Acad Sci U S A 91:6486-6490.
McPherson PS, Garcia EP, Slepnev VI, David C, Zhang X, Grabs D, Sossin WS, Bauerfeind R, Nemoto Y, De Camilli P (1996) A presynaptic inositol-5-phosphatase. Nature 379:353-357.
Meijer AJ, Codogno P (2004) Regulation and role of autophagy in mammalian cells. Int J Biochem Cell Biol 36:2445-2462.
Meyer MP, Smith SJ (2006) Evidence from in vivo imaging that synaptogenesis guides the growth and branching of axonal arbors by two distinct mechanisms. In: J Neurosci, pp 3604-3614. United States.
Miesenbock G, De Angelis DA, Rothman JE (1998) Visualizing secretion and synaptic transmission with pH-sensitive green fluorescent proteins. Nature 394:192-195.
Mizushima N (2005) The pleiotropic role of autophagy: from protein metabolism to bactericide. Cell Death Differ 12 Suppl 2:1535-1541.
Monastyrska I, Rieter E, Klionsky DJ, Reggiori F (2009) Multiple roles of the cytoskeleton in autophagy. Biol Rev Camb Philos Soc 84:431-448.
Moreau K, Ravikumar B, Puri C, Rubinsztein DC (2012) Arf6 promotes autophagosome formation via effects on phosphatidylinositol 4,5-bisphosphate and phospholipase D. The Journal of cell biology 196:483-496.

Morris AC, Fadool JM (2005) Studying rod photoreceptor development in zebrafish. Physiol Behav 86:306-313.
Mullock BM, Bright NA, Fearon CW, Gray SR, Luzio JP (1998) Fusion of lysosomes with late endosomes produces a hybrid organelle of intermediate density and is NSF dependent. The Journal of cell biology 140:591-601.
Muto A, Orger MB, Wehman AM, Smear MC, Kay JN, Page-McCaw PS, Gahtan E, Xiao T, Nevin LM, Gosse NJ, Staub W, Finger-Baier K, Baier H (2005) Forward genetic analysis of visual behavior in zebrafish. PLoS Genet 1:e66.
Nicot AS, Fares H, Payrastre B, Chisholm AD, Labouesse M, Laporte J (2006) The phosphoinositide kinase PIKfyve/Fab1p regulates terminal lysosome maturation in Caenorhabditis elegans. Mol Biol Cell 17:3062-3074.
Nixon RA (2013) The role of autophagy in neurodegenerative disease. Nat Med 19:983-997.
Nixon RA, Yang DS, Lee JH (2008) Neurodegenerative lysosomal disorders: a continuum from development to late age. Autophagy 4:590-599.
O'Day WT, Young RW (1978) Rhythmic daily shedding of outer-segment membranes by visual cells in the goldfish. J Cell Biol 76:593-604.
Obara K, Noda T, Niimi K, Ohsumi Y (2008) Transport of phosphatidylinositol 3-phosphate into the vacuole via autophagic membranes in Saccharomyces cerevisiae. Genes Cells 13:537-547.
Obholzer N, Wolfson S, Trapani JG, Mo W, Nechiporuk A, Busch-Nentwich E, Seiler C, Sidi S, Sollner C, Duncan RN, Boehland A, Nicolson T (2008) Vesicular glutamate transporter 3 is required for synaptic transmission in zebrafish hair cells. In: J Neurosci, pp 2110-2118. United States.
Odorizzi G, Babst M, Emr SD (2000) Phosphoinositide signaling and the regulation of membrane trafficking in yeast. Trends in biochemical sciences 25:229-235.
Ooms LM, Horan KA, Rahman P, Seaton G, Gurung R, Kethesparan DS, Mitchell CA (2009) The role of the inositol polyphosphate 5-phosphatases in cellular function and human disease. In: Biochem J, pp 29-49. England.
Papermaster DS, Schneider BG, Besharse JC (1985) Vesicular transport of newly synthesized opsin from the Golgi apparatus toward the rod outer segment. Ultrastructural immunocytochemical and autoradiographic evidence in Xenopus retinas. Invest Ophthalmol Vis Sci 26:1386-1404.
Papermaster DS, Schneider BG, DeFoe D, Besharse JC (1986) Biosynthesis and vectorial transport of opsin on vesicles in retinal rod photoreceptors. J Histochem Cytochem 34:5-16.
Parrish WR, Stefan CJ, Emr SD (2004) Essential role for the myotubularin-related phosphatase Ymr1p and the synaptojanin-like phosphatases Sjl2p and Sjl3p in regulation of phosphatidylinositol 3-phosphate in yeast. Mol Biol Cell 15:3567-3579.
Patterson D (2009) Molecular genetic analysis of Down syndrome. Hum Genet 126:195-214.
Pearring JN, Salinas RY, Baker SA, Arshavsky VY (2013) Protein sorting, targeting and trafficking in photoreceptor cells. Progress in retinal and eye research 36:24-51.
Pfeffer SR (2009) Multiple routes of protein transport from endosomes to the trans Golgi network. FEBS Lett 583:3811-3816.

Posor Y, Eichhorn-Gruenig M, Puchkov D, Schoneberg J, Ullrich A, Lampe A, Muller R, Zarbakhsh S, Gulluni F, Hirsch E, Krauss M, Schultz C, Schmoranzer J, Noe F, Haucke V (2013) Spatiotemporal control of endocytosis by phosphatidylinositol-3,4-bisphosphate. Nature 499:233-237.
Prescott ED, Zenisek D (2005) Recent progress towards understanding the synaptic ribbon. Curr Opin Neurobiol 15:431-436.
Puri C, Renna M, Bento CF, Moreau K, Rubinsztein DC (2013) Diverse autophagosome membrane sources coalesce in recycling endosomes. Cell 154:1285-1299.
Quadri M, Fang M, Picillo M, Olgiati S, Breedveld GJ, Graafland J, Wu B, Xu F, Erro R, Amboni M, Pappata S, Quarantelli M, Annesi G, Quattrone A, Chien HF, Barbosa ER, Oostra BA, Barone P, Wang J, Bonifati V (2013) Mutation in the SYNJ1 gene associated with autosomal recessive, early-onset Parkinsonism. Human mutation 34:1208-1215.
Qualmann B, Kessels MM (2002) Endocytosis and the cytoskeleton. Int Rev Cytol 220:93-144.
Rajala A, Daly RJ, Tanito M, Allen DT, Holt LJ, Lobanova ES, Arshavsky VY, Rajala RV (2009) Growth factor receptor-bound protein 14 undergoes light-dependent intracellular translocation in rod photoreceptors: functional role in retinal insulin receptor activation. Biochemistry 48:5563-5572.
Rajala RV, Rajala A, Morris AJ, Anderson RE (2014) Phosphoinositides: minor lipids make a major impact on photoreceptor cell functions. Sci Rep 4:5463.
Ramamurthy V, Cayouette M (2009) Development and disease of the photoreceptor cilium. Clin Genet 76:137-145.
Ramjaun AR, McPherson PS (1996) Tissue-specific alternative splicing generates two synaptojanin isoforms with differential membrane binding properties. J Biol Chem 271:24856-24861.
Ravikumar B, Moreau K, Jahreiss L, Puri C, Rubinsztein DC (2010) Plasma membrane contributes to the formation of pre-autophagosomal structures. Nat Cell Biol 12:747-757.
Regus-Leidig H, Brandstatter JH (2012) Structure and function of a complex sensory synapse. Acta physiologica 204:479-486.
Riedl J, Crevenna AH, Kessenbrock K, Yu JH, Neukirchen D, Bista M, Bradke F, Jenne D, Holak TA, Werb Z, Sixt M, Wedlich-Soldner R (2008) Lifeact: a versatile marker to visualize F-actin. Nat Methods 5:605-607.
Ringstad N, Nemoto Y, De Camilli P (1997) The SH3p4/Sh3p8/SH3p13 protein family: binding partners for synaptojanin and dynamin via a Grb2-like Src homology 3 domain. Proc Natl Acad Sci U S A 94:8569-8574.
Roderick HL, Campbell AK, Llewellyn DH (1997) Nuclear localisation of calreticulin in vivo is enhanced by its interaction with glucocorticoid receptors. FEBS Lett 405:181-185.
Rodieck RW (1973) The vertebrate retina; principles of structure and function. San Francisco: Freeman.
Rong Y, Liu M, Ma L, Du W, Zhang H, Tian Y, Cao Z, Li Y, Ren H, Zhang C, Li L, Chen S, Xi J, Yu L (2012) Clathrin and phosphatidylinositol-4,5-bisphosphate regulate autophagic lysosome reformation. Nature cell biology 14:924-934.

Rowland AM, Richmond JE, Olsen JG, Hall DH, Bamber BA (2006) Presynaptic terminals independently regulate synaptic clustering and autophagy of GABAA receptors in Caenorhabditis elegans. The Journal of neuroscience : the official journal of the Society for Neuroscience 26:1711-1720.
Sarkes D, Rameh LE (2010) A novel HPLC-based approach makes possible the spatial characterization of cellular PtdIns5P and other phosphoinositides. Biochem J 428:375-384.
Schmied R, Holtzman E Involvement of the Golgi apparatus in sorting of materials to opposite ends of frog rod retinal photoreceptors. Journal of Neurobiology 20:115-138.
Schmied R, Holtzman E (1989) Involvement of the Golgi apparatus in sorting of materials to opposite ends of frog rod retinal photoreceptors. Journal of Neurobiology 20:115-138.
Schmitt EA, Dowling JE (1999) Early retinal development in the zebrafish, Danio rerio: light and electron microscopic analyses. J Comp Neurol 404:515-536.
Seglen PO, Berg TO, Blankson H, Fengsrud M, Holen I, Stromhaug PE (1996) Structural aspects of autophagy. Adv Exp Med Biol 389:103-111.
Shen HM, Mizushima N (2014) At the end of the autophagic road: an emerging understanding of lysosomal functions in autophagy. Trends Biochem Sci 39:61-71.
Shen W, Ganetzky B (2009) Autophagy promotes synapse development in Drosophila. The Journal of cell biology 187:71-79.
Shin HW (2005) An enzymatic cascade of Rab5 effectors regulates phosphoinositide turnover in the endocytic pathway. J Cell Biol 170:607-618.
Shvets E, Fass E, Elazar Z (2008) Utilizing flow cytometry to monitor autophagy in living mammalian cells. Autophagy 4:621-628.
Singer-Kruger B, Nemoto Y, Daniell L, Ferro-Novick S, De Camilli P (1998) Synaptojanin family members are implicated in endocytic membrane traffic in yeast. J Cell Sci 111 (Pt 22):3347-3356.
Stack JH, Horazdovsky B, Emr SD (1995) Receptor-mediated protein sorting to the vacuole in yeast: roles for a protein kinase, a lipid kinase and GTP-binding proteins. Annu Rev Cell Dev Biol 11:1-33.
Stefan CJ, Audhya A, Emr SD (2002) The yeast synaptojanin-like proteins control the cellular distribution of phosphatidylinositol (4,5)-bisphosphate. Mol Biol Cell 13:542-557.
Stein MP, Feng Y, Cooper KL, Welford AM, Wandinger-Ness A (2003) Human VPS34 and p150 are Rab7 interacting partners. Traffic 4:754-771.
Sterling P, Matthews G (2005) Structure and function of ribbon synapses. Trends Neurosci 28:20-29.
Stolz LE, Huynh CV, Thorner J, York JD (1998) Identification and characterization of an essential family of inositol polyphosphate 5-phosphatases (INP51, INP52 and INP53 gene products) in the yeast Saccharomyces cerevisiae. Genetics 148:1715-1729.
Strauss O (2005) The retinal pigment epithelium in visual function. Physiol Rev 85:845-881.

Stuart GW, McMurray JV, Westerfield M (1988) Replication, integration and stable germ-line transmission of foreign sequences injected into early zebrafish embryos. Development (Cambridge, England) 103:403-412.
Sung CH, Chuang JZ (2010) The cell biology of vision. J Cell Biol 190:953-963.
Suzuki SC, Bleckert A, Williams PR, Takechi M, Kawamura S, Wong RO (2013) Cone photoreceptor types in zebrafish are generated by symmetric terminal divisions of dedicated precursors. Proc Natl Acad Sci U S A.
Tai HC, Schuman EM (2008) Ubiquitin, the proteasome and protein degradation in neuronal function and dysfunction. Nat Rev Neurosci 9:826-838.
Takasuga S, Sasaki T (2013) Phosphatidylinositol-3,5-bisphosphate: metabolism and physiological functions. Journal of biochemistry 154:211-218.
Tanaka K, Matsuda N (2014) Proteostasis and neurodegeneration: the roles of proteasomal degradation and autophagy. Biochim Biophys Acta 1843:197-204.
Tofaris GK (2012) Lysosome-dependent pathways as a unifying theme in Parkinson's disease. Mov Disord 27:1364-1369.
Trapani JG, Obholzer N, Mo W, Brockerhoff SE, Nicolson T (2009) Synaptojanin1 is required for temporal fidelity of synaptic transmission in hair cells. PLoS Genet 5:e1000480.
Tsujikawa M, Malicki J (2004) Intraflagellar transport genes are essential for differentiation and survival of vertebrate sensory neurons. Neuron 42:703-716.
Ullrich B, Südhof TC (1994) Distribution of synaptic markers in the retina: Implications for synaptic vesicle traffic in ribbon synapses. 88:249–257.
Van Epps HA, Yim CM, Hurley JB, Brockerhoff SE (2001) Investigations of photoreceptor synaptic transmission and light adaptation in the zebrafish visual mutant nrc. Invest Ophthalmol Vis Sci 42:868-874.
Van Epps HA, Hayashi M, Lucast L, Stearns GW, Hurley JB, De Camilli P, Brockerhoff SE (2004) The zebrafish nrc mutant reveals a role for the polyphosphoinositide phosphatase synaptojanin 1 in cone photoreceptor ribbon anchoring. J Neurosci 24:8641-8650.
Vergne I, Deretic V (2010) The role of PI3P phosphatases in the regulation of autophagy. FEBS Lett 584:1313-1318.
Vergne I, Roberts E, Elmaoued RA, Tosch V, Delgado MA, Proikas-Cezanne T, Laporte J, Deretic V (2009) Control of autophagy initiation by phosphoinositide 3-phosphatase Jumpy. Embo j 28:2244-2258.
Verstreken P, Koh T-W, Schulze KL, Zhai RG, Hiesinger PR, Zhou Y, Mehta SQ, Cao Y, Roos J, Bellen HJ (2003) Synaptojanin is recruited by endophilin to promote synaptic vesicle uncoating. Neuron 40:733-748.
Vicinanza M, D'Angelo G, Di Campli A, De Matteis MA (2008a) Phosphoinositides as regulators of membrane trafficking in health and disease. Cell Mol Life Sci 65:2833-2841.
Vicinanza M, D'Angelo G, Di Campli A, De Matteis MA (2008b) Function and dysfunction of the PI system in membrane trafficking. In: EMBO J, pp 2457-2470. England.
Vicinanza M, Korolchuk VI, Ashkenazi A, Puri C, Menzies FM, Clarke JH, Rubinsztein DC (2015) PI(5)P Regulates Autophagosome Biogenesis. Mol Cell.

Vidal RL, Matus S, Bargsted L, Hetz C (2014) Targeting autophagy in neurodegenerative diseases. Trends Pharmacol Sci 35:583-591.
Vitelli R, Santillo M, Lattero D, Chiariello M, Bifulco M, Bruni CB, Bucci C (1997) Role of the small GTPase Rab7 in the late endocytic pathway. J Biol Chem 272:4391-4397.
Vollrath L, Spiwoks-Becker I (1996) Plasticity of retinal ribbon synapses. Microsc Res Tech 35:472-487.
Vollrath L, Meyer A, Buschmann F (1989) Ribbon synapses of the mammalian retina contain two types of synaptic bodies--ribbons and spheres. J Neurocytol 18:115-120.
Voronov SV, Frere SG, Giovedi S, Pollina EA, Borel C, Zhang H, Schmidt C, Akeson EC, Wenk MR, Cimasoni L, Arancio O, Davisson MT, Antonarakis SE, Gardiner K, De Camilli P, Di Paolo G (2008) Synaptojanin 1-linked phosphoinositide dyshomeostasis and cognitive deficits in mouse models of Down's syndrome. Proc Natl Acad Sci U S A 105:9415-9420.
Wan L, Almers W, Chen W (2005) Two ribeye genes in teleosts: the role of Ribeye in ribbon formation and bipolar cell development. The Journal of neuroscience : the official journal of the Society for Neuroscience 25:941-949.
Wang J, Deretic D (2014) Molecular complexes that direct rhodopsin transport to primary cilia. Progress in retinal and eye research 38:1-19.
Westerfield M (1995) The Zebrafish Book: A Guide for the Laboratory Use of Zebrafish (*Brachydanio rerio)*. Eugene: University of Oregon Press.
Wheeler TC, Chin L-S, Li Y, Roudabush FL, Li L (2002) Regulation of Synaptophysin Degradation by Mammalian Homologues of Seven in Absentia.
Whisstock JC, Romero S, Gurung R, Nandurkar H, Ooms LM, Bottomley SP, Mitchell CA (2000) The inositol polyphosphate 5-phosphatases and the apurinic/apyrimidinic base excision repair endonucleases share a common mechanism for catalysis. J Biol Chem 275:37055-37061.
Wright AF, Chakarova CF, El-Aziz MMA, Bhattacharya SS (2010) Photoreceptor degeneration: genetic and mechanistic dissection of a complex trait. Nature Reviews Genetics 11:273-284.
Yau KW, Hardie RC (2009) Phototransduction motifs and variations. Cell 139:246-264.
Young RW (1967) The renewal of photoreceptor cell outer segments. J Cell Biol 33:61-72.
Zhang Y, Zolov SN, Chow CY, Slutsky SG, Richardson SC, Piper RC, Yang B, Nau JJ, Westrick RJ, Morrison SJ, Meisler MH, Weisman LS (2007) Loss of Vac14, a regulator of the signalling lipid phosphatidylinositol 3,5-bisphosphate, results in neurodegeneration in mice. Proc Natl Acad Sci USA 104:17518-17523.
Zhu L, Zhong M, Zhao J, Rhee H, Caesar I, Knight EM, Volpicelli-Daley L, Bustos V, Netzer W, Liu L, Lucast L, Ehrlich ME, Robakis NK, Gandy SE, Cai D (2013) Reduction of synaptojanin 1 accelerates Abeta clearance and attenuates cognitive deterioration in an Alzheimer mouse model. J Biol Chem 288:32050-32063.
Zolov SN, Bridges D, Zhang Y, Lee WW, Riehle E, Verma R, Lenk GM, Converso-Baran K, Weide T, Albin RL, Saltiel AR, Meisler MH, Russell MW, Weisman LS (2012) In vivo, Pikfyve generates PI(3,5)P2, which serves as both a signaling

lipid and the major precursor for PI5P. Proc Natl Acad Sci U S A 109:17472-17477.